Studies of the N-end Rule Pathway in Bacteria and Mammals

Thesis by

Tri Vu

In Partial Fulfillment of the Requirements for

the Degree of

Doctor of Philosophy

CALIFORNIA INSTITUTE OF TECHNOLOGY

Pasadena, California

2017

(Defended June 14th 2016)

ACKNOWLEDGEMENTS

I would like to thank my advisor, Alexander Varshavsky, who has guided me through all the work in this thesis. Alex's creativity and enthusiasm for science is rare and exceptional. It is a great honor for me to work with Alex.

I would like to thank Konstatin Piatkov with whom I collaborated for the work in this thesis. Konstatin is an exceptional scientist who had taught me much about bench work.

I would like to thank members of the Varshavsky lab who have helped me over the years: Brandon Wadas who gave me advice and ideas, Chris Brower who taught me mouse techniques, and Elena Udartseva who assisted me with managing the mouse colony.

I would like to thank other members of Caltech: Natalie Verduzco who took care of much of my mouse colony, Shirley Pease who assisted me with generating mutant mice, and Natalia Malkova who gave me advice on mouse behavior studies.

I would like to thank my committee, Bil Clemon, Shu-ou Shan, and David Chan for their support during my time at Caltech. I also want to thank Bil for organizing the Biochemistry Seminars allowing the students to discuss with the speakers about their work. I had many stimulating discussions in these seminars.

I would like to dedicate this thesis to my parents and my grandparents Vũ Minh Khương, Trần Hoàng Châu Sa, Trần Đình Khôi, Hoàng Thị Mộng Hiền, Vũ Minh Chính, and Phạm Thị Dung for always supporting what I do.

ABSTRACT

Many intracellular proteins are either conditionally or constitutively short-lived, with *in vivo* half-lives that can be as brief as a minute or so. The regulated and processive degradation of intracellular proteins is carried out largely by the ubiquitin (Ub)-proteasome system (UPS), in conjunction with molecular chaperones, autophagy, and lysosomal proteolysis. The N-end rule pathway, the first specific pathway of UPS to be discovered, relates the *in vivo* half-life of a protein to the identity of its N-terminal residue. Physiological functions of the N-end rule pathway are strikingly broad and continue to be discovered.

In bacteria and in eukaryotic organelles mitochondria and chloroplasts all nascent proteins bear the pretranslationally formed N-terminal formyl-methionine (fMet) residue. What is the main biological function of this metabolically costly, transient, and not strictly essential modification of N-terminal Met, and why has Met formylation not been eliminated during bacterial evolution? One possibility is that the formyl groups of N-terminal Met in Nt-formylated bacterial proteins may signify a proteolytic role of Nt-formylation. My colleagues and I addressed this hypothesis experimentally, as described in Chapter 3 of this thesis.

Among the multitude of biological functions of the mammalian Arg/N-end rule pathway are its roles in the brain, including the regulation of synaptic transmission and the regulation of brain's G-protein circuits. This regulation is mediated, in part, by the its Ate1-mediated arginylation branch of the Arg/N-end rule pathway. One role of the Ate1 arginyltransferase (R-transferase) is to mediate the conditional degradation of three G-protein down-regulators, Rgs4, Rgs5, and Rgs16. *Ate1*$^{-/-}$ mice, which lack the Ate1 R-

transferase, exhibit a variety of abnormal phenotypes. Chapter 4 describes our studies of neurological abnormalities in *Ate1*$^{-/-}$ mice (and also in mice that express Ate1 conditionally, upon the addition of doxycycline), with an emphasis on the propensity of these mice to epileptic seizures.

PUBLISHED CONTENT AND CONTRIBUTIONS

Piatkov, K. I. et al. (2015). “Formyl-methionine as a degradation signal at the N-termini of bacterial proteins”. In: *Microbial Cell*, Vol. 2, No.10, pp. 376–393. doi: 10.15698/mic2015.10.231.

T.T.M.V participated in the project, prepared and analyzed the data, and participated in the writing of the manuscript.

TABLE OF CONTENTS

LIST OF FIGURES AND TABLES

Table *Page*

CHAPTER 1:
INTRODUCTION TO THE N-END RULE PATHWAY

Many intracellular proteins are either conditionally or constitutively short-lived, with *in vivo* half-lives that can be as brief as a minute or so. In some cases, a proteolytic pathway targets and destroys a protein cotranslationally (*1, 2*). The regulated and processive degradation of intracellular proteins is carried out largely by the ubiquitin (Ub)-proteasome system (UPS), in conjunction with molecular chaperones, autophagy and lysosomal proteolysis. Other mediators of intracellular protein degradation include nonprocessive proteases such as caspases, calpains, and separases. These and other proteases can function as "upstream" components of the UPS, generating protein fragments that are targeted and degraded to short peptides by specific Ub-dependent proteases. Proteins that are damaged, misfolded, or otherwise abnormal are often recognized as such and selectively destroyed by the UPS. Physiologically important exceptions include conformationally perturbed proteins and/or their aggregates that are harmful but cannot be efficaciously repaired or removed. The resulting proteotoxicity underlies both aging and specific diseases, including neurodegeneration (*3*).

One major role of the UPS is the regulation of proteins whose concentrations must vary with time and alterations in the state of a cell. Short *in vivo* half-lives of such proteins provide a way to generate their spatial gradients and to rapidly adjust their concentration or subunit composition through changes in the rate of their degradation. In addition, a short half-life of a protein would lead to a rapid decrease in its concentration upon cessation of its synthesis. This way, transcriptional or translational control of specific regulatory proteins can acquire switch-like properties, because a short-lived protein that is no longer made would not persist in a cell, in contrast to a metabolically stable protein. Proteolysis can also serve to activate or otherwise modulate protein molecules and

specific circuits. These and other properties of the UPS make it, among other things, a major regulator of gene expression (*3*).

The field of Ub and regulated protein degradation was created in the 1980s, largely through the complementary discoveries by the laboratory of A. Hershko and the laboratory of A. Varshavsky. In 1978-1985, Hershko and colleagues analyzed Ub-mediated protein degradation *in vitro* (in cell extracts), including the isolation of enzymes that mediate Ub conjugation. In 1982–1990, Varshavsky and colleagues discovered the biological fundamentals of the UPS, including the first demonstration that the bulk of protein degradation in a living cell requires Ub conjugation and the identification of the first Ub-conjugating (E2) enzymes (see below for the enzymology of the UPS) with specific physiological functions, in the cell cycle (Cdc34 E2) and DNA repair (Rad6 E2). These advances initiated the understanding of the massive, multilevel involvement of the UPS in the regulation of the cell cycle and DNA damage response (*3*).

In 1990, Varshavsky and colleagues identified and cloned an E3 ligase termed Ubr1 (see below for enzymology of the UPS), the first molecularly cloned and analyzed E3 Ub ligase. Together with the Rad6 E2 and Cdc34 E2 results, the cloning and characterization of the Ubr1 E3 opened up a particularly large field, as we now know that the mammalian genome encodes about 1,000 distinct E3s. The targeting of many distinct degrons in cellular proteins by this enormous diversity of specific E3 Ub ligases underlies the unprecedented functional reach of the Ub system (*3*). In 1986, Varshavsky and colleagues discovered the first primary degradation signals (degrons) in short-lived proteins. (Specific features of proteins that mark them for conjugation to Ub were presumed to exist, but their nature was a mystery.) These new signals included degrons that give rise to the N-end rule,

which relates the *in vivo* half-life of a protein to the identity of its N-terminal residue. The N-end rule pathway (it mediates the N-end rule) was the first specific pathway of the Ub system. Other foundational discoveries of the Varshavsky laboratory in the 1980s included the first substrate-linked poly-Ub chains, their specific topology, and their necessity for proteolysis; the subunit selectivity of protein degradation; the first physiological substrate of the UPS (the MATα2 repressor; before this advance, the UPS was examined using artificial substrates); and first genes that encode Ub precursors (linear poly-Ub and Ub fusions to specific ribosomal proteins. By the end of the 1980s, these and related studies by the Varshavsky laboratory had revealed the major biological functions of the UPS as well as the basis for its specificity, i. e., the first degradation signals in short-lived proteins (3).

Enzymology of the UPS

Ub is a 76-residue protein that mediates protein degradation through the enzymatic conjugation of Ub to proteins that contain primary degradation signals, called degrons (*4*). Ub-protein conjugation marks proteins for their recognition and degradation by the 26S proteasome, a processive, ATP-dependent protease. Ub is conjugated to proteins either as a single moiety or as a poly-Ub chain that is linked (in most cases) to the ε-amino group of an internal Lys residue in a substrate protein. Ub is a "secondary" degron, in that Ub is conjugated to proteins because they contain primary degradation signals. Ub has nonproteolytic functions as well (*5*).

Ub is activated for conjugation to other proteins by a Ub-activating enzyme (E1), which couples ATP hydrolysis to the formation of a high-energy thioester bond between Gly76 of Ub and a specific Cys residue of E1 (*6, 7*). The E1-linked Ub moiety is moved, in a transesterification reaction, from E1 to a Cys residue of an Ub-conjugating enzyme (E2), and from there to a Lys residue

of an ultimate acceptor protein, yielding an Ub-protein conjugate. This last step requires the participation of another component, called E3 ligase, which selects a protein for ubiquitylation through an interaction with its degron (*7, 8*).

Repeated ubiquitylation at the same substrate's site results in a poly-Ub chain. In these structures, the C-terminal Gly of one Ub is joined to an internal Lys of the adjacent Ub moiety, resulting in a chain of Ub-Ub conjugates containing two or more Ub moieties (*9, 10*). Ub has seven lysines; thus, a poly-Ub chain in which no Ub moiety has more than one Lys residue linked to another Ub moiety can have, *a priori*, any of the seven 'pure' topologies or a far greater number of 'mixed' topologies. The first poly-Ub chain to be discovered had its Ub moieties conjugated through the Lys48 residue of Ub (*9*). Other poly-Ub chains involve Lys63 or Lys29 of Ub (*11, 12*). A chain linked through the Lys63 residues of its Ub moieties has a role in a pathway of DNA repair (*11*). One function of the Lys48 linkage chain is to facilitate the degradation of the substrate by the 26S proteasome.

The covalent bond between Ub and other proteins can be cleaved. There are multiple ATP independent proteases that recognize an Ub moiety and cleave at the Ub adduct junction (*7, 13, 14*). One cause of the multiplicity of deubiquitylases (DUBs) is the diversity of their targets, which include linear Ub fusions, Ub adducts with small nucleophiles such as glutathione, and also free or substrate linked poly-Ub chains (*11, 12, 15, 16*). The junctions in linear Ub adducts are structurally distinct from the junctions in branched Ub conjugates. Thus, some DUBs may have preferences for either linear or branched Ub adducts. In addition, a Ub conjugate can be spatially confined in a cell,

making it accessible only to some DUBs. For example, DUBs associated with the 26S proteasome have privileged access to a poly-Ub chain of a proteasome-bound substrate (*7*).

The N-end rule pathway in eukaryotes

In 1986, Varshavsky and colleagues discovered the first primary degradation signals in short-lived proteins. These signals included degrons that give rise to the N-end rule, which relates the *in vivo* half-life of a protein to the identity of its N-terminal residue (*17*). In eukaryotes, the N-end rule pathway comprises two major branches, one of which is termed the Arg/N-end rule pathway. This branch involves the N-terminal deamidation (Nt-deamidation) and N-terminal arginylation (Nt-arginylation) of protein substrates, and also the recognition of specific unmodified N-terminal residues by the pathway's E3 Ub ligases, termed N-recognins. The other branch of the N-end rule pathway is called the Ac/N-end rule pathway (*18*). It involves the cotranslational N^{α}-terminal acetylation (Nt-acetylation) of cellular proteins (*19-21*) whose N-termini bear either Met or the small uncharged residues Ala, Val, Ser, Thr, or Cys (*22, 23*). Nt-acetylated proteins are targeted for regulated degradation by specific Ub ligases (called Ac/N-recognins) of the Ac/N-end rule pathway (*18*). Approximately 90% of human proteins are cotranslationally Nt-acetylated (*19*). Many, possibly most, Nt-acetylated proteins contain Ac/N-degrons (*18, 24-26*).

In the Arg/N-end rule pathway, the N-terminal Arg, Lys, His, Leu, Phe, Tyr, Trp, Ile, Asp, Glu, Asn, Gln, and Cys residues comprise the main determinants of N-degrons. Among these N-degrons, the unmodified basic (Arg, Lys, His) and bulky hydrophobic (Leu, Phe, Tyr, Trp, Ile) N-terminal residues are recognized directly by cognate E3 N-recognins. These E3s contain highly spalogous (spatially similar (*27*)) ~80-residue regions called UBR domains or Type-1 binding sites

(*28*). Folded around three zinc ions, a UBR domain binds to N-terminal Arg, Lys, or His, the Type-1 primary destabilizing residues of N-end rule substrates. Another region of UBR-type N-recognins, called the Type-2 binding site, recognizes N-terminal Leu, Phe, Tyr, Trp, or Ile, which are called the Type-2 primary destabilizing residues (*28-30*).

In contrast to N-terminal Arg, Lys, His, Leu, Phe, Tyr, Trp, and Ile, the N-terminal Asp, Glu, Asn, Gln, and Cys function as destabilizing residues through their preliminary chemical modifications. One of these modifications is Nt-arginylation. Arg-tRNA-protein transferase (R-transferase) conjugates Arg to N-terminal Asp, Glu, or (oxidized) Cys of proteins or short peptides, with Arg-tRNA as the cosubstrate and the donor of Arg. R-transferases are encoded by *Ate1* and its sequelogs from yeast to mammals but are absent from examined prokaryotes (*31-33*). In contrast to N-terminal Asp, Glu and oxidized Cys, the N-terminal Asn and Gln residues cannot be arginylated by R-transferase. However, the Arg/N-end rule pathway contains specific N-terminal amidases (Nt-amidases) that convert N-terminal Asn and Gln to Asp and Glu, respectively, followed by their Nt-arginylation (*34-37*). N-terminal Asp, Glu, Asn, Gln, and Cys that are targeted by the Arg/N-end rule pathway are termed “secondary” or “tertiary” destabilizing residues, depending on the number of specific steps that precede their targeting by *N*-recognins (*31, 36, 38, 39*).

The substrate range of the Arg/N-end rule pathway was recently expanded as a result of the discovery that both *S. cerevisiae* Ubr1 and mammalian Ubr1 and Ubr2 can recognize the N-termini of Met-Φ proteins through their unacetylated N-terminal Met residues, resulting in the processive degradation of these proteins. (A Met-Φ protein bears N-terminal Met followed by a large hydrophobic [Φ] non-Met residue, i.e., Leu, Phe, Tyr, Trp or Ile.) On the other hand, Nt-acetylation

would convert a Met^{Φ}/N-degron into an $AcMet^{\Phi}$/N-degron, and thereby would shift the targeting of the resulting Ac-Met-Φ protein to the Ac/N-end rule pathway. The resulting functional complementarity between the Arg/N-end rule and the Ac/N-end rule pathways makes possible the proteolysis-mediated control of Met-Φ proteins irrespective of the extent of their Nt-acetylation (*24, 25*).

An *N*-degron can be produced through a cotranslational or posttranslational proteolytic cleavage. Ribosome-associated Met-aminopeptidases cleave off the Met residue from the N-terminus of a nascent protein if and only if the residue at position 2, to become N-terminal after cleavage, is not larger than Val (*22*). Of the 13 residues that are destabilizing in the mammalian Arg/N-end rule pathway, only Cys can be made N-terminal by Met-aminopeptidases. The second-position Ala, Val, Ser, Thr, or Cys can also be made N-terminal by Met-aminopeptidases. These residues are usually Nt-acetylated and are a part of the Ac/N-end rule pathway. If N-terminal Met is followed by a residue larger than Val, this Met is not cleaved off, and is usually Nt-acetylated. In these nascent proteins, their N-terminal Met is, most cases, cotranslationally Nt-acetylated, thereby generating Ac/N-degrons recognized the Ac/N-end rule pathway (*1*).

N-degrons of the Arg/N-end rule pathway can also be produced by non-MetAP nonprocessive proteases, including caspases (*40, 41*), calpains (*42*), separase (*43*), taspase (*44*), MALT1 protease (*45*), γ-secretase (*46*), proteinase-3 (PR3) (*47*), viral proteases (*48, 49*), and other such proteases as well. Thus, operationally, these proteases function as upstream components of the N-end rule pathway, generating its substrates, which comprise C-terminal

fragments of naturally cleaved proteins (*29, 38*). In sum, a majority of cellular proteins can be targeted for regulated degradation by the Arg/N-end rule and Ac/N-end rule pathways, which can act, on a given protein, either separately or together, depending on the protein's N-terminal sequence and the state of its modification.

Physiological functions of the N-end rule pathway are strikingly broad and continue to be discovered. Regulated degradation of proteins by the eukaryotic Arg/N-end rule pathway mediates the sensing of heme, NO, oxygen, and short peptides; the selective elimination of misfolded proteins; the regulation of DNA repair (at least in part through the degradation of Mgt1, a DNA repair protein); the cohesion/segregation of chromosomes (through the degradation of a subunit of cohesin); the signaling by transmembrane receptors (through the degradation of the G-protein regulators Rgs4, Rgs5, and Rgs16); the control of peptide import (through the degradation of Cup9, the import's transcriptional repressor); the regulation of apoptosis, meiosis, viral and bacterial infections, fat metabolism, cell migration, actin filaments, cardiovascular development, spermatogenesis, neurogenesis, and memory; the functioning of adult organs, including the brain, muscle, testis, and pancreas; and the regulation of leaf and shoot development, leaf senescence, and seed germination in plants (*18, 29, 31, 33, 35, 38, 48-63*). Mutations in UBR1, an E3 *N*-recognin of the human Arg/N-end rule pathway, cause Johanson–Blizzard syndrome (JBS). It comprises, among other defects, physical malformations, insufficiency and inflammation of the exocrine pancreas, frequent mental retardation, and deafness (*52*). An *N*-recognin such as mammalian UBR2 can also function to protect specific proteins from degradation (*64*). The Ac/N-end rule pathway mediates, among other things,

protein quality control and the regulation of *in vivo* stoichiometry of proteins that form multisubunit complexes (*26*).

Regulation of G proteins and the N-end rule pathway

As mentioned in the preceding section, the functions of the mammalian Arg/N-end rule pathway include the sensing of NO and oxygen and the regulation of specific G proteins that are coupled to transmembrane receptors. These processes involve the NO/O_2-dependent degradation of Rgs4, Rgs5, and Rgs16, a set of G-protein regulators (*31, 33, 39*). The conditional Nt-arginylation and degradation of these RGS proteins by the Arg/N-end rule pathway alters the activity of cognate G-protein circuits (*31, 33*). Rgs4 is an inhibitor of tubulogenesis, a process that underlies the development and homeostasis of blood vessels and other tubular structures, such as those in the mammary gland, kidney and lung (*65*). Rgs4 and Rgs16 block signaling by the vascular endothelial growth factor (VEGF), and Rgs5 regulates vessel remodeling during neovascularization (*66*). Rgs4 is also known to be a negative modulator of the myocardial hypertrophic response (*67*). The rate of degradation of Rgs4, largely by the Arg/N-end rule pathway, influences other physiological and pathophysiological processes, including the invasiveness of breast cancer, responses of neurons to opiates, and responses of cells in culture to fluxes of calcium ions (*68, 69*).

The Cre recombinase-induced postnatal loss of the Ate1 R-transferase and Nt-arginylation in adult mice leads to a more than 10-fold increase in the level of the metabolically stabilized Rgs4 in the resulting Ate1-deficient mice, suggesting a major decrease in signaling by Rgs4-regulated G proteins (*70*). The loss of Nt-arginylation results in a number of phenotypic

alterations in Ate1-deficient mice. Studies described in this thesis explore, in particular, the physiology of Ate1 deficiency and the upregulation of Rgs4, Rgs5, and Rgs16 in Ate1-deficient mice.

In addition, the two branches of the N-end rule pathway, Ac/N-end rule and Arg/N-end rule pathways, were recently found to regulate Rgs2. This regulator of G proteins lowers blood pressure by decreasing signaling through Gαq. Human patients expressing Met-Leu-Rgs2 (ML-Rgs2) or Met-Arg-Rgs2 (MR-Rgs2) are hypertensive relative to people expressing wild-type Met-Gln-Rgs2 (MQ-Rgs2). Park and colleagues found that wild-type MQ-Rgs2 and its mutant, MR-Rgs2, were destroyed by the Ac/N-end rule pathway, which recognizes Nt-acetylated proteins (*24*). The shortest-lived mutant, ML-Rgs2, was targeted by both the Ac/N-end rule and Arg/N-end rule pathways. The latter pathway recognizes unacetylated N-terminal residues. Thus, the Nt-acetylated Ac-MX-Rgs2 (X = Arg, Gln, Leu) proteins are specific substrates of the mammalian Ac/N-end rule pathway. Furthermore, the Ac/N-degron of Ac-MQ-Rgs2 was conditional, and Teb4, an endoplasmic reticulum (ER) membrane-embedded ubiquitin ligase, was able to regulate G protein signaling by targeting Ac-MX-Rgs2 proteins for degradation through their N^{α}-terminal acetyl group.

The N-end rule pathway in bacteria

Although bacteria lack a bona fide Ub system, they contain a Ub-independent version of the N-end rule pathway, termed the Leu/N-end rule pathway. The Leu/N-end rule pathway was discovered in 1991 by the Varshavsky laboratory (*71*), and was characterized in gram-negative bacteria *Escherichia coli* and *Vibrio vulnificus (50, 72).* It comprises the following components.

(1) ClpAP, a proteasome-like, ATP-dependent protease;

(2) ClpS, the 12-kDa *N*-recognin of the Leu/N-end rule pathway that binds to N-terminal Leu, Phe, Trp or Tyr and delivers N-end rule substrates to the ClpAP protease (*50, 73-76*);

(3) Aat, an L/F-transferase that uses Leu-tRNA or Phe-tRNA as a cosubstrate to conjugate largely Leu (and occasionally Phe) to the N-termini of proteins bearing N-terminal Lys or Arg, the secondary destabilizing residues of the Leu/N-end rule pathway;

(4) Bpt, an L-transferase that uses Leu-tRNA to conjugate Leu to N-terminal Asp, Glu, and (possibly) oxidized Cys (*1*).

V. vulnificus contains both the Aat and Bpt L-transferases, while *E. coli* contains only Aat. Therefore N-terminal Arg, Lys, Asp and Glu are secondary destabilizing residues in *V. vulnificus*, whereas in *E. coli* the N-terminal Asp and Glu are stabilizing ("non-destabilizing") residues (*72*). In *V. vulnificus*, the two L-transferases are encoded by the *aat-bpt* operon, but in several other gram-negative bacteria these two genes are unlinked, and some gram-negatives lack one or the other of these L-transferases (for example, *E. coli* lacks Bpt) (*1*).

Two physiological substrates of the Leu/N-end rule pathway have been described so far, in addition to a more tentatively identified (potential) substrate (*76, 77*), One of these substrates is Dps, an 18-kDa DNA-binding protein that compacts the nucleoid of *E. coli* in starving cells, forming highly ordered, crystal-like structures. An unknown protease removes 5 residues from the initial N-terminus of Dps, generating N-terminal Leu and thereby making Dps a short-lived N-end rule substrate. The other identified N-end rule substrate is the *E. coli* YgjG putrescine-

aminotransferase (PATase). It is targeted for degradation by the Leu/N-end rule pathway through a (so far) unique route that requires Nt-leucylation, by the Aat L/F-transferase, of the (initial) N-terminal Met residue of PATase (*77*). The “non-cognate” specificity of L/F-transferase, in this setting, remains to be confirmed. One possibility is that the active site of the Aat L/F-transferase might be able to accommodate the N-terminal Met of a substrate for its conjugation to Leu if the substrate's second residue is, for example, Asn, a small hydrophilic residue (*1*).

Both gram-negative and gram-positive bacteria use the Nt-formylated Met residue (fMet) to initiate the synthesis of a polypeptide chain. The resulting N-terminal fMet of nascent bacterial proteins is cotranslationally deformylated by a ribosome-bound deformylase (*78*). In the next two chapters of this thesis, I will describe and discuss experimental data that support the hypothesis about fMet-based degradation signals, termed fMet/N-degrons.

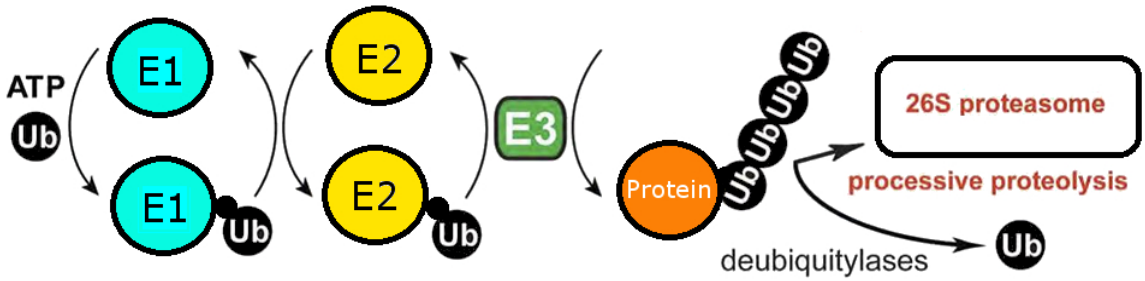

Figure 1.1. The ubiquitin-proteasome system. Ub-protein conjugation marks proteins for their recognition and degradation by the 26S proteasome, a processive, ATP-dependent protease. Ub is conjugated to proteins as a poly-Ub chain that is linked to the ε-amino group of an internal Lys residue in a substrate protein. Ub is activated for conjugation to other proteins by an Ub-activating enzyme (E1), which couples ATP hydrolysis to the formation of a high-energy thioester bond between Gly76 of Ub and a specific Cys residue of E1 (*6, 7*). The E1-linked Ub moiety is moved, in a transesterification reaction, from E1 to a Cys residue of an Ub-conjugating enzyme (E2), and from there to a Lys residue of an ultimate acceptor protein, yielding an Ub-protein conjugate. This last step requires the participation of another component, called E3 Ub ligase, which selects a protein for ubiquitylation through an interaction with its degradation signal.

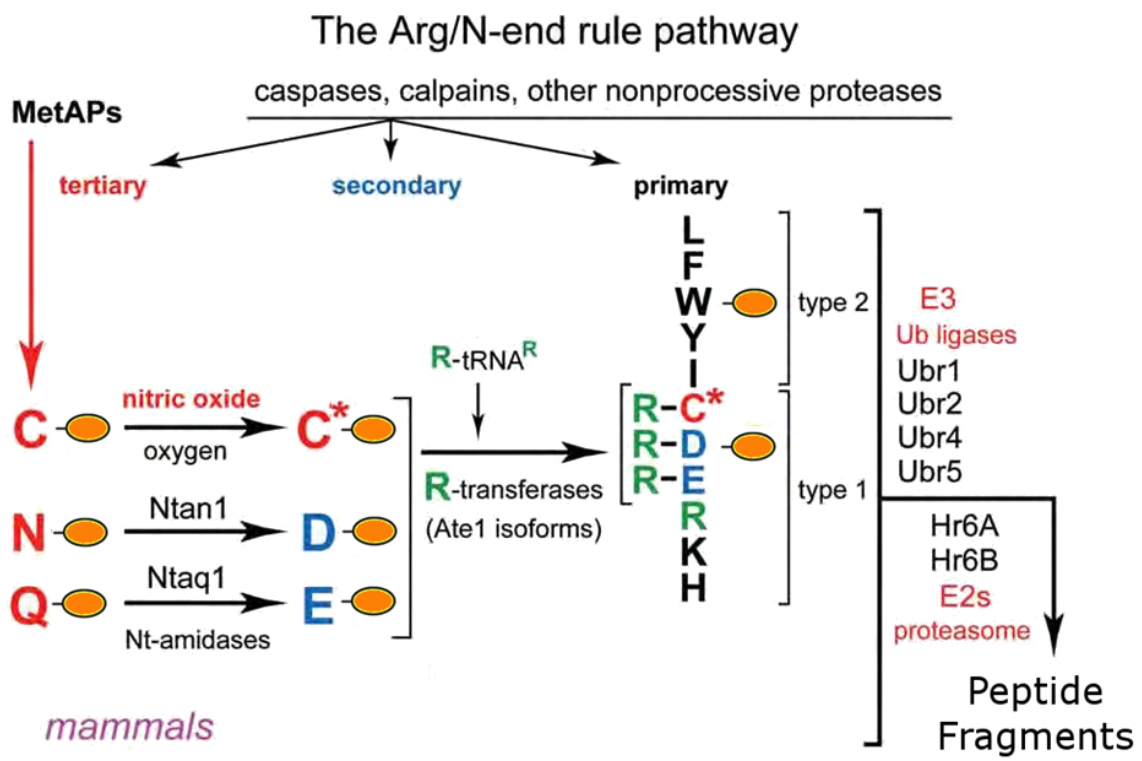

Figure 1.2. The Arg/N-end rule pathway in mammals. An *N*-degron can be produced through a cotranslational or posttranslational proteolytic cleavage by the methionine aminopeptidases (MetAPs), caspases, calpains, or other non-possessive proteases. N-terminal Arg, Lys, His, Leu, Phe, Tyr, Trp, Ile, Asp, Glu, Asn, Gln, and Cys comprise the main determinants of N-degrons. The unmodified Type-1 basic (Arg, Lys, His) and Type-2 bulky hydrophobic (Leu, Phe, Tyr, Trp, Ile) N-terminal residues are recognized directly by cognate E3 N-recognins Ubr1, Ubr2, Ubr4, and Ubr5. The N-terminal Asp, Glu, Asn, Gln, and Cys function as destabilizing residues through their preliminary modifications. Arg-tRNA-protein transferase (R-transferase) conjugates Arg to N-terminal Asp, Glu, or oxidized Cys of proteins or short peptides, with Arg-tRNA as the cosubstrate and the donor of Arg. The N-terminal Asn and Gln residues are converted by the N-terminal amidases to Asp and Glu. N-terminal Asp, Glu, Asn, Gln, and Cys that are targeted by the Arg/N-end rule pathway are termed "secondary" or "tertiary" destabilizing residues, depending on the number of specific steps that precede their targeting by *N*-recognins.

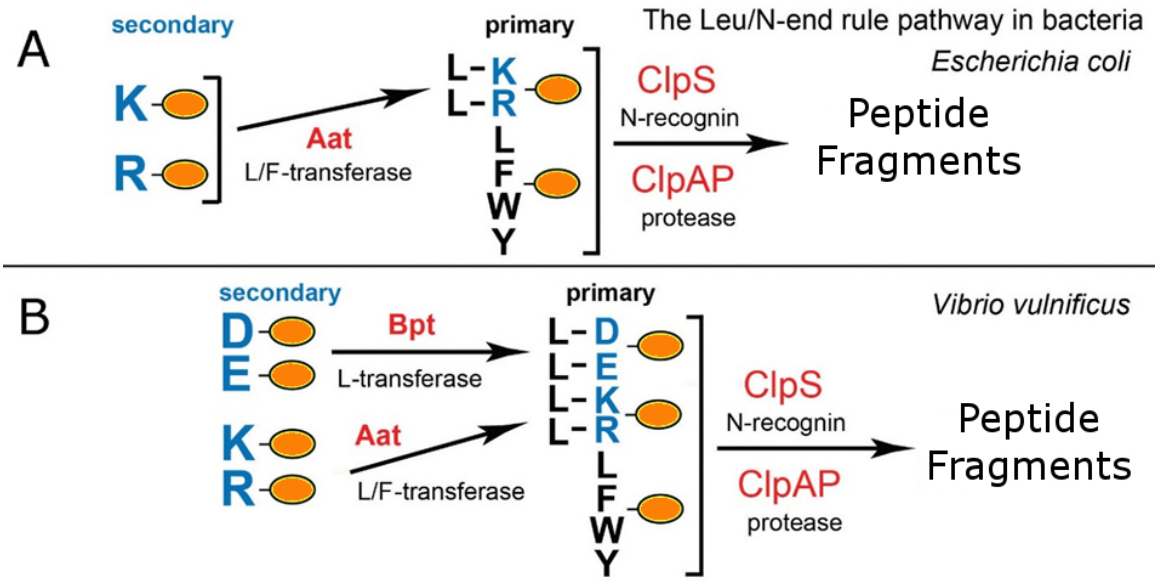

Figure 1.3 The bacterial Leu/N-end rule pathway. (A) In *Escherichia coli*, Aat, an L/F-transferase, uses Leu-tRNA or Phe-tRNA as a cosubstrate to conjugate largely Leu (and occasionally Phe) to the N-termini of proteins bearing N-terminal Lys or Arg, the secondary destabilizing residues of the Leu/N-end rule pathway. ClpS, the 12-kDa *N*-recognin of the Leu/N-end rule pathway that binds to N-terminal Leu, Phe, Trp or Tyr and delivers N-end rule substrates to the ClpAP protease. (B) In *V. vulnificus*, in addition to the machinery *E. coli* possesses, there is also Bpt, an L-transferase that uses Leu-tRNA to conjugate Leu to N-terminal Asp, Glu, and (possibly) oxidized Cys.

REFERENCES

1. A. Varshavsky, The N-end rule pathway and regulation by proteolysis. *Protein science : a publication of the Protein Society* **20**, 1298-1345 (2011).
2. G. C. Turner, A. Varshavsky, Detecting and measuring cotranslational protein degradation *in vivo*. *Science* **289**, 2117-2120 (2000).
3. A. Varshavsky, The Ubiquitin System, an Immense Realm. *Annual Review of Biochemistry* **81**, 167-176 (2012).
4. A. Varshavsky, Naming a targeting signal. *Cell* **64**, 13-15 (1991).
5. A. Varshavsky, The ubiquitin system. *Trends in Biochemical Sciences* **22**, 383-387 (1997).
6. A. Hershko, Lessons from the discovery of the ubiquitin system. *Trends in Biochemical Sciences* **21**, 445-449 (1996).
7. M. Hochstrasser, Ubiquitin-dependent protein degradation. *Annual review of genetics* **30**, 405-439 (1996).
8. A. Varshavsky, The N-end rule: functions, mysteries, uses. *Proceedings of the National Academy of Sciences of the United States of America* **93**, 12142-12149 (1996).
9. V. Chau *et al.*, A multiubiquitin chain is confined to specific lysine in a targeted short-lived protein. *Science (New York, N.Y.)* **243**, 1576-1583 (1989).
10. R. Beal, Q. Deveraux, G. Xia, M. Rechsteiner, C. Pickart, Surface hydrophobic residues of multiubiquitin chains essential for proteolytic targeting. *Proceedings of the National Academy of Sciences* **93**, 861-866 (1996).
11. J. Spence, S. Sadis, A. L. Haas, D. Finley, A ubiquitin mutant with specific defects in DNA repair and multiubiquitination. *Molecular and Cellular Biology* **15**, 1265-1273 (1995).
12. E. Johnson, P. Ma, I. Ota, A. Varshavsky, A Proteolytic Pathway That Recognizes Ubiquitin as a Degradation Signal. *Journal of Biological Chemistry* **270**, 17442-17456 (1995).
13. K. Wilkinson *et al.*, Metabolism of the polyubiquitin degradation signal: structure, mechanism, and role of isopeptidase T. *Biochemistry* **34**, 14535-14546 (1995).

14. R. T. Baker, J. W. Tobias, A. Varshavsky, Ubiquitin-specific proteases of Saccharomyces cerevisiae. Cloning of UBP2 and UBP3, and functional analysis of the UBP gene family. *The Journal of biological chemistry* **267**, 23364-23375 (1992).
15. D. Finley, B. Bartel, A. Varshavsky, The tails of ubiquitin precursors are ribosomal proteins whose fusion to ubiquitin facilitates ribosome biogenesis. *Nature* **338**, 394-401 (1989).
16. C. M. Pickart, I. A. Rose, Ubiquitin carboxyl-terminal hydrolase acts on ubiquitin carboxyl-terminal amides. *Journal of Biological Chemistry* **260**, 7903-7910 (1985).
17. A. Varshavsky, The early history of the ubiquitin field. *Protein Science* **15**, 647-654 (2006).
18. C.-S. Hwang, A. Shemorry, A. Varshavsky, N-terminal acetylation of cellular proteins creates specific degradation signals. *Science (New York, N.Y.)* **327**, 973-977 (2010).
19. T. Arnesen *et al.*, Proteomics analyses reveal the evolutionary conservation and divergence of N-terminal acetyltransferases from yeast and humans. *Proceedings of the National Academy of Sciences of the United States of America* **106**, 8157-8162 (2009).
20. B. Polevoda, S. Brown, T. Cardillo, S. Rigby, F. Sherman, Yeast N(alpha)-terminal acetyltransferases are associated with ribosomes. *Journal of cellular biochemistry* **103**, 492-508 (2008).
21. S. Goetze *et al.*, Identification and functional characterization of N-terminally acetylated proteins in Drosophila melanogaster. *PLoS biology* **7**, e1000236 (2009).
22. F. Frottin *et al.*, The Proteomics of N-terminal Methionine Cleavage. *Molecular & Cellular Proteomics* **5**, 2336-2349 (2006).
23. A. Addlagatta, X. Hu, J. Liu, B. Matthews, Structural basis for the functional differences between type I and type II human methionine aminopeptidases. *Biochemistry* **44**, 14741-14749 (2005).
24. S.-E. Park *et al.*, Control of mammalian G protein signaling by N-terminal acetylation and the N-end rule pathway. *Science (New York, N.Y.)* **347**, 1249-1252 (2015).
25. H.-K. Kim *et al.*, The N-terminal methionine of cellular proteins as a degradation signal. *Cell* **156**, 158-169 (2014).

26. A. Shemorry, C.-S. Hwang, A. Varshavsky, Control of protein quality and stoichiometries by N-terminal acetylation and the N-end rule pathway. *Molecular cell* **50**, 540-551 (2013).
27. A. Varshavsky, 'Spalog' and 'sequelog': neutral terms for spatial and sequence similarity. *Current biology : CB* **14**, (2004).
28. S. Sriram, Y. T. Kwon, The molecular principles of N-end rule recognition. *Nature structural & molecular biology* **17**, 1164-1165 (2010).
29. A. Varshavsky, Discovery of Cellular Regulation by Protein Degradation. *Journal of Biological Chemistry* **283**, 34469-34489 (2008).
30. T. Tasaki *et al.*, The substrate recognition domains of the N-end rule pathway. *The Journal of biological chemistry* **284**, 1884-1895 (2009).
31. R.-G. Hu *et al.*, The N-end rule pathway as a nitric oxide sensor controlling the levels of multiple regulators. *Nature* **437**, 981-986 (2005).
32. R.-G. Hu *et al.*, Arginyltransferase, Its Specificity, Putative Substrates, Bidirectional Promoter, and Splicing-derived Isoforms. *Journal of Biological Chemistry* **281**, 32559-32573 (2006).
33. R.-G. Hu, H. Wang, Z. Xia, A. Varshavsky, The N-end rule pathway is a sensor of heme. *Proceedings of the National Academy of Sciences* **105**, 76-81 (2008).
34. R. T. Baker, A. Varshavsky, Yeast N-terminal amidase. A new enzyme and component of the N-end rule pathway. *The Journal of biological chemistry* **270**, 12065-12074 (1995).
35. Y. T. Kwon *et al.*, Altered activity, social behavior, and spatial memory in mice lacking the NTAN1p amidase and the asparagine branch of the N-end rule pathway. *Molecular and cellular biology* **20**, 4135-4148 (2000).
36. H. Wang, K. Piatkov, C. Brower, A. Varshavsky, Glutamine-specific N-terminal amidase, a component of the N-end rule pathway. *Molecular cell* **34**, 686-695 (2009).
37. S. Grigoryev *et al.*, A Mouse Amidase Specific for N-terminal Asparagine. *Journal of Biological Chemistry* **271**, 28521-28532 (1996).
38. T. Tasaki, Y. Kwon, The mammalian N-end rule pathway: new insights into its components and physiological roles. *Trends in Biochemical Sciences* **32**, 520-528 (2007).

39. M. J. Lee *et al.*, RGS4 and RGS5 are *in vivo* substrates of the N-end rule pathway. *Proceedings of the National Academy of Sciences of the United States of America* **102**, 15030-15035 (2005).

40. U. Fischer, R. U. Janicke, K. Schulze-Osthoff, Many cuts to ruin: a comprehensive update of caspase substrates. *Cell Death & Differentiation* **10**, 76-100 (2003).

41. C. Pop, G. Salvesen, Human caspases: activation, specificity, and regulation. *The Journal of biological chemistry* **284**, 21777-21781 (2009).

42. S. Storr, N. Carragher, M. Frame, T. Parr, S. Martin, The calpain system and cancer. *Nature reviews. Cancer* **11**, 364-374 (2011).

43. F. Uhlmann, The mechanism of sister chromatid cohesion. *Experimental cell research* **296**, 80-85 (2004).

44. J. J. D. Hsieh, E. H. Y. Cheng, S. Korsmeyer, Taspase1: a threonine aspartase required for cleavage of MLL and proper HOX gene expression. *Cell* **115**, 293-303 (2003).

45. S. Hailfinger *et al.*, Essential role of MALT1 protease activity in activated B cell-like diffuse large B-cell lymphoma. *Proceedings of the National Academy of Sciences of the United States of America* **106**, 19946-19951 (2009).

46. P. Marambaud *et al.*, A presenilin-1/gamma-secretase cleavage releases the E-cadherin intracellular domain and regulates disassembly of adherens junctions. *The EMBO journal* **21**, 1948-1956 (2002).

47. V. Witko-Sarsat *et al.*, Cleavage of p21waf1 by proteinase-3, a myeloid-specific serine protease, potentiates cell proliferation. *The Journal of biological chemistry* **277**, 47338-47347 (2002).

48. R. J. de Groot, T. Rümenapf, R. J. Kuhn, E. G. Strauss, J. H. Strauss, Sindbis virus RNA polymerase is degraded by the N-end rule pathway. *Proceedings of the National Academy of Sciences of the United States of America* **88**, 8967-8971 (1991).

49. L. C. Mulder, M. A. Muesing, Degradation of HIV-1 integrase by the N-end rule pathway. *The Journal of biological chemistry* **275**, 29749-29753 (2000).

50. A. Mogk, R. Schmidt, B. Bukau, The N-end rule pathway for regulated proteolysis: prokaryotic and eukaryotic strategies. *Trends in cell biology* **17**, 165-172 (2007).

51. E. Graciet, F. Wellmer, The plant N-end rule pathway: structure and functions. *Trends in plant science* **15**, 447-453 (2010).
52. M. Zenker *et al.*, Deficiency of UBR1, a ubiquitin ligase of the N-end rule pathway, causes pancreatic dysfunction, malformations and mental retardation (Johanson-Blizzard syndrome). *Nature genetics* **37**, 1345-1350 (2005).
53. C.-S. Hwang, A. Shemorry, A. Varshavsky, Two proteolytic pathways regulate DNA repair by cotargeting the Mgt1 alkylguanine transferase. *Proceedings of the National Academy of Sciences of the United States of America* **106**, 2142-2147 (2009).
54. C.-S. Hwang, A. Varshavsky, Regulation of peptide import through phosphorylation of Ubr1, the ubiquitin ligase of the N-end rule pathway. *Proceedings of the National Academy of Sciences* **105**, 19188-19193 (2008).
55. E. Graciet *et al.*, The N-end rule pathway controls multiple functions during Arabidopsis shoot and leaf development. *Proceedings of the National Academy of Sciences of the United States of America* **106**, 13618-13623 (2009).
56. M. Carpio, C. López Sambrooks, E. Durand, M. Hallak, The arginylation-dependent association of calreticulin with stress granules is regulated by calcium. *The Biochemical journal* **429**, 63-72 (2010).
57. S. H. Lecker *et al.*, Ubiquitin conjugation by the N-end rule pathway and mRNAs for its components increase in muscles of diabetic rats. *The Journal of clinical investigation* **104**, 1411-1420 (1999).
58. F. Zhang, S. Saha, S. Shabalina, A. Kashina, Differential Arginylation of Actin Isoforms Is Regulated by Coding Sequence–Dependent Degradation. *Science* **329**, 1534-1537 (2010).
59. S. Kurosaka *et al.*, Arginylation-dependent neural crest cell migration is essential for mouse development. *PLoS genetics* **6**, (2010).
60. P. Schnupf, J. Zhou, A. Varshavsky, D. Portnoy, Listeriolysin O secreted by Listeria monocytogenes into the host cell cytosol is degraded by the N-end rule pathway. *Infection and immunity* **75**, 5135-5147 (2007).
61. Y. Ouyang *et al.*, Loss of Ubr2, an E3 ubiquitin ligase, leads to chromosome fragility and impaired homologous recombinational repair. *Mutation research* **596**, 64-75 (2006).

62. N. Nillegoda *et al.*, Ubr1 and Ubr2 Function in a Quality Control Pathway for Degradation of Unfolded Cytosolic Proteins. *Molecular biology of the cell* **21**, 2102-2116 (2010).

63. J. Heck, S. Cheung, R. Hampton, Cytoplasmic protein quality control degradation mediated by parallel actions of the E3 ubiquitin ligases Ubr1 and San1. *Proceedings of the National Academy of Sciences of the United States of America* **107**, 1106-1111 (2010).

64. F. Yang *et al.*, The ubiquitin ligase Ubr2, a recognition E3 component of the N-end rule pathway, stabilizes Tex19.1 during spermatogenesis. *PloS one* **5**, (2010).

65. A. Albig, W. Schiemann, Identification and characterization of regulator of G protein signaling 4 (RGS4) as a novel inhibitor of tubulogenesis: RGS4 inhibits mitogen-activated protein kinases and vascular endothelial growth factor signaling. *Molecular biology of the cell* **16**, 609-625 (2005).

66. M. Berger, G. Bergers, B. Arnold, G. Hämmerling, R. Ganss, Regulator of G-protein signaling-5 induction in pericytes coincides with active vessel remodeling during neovascularization. *Blood* **105**, 1094-1101 (2005).

67. D. Tirziu *et al.*, Myocardial hypertrophy in the absence of external stimuli is induced by angiogenesis in mice. *The Journal of clinical investigation* **117**, 3188-3197 (2007).

68. Y. Xie *et al.*, Breast cancer migration and invasion depend on proteasome degradation of regulator of G-protein signaling 4. *Cancer research* **69**, 5743-5751 (2009).

69. B. Sjögren, R. Neubig, Thinking Outside of the "RGS Box": New Approaches to Therapeutic Targeting of Regulators of G Protein Signaling. *Molecular Pharmacology* **78**, 550-557 (2010).

70. C. Brower, A. Varshavsky, Ablation of Arginylation in the Mouse N-End Rule Pathway: Loss of Fat, Higher Metabolic Rate, Damaged Spermatogenesis, and Neurological Perturbations. *PLoS ONE* **4**, e7757 (2009).

71. J. W. Tobias, T. E. Shrader, G. Rocap, A. Varshavsky, The N-end rule in bacteria. *Science (New York, N.Y.)* **254**, 1374-1377 (1991).

72. E. Graciet *et al.*, Aminoacyl-transferases and the N-end rule pathway of prokaryotic/eukaryotic specificity in a human pathogen. *Proceedings of the National Academy of Sciences of the United States of America* **103**, 3078-3083 (2006).

73. A. Erbse *et al.*, ClpS is an essential component of the N-end rule pathway in Escherichia coli. *Nature* **439**, 753-756 (2006).

74. J. Hou, R. Sauer, T. Baker, Distinct structural elements of the adaptor ClpS are required for regulating degradation by ClpAP. *Nature structural & molecular biology* **15**, 288-294 (2008).

75. G. M. De Donatis, S. Singh, S. Viswanathan, M. Maurizi, A single ClpS monomer is sufficient to direct the activity of the ClpA hexamer. *The Journal of biological chemistry* **285**, 8771-8781 (2010).

76. R. Schmidt, R. Zahn, B. Bukau, A. Mogk, ClpS is the recognition component for *Escherichia coli* substrates of the N-end rule degradation pathway. *Molecular Microbiology* **72**, 506-517 (2009).

77. R. Ninnis, S. Spall, G. Talbo, K. Truscott, D. Dougan, Modification of PATase by L/F-transferase generates a ClpS-dependent N-end rule substrate in *Escherichia coli*. *The EMBO journal* **28**, 1732-1744 (2009).

78. R. Bingel-Erlenmeyer *et al.*, A peptide deformylase|[ndash]|ribosome complex reveals mechanism of nascent chain processing. *Nature* **452**, 108-111 (2008).

CHAPTER 2:
FORMYL-METHIONINE AS A DEGRADATION SIGNAL AT THE N-TERMINI OF BACTERIAL PROTEINS

Abstract

In bacteria, all nascent proteins bear the pretranslationally formed N-terminal formyl-methionine (fMet) residue. The fMet residue is cotranslationally deformylated by a ribosome-associated deformylase. The formylation of N-terminal Met in bacterial proteins is not essential for either translation or cell viability. Moreover, protein synthesis by the cytosolic ribosomes of eukaryotes does not involve the formylation of N-terminal Met. What, then, is the main biological function of this metabolically costly, transient, and not strictly essential modification of N-terminal Met, and why has Met formylation not been eliminated during bacterial evolution? One possibility is that the similarity of the formyl and acetyl groups, their identical locations in N-terminally formylated (Nt-formylated) and Nt-acetylated proteins, and the recently discovered proteolytic function of Nt-acetylation in eukaryotes might also signify a proteolytic role of Nt-formylation in bacteria. We addressed this hypothesis about fMet-based degradation signals, termed fMet/N-degrons, using specific *E. coli* mutants, pulse-chase degradation assays, and protein reporters whose deformylation was altered, through site-directed mutagenesis, to be either rapid or relatively slow. Our findings strongly suggest that the formylated N-terminal fMet can act as a degradation signal, largely a cotranslational one. One likely function of fMet/N-degrons is the control of protein quality. In bacteria, the rate of polypeptide chain elongation is nearly an order of magnitude higher than in eukaryotes. We suggest that the faster emergence of nascent proteins from bacterial ribosomes is one mechanistic and evolutionary reason for the pretranslational design of bacterial fMet/N-degrons, in contrast to the cotranslational design of analogous Ac/N-degrons in eukaryotes.

Introduction

Nascent polypeptides bear the N-terminal Met residue, encoded by the AUG initiation codon. In bacteria and in eukaryotic organelles mitochondria and chloroplasts (remote descendants of bacteria), this Met is N^{α}-terminally formylated (Nt-formylated) through a "pretranslational" mechanism. Formyltransferase (FMT) uses 10-formyltetrahydrofolate to formylate the α-amino group of the Met moiety in the initiator Met-$tRNA_i^{Met}$ [1-8]. The resulting formyl-Met (fMet) becomes the first residue of a nascent polypeptide that emerges from a bacterial ribosome (Fig. 1A) [9-13]. The formyl moiety of N-terminal fMet is cotranslationally removed by peptide deformylase (PDF), which is reversibly bound to the ribosome near the exit from the ribosomal tunnel (Fig. 1B) [4, 14-27]. A ribosome-associated chaperone called trigger factor (TF) interacts with proteins emerging from the tunnel [28-42]. The signal recognition particle (SRP) also binds to some nascent proteins, recognizing specific sequence motifs (signal sequences) and directing SRP-associated proteins for translocation through the inner membrane [42-45].

Once N-terminal fMet of a nascent protein is deformylated by PDF, the resulting Met can be cleaved off by Met-aminopeptidase (MetAP) (Fig. 1B). The removal of (deformylated) Met by MetAP requires that a residue at position 2, to be made N-terminal by the cleavage, is not larger than Val [26, 46-48]. The *Escherichia coli* PDF deformylase binds to the 50S ribosomal subunit in part through contacts with the L22 ribosomal protein [23, 26]. PDF and MetAP act sequentially in their cotranslational

processing of nascent proteins and compete with each other for interactions with their overlapping binding sites on the ribosome near the tunnel's exit [26].

High-affinity interactions of the TF chaperone with a nascent protein begin to take place after the first ~100 residues of the protein have been synthesized [28]. Deformylation of N-terminal fMet by PDF (Fig. 1B) is impeded in cells engineered to overproduce TF [28]. Consequently, it is likely that in wild-type cells, by the time a nascent protein becomes larger than ~100 residues, i.e., shortly before the binding of TF to this protein [28], its N-terminal fMet had already been, in most cases, deformylated by the ribosome-associated PDF. The rate of chain elongation by bacterial ribosomes *in vivo* at 37°C is 10-20 residues/sec [49-52]. Thus, the *in vivo* lifespan of the formyl group, from the moment fMet becomes the first residue of a newly initiated protein to the moment of fMet deformylation, is usually less than a minute. Given the delay in high-affinity binding of TF to a nascent protein [28], its first ~100 residues, which require 5-10 sec to be made, may be unassociated, during a fraction of those 5-10 sec, with any chaperone.

Although the fMet moiety of bacterial fMet-$tRNA_i^{Met}$ interacts with the initiation factor IF2 and thereby contributes to the efficacy of translation initiation [5, 7, 53-55], the formylation of N-terminal Met is not strictly essential for protein synthesis and cell viability. For example, *E. coli fmt* mutants lacking formyltransferase are viable. Their abnormal phenotypes include slow growth and hypersensitivity to stresses [3, 4, 7]. In *Salmonella enterica*, the slow growth of *fmt* mutants can be alleviated, during serial passaging, through the emergence of mutants that overexpress the initiator $tRNA_i^{Met}$ [56]. In *Pseudomonas aeruginosa*, an engineered overexpression of IF2 can alleviate slow

growth of *fmt* mutants in minimal media [57]. Moreover, in *P. aeroginosa* and some other bacteria (other than *E. coli*), the ablation of *fmt* results in cells whose growth rates in rich media are nearly identical to those of wild-type cells [57, 58].

In contrast, deformylation of the bulk of N-terminal fMet in nascent proteins is required for cell viability. Either a strong inhibition of PDF by the antibiotic actinonin or ablation of the PDF-encoding *def* gene are lethal, because MetAP is unable to cleave off the formyl-bearing N-terminal fMet [46]. (The inability to remove N-terminal Met leads to cell death in part because specific non-Met residues, e.g., Thr, must become N-terminal in some essential enzymes, in which these non-Met residues are parts of enzymes' active sites [59].) However, double *fmt def* mutants, which lack both FMT and PDF and therefore can neither deformylate fMet nor formylate it in the first place, are viable, with phenotypes similar to those of single *fmt* mutants [23].

In eukaryotes, protein synthesis by the cytosolic ribosomes does not involve the formylation of Met, indicating that it was feasible, during evolution, to either lose the formylation of Met or not to acquire it in the first place. (It is unknown whether formylation of Met was a part of translation in the last common ancestor of extant organisms.) Innate immune responses involve the recognition of Nt-formylated bacterial proteins and short peptides. They are present in infected animals at high enough levels to act as chemoattractants for macrophages and neutrophils [60, 61]. Consequently, the formylation of Met can be a detriment to bacterial fitness.

Given these properties of fMet, why do all examined wild-type bacteria contain formyltransferase, deformylase, and use fMet, rather than Met, to initiate translation? Why has this pervasive, metabolically costly, transient, and not strictly essential

modification of N-terminal Met not been eliminated during bacterial evolution? This conundrum suggested to us that the main biological function of fMet, the one that underlies the universal presence of N-terminal fMet in extant wild-type bacteria, remained to be discovered.

Previous work identified the N-terminus of an intracellular protein as the site of degradation signals (degrons [62]) that are targeted by the N-end rule pathway (Fig. S1). This pathway is a set of proteolytic systems whose unifying feature is their ability to recognize proteins containing N-terminal degradation signals called N-degrons and to cause the processive degradation of such proteins by the 26S proteasome in eukaryotes (Fig. S1A, B) [63-74] or by the proteasome-like protease ClpAP in bacteria (Fig. S1C, D) [75-80]. In eukaryotes, N-degrons can also mediate the degradation of specific proteins (and their noncovalently bound protein ligands) by autophagy, as distinguished from the proteasome [74]. The main determinant of an N-degron is either an unmodified or chemically modified "destabilizing" N-terminal residue of a protein. Recognition components of the N-end rule pathway are called N-recognins. In eukaryotes, N-recognins are specific E3 ubiquitin (Ub) ligases that recognize N-degrons and polyubiquitylate proteins bearing them [71-73]. Bacteria lack the bona fide Ub system. The bacterial N-end rule pathway employs the ClpS N-recognin (but no ubiquitylation) to deliver targeted N-end rule substrates to the ClpAP protease (Fig. S1C, D) [75, 76, 79-93].

In eukaryotes, the N-end rule pathway consists of two branches. One of these branches, called the Arg/N-end rule pathway, targets proteins bearing N-terminal Arg, Lys, His, Leu, Phe, Tyr, Trp, Ile, Asn, Gln, Asp, Glu, and Cys (Fig. 1B) [63, 65, 71-73, 94-97]. This pathway can also target unmodified N-terminal Met, if Met is followed by a bulky

hydrophobic residue (Fig. S1A). Among these N-terminal residues, Asn, Gln, Asp, Glu, and Cys are destabilizing owing to their preliminary enzymatic modifications, which include N-terminal deamidation (Nt-deamidation) of Asn and Gln and Nt-arginylation of Asp, Glu and Cys (the latter after its conditional oxidation) [66, 96, 98, 99]. The substrate specificity of the bacterial N-end rule pathway is similar to the targeting range of the Arg/N-end rule pathway but is not as broad (Fig. S1C, D) [71, 77, 78].

The other branch of the eukaryotic N-end rule pathway is called the Ac/N-end rule pathway. It recognizes proteins through their N^{α}-terminally acetylated (Nt-acetylated) residues (Fig. S1B) [67-70]. The degrons and N-recognins of the Ac/N-end rule pathway are called Ac/N-degrons and Ac/N-recognins, respectively. Nt-acetylation of eukaryotic proteins is largely cotranslational, being mediated by ribosome-associated Nt-acetylases [100-102]. At least 60% and about 90% of proteins are Nt-acetylated in the yeast *S. cerevisiae* and in human cells, respectively [103-106]. Nt-acetylation is apparently irreversible, i.e., a protein molecule acquires the N^{α}-acetyl group largely at birth and retains this group for the rest of that molecule's lifetime in a cell. While Nt-acetylation also takes place in bacteria, it involves less than 10% of bacterial proteins and can occur only after the PDF-mediated deformylation of N-terminal fMet [107, 108]. Nothing is known about whether or not a version of the Ac/N-end rule pathway exists in bacteria as well.

The acetyl and formyl groups differ by the CH_3 moiety vs. the hydrogen atom. It occurred to us that the similarity of acetyl and formyl, their identical locations in Nt-acetylated and Nt-formylated proteins, and the recently discovered proteolytic function of Nt-acetylation in eukaryotes [67-71] might also signify the proteolytic role of Nt-formylation in bacteria, despite the transiency of the formyl group in fMet of nascent

bacterial proteins. We proposed this hypothesis in 2010 [67] and carried out experiments to verify it in the present study.

The evidence below (Figs. 2-4) strongly suggests that N-terminal fMet can act as an N-degron, termed fMet/N-degron. In bacteria, the rate of polypeptide chain elongation is nearly an order of magnitude higher than in eukaryotes. We suggest that the faster emergence of nascent proteins from bacterial ribosomes may be the mechanistic and evolutionary reason for the pretranslational design of bacterial fMet/N-degrons (Fig. 1A), in contrast to the cotranslational design of Ac/N-degrons in eukaryotes (Fig. S1B). By analogy with Ac/N-degrons [67-71], one function of bacterial fMet/N-degrons is likely to be the quality control of both nascent proteins and just released, newly formed proteins. Specifically, fMet/N-degrons are envisioned to augment the quality of bacterial proteome through a preferential and largely cotranslational degradation of Nt-formylated misfolded proteins. This would happen at the price of eliminating a subset of normal proteins as well, given the stochasticity of both the PDF-mediated deformylation of fMet and the alternative, competing process of targeting and destroying Nt-formylated proteins through their fMet/N-degrons.

Results

Inhibition of fMet deformylation decreases the levels of larger pulse-labeled proteins

Wild-type *E. coli* were pulse-labeled for 1 min at 37°C with ^{35}S-methionine/cysteine in (Fig. 2A). The pulse was followed by a chase (in the presence of translation inhibitor chloramphenicol), preparation of cell extracts, SDS-PAGE, and autoradiography. Actinonin, a specific inhibitor of PDF, was either absent or present, at

indicated concentrations, throughout pulse chases. The inhibition of fMet deformylation by actinonin was found to cause a significant decrease in the levels of larger (more than ~35 kDa) ^{35}S-labeled proteins and a concomitant increase of smaller (less than ~20 kDa) proteins (Fig. 2A).

Additional ^{35}S-pulse-chases (this time in the absence of chloramphenicol) with wild-type vs. formyltransferase-lacking *fmt E. coli* showed that the above effect of actinonin required the formylation of N-terminal Met, because ^{35}S-protein patterns in *fmt* cells were essentially the same in the presence or absence of actinonin (Fig. 2B). These results (Fig. 2) were consistent with the fMet/N-degron hypothesis (Fig. 1C-E), as it predicts that the probability of destruction of an fMet-bearing nascent protein would be higher, on average, for a larger protein, because its polypeptide chain, i.e., its ribosome-associated peptidyl-tRNA, would dwell in the vicinity of a translating ribosome for a longer time than would be the case for a smaller fMet-bearing nascent protein. The postulated fMet/N-recognin/protease (Fig. 1E) or at least its fMet/N-recognin part is envisioned to be reversibly associated with the ribosomes (see Discussion). Thus, the probability of capture of larger Nt-formylated proteins by this protease would be higher than the corresponding probability for smaller fMet-bearing nascent proteins, because the latter would be released sooner and diffuse into the bulk solvent, i.e., into regions with (presumably) lower levels of the fMet/N-recognin/protease.

An alternative interpretation of these results is that actinonin might increase the probability of premature chain termination. This increase would lead to a lower relative abundance of larger (as compared to smaller) pulse-labeled proteins in the presence of actinonin, thereby accounting for our results (Fig. 2) without invoking a preferential

degradation of these proteins. However, this interpretation was made unlikely by the fact that the observed effect of actinonin required the formylated state of N-terminal Met, i.e. this effect of actinonin was not observed with *fmt* cells, in contrast to wild-type cells (Fig. 2B).

Higher levels of a protein reporter in formylation-lacking mutants

One prediction of the fMet/N-degron hypothesis is as follows: even in the case of a nascent protein whose N-terminal amino acid sequence makes it an efficacious PDF substrate, some molecules of this protein would still be expected to be destroyed through the protein's fMet/N-degron, given the stochasticity of deformylation of N-terminal fMet by PDF and the alternative, competing process of targeting an fMet-bearing protein for degradation (Fig. 1C-E). Consequently, the ribosome-associated PDF deformylase would be expected to occasionally lose the competition for N-terminal fMet to a postulated fMet/N-recognin/protease, resulting in the degradation of a targeted nascent protein. The kinetic advantage of PDF may be decreased if a nascent N-terminal segment of a protein would be either unfolded (with N-terminal fMet partly obscured within a "molten globule") or misfolded in a way that decreases the time-averaged solvent exposure of N-terminal fMet (Fig. 1C-E and Discussion). If so, the steady-state level of such a protein would be expected to increase in formyltransferase-lacking *fmt* mutants.

We addressed this prediction through a reporter bearing the N-terminal sequence of a protein called D2. Earlier studies of D2 protein in plant chloroplasts, by Giglione, Meinnel and colleagues [109, 110], were relevant to experiments of the present study. Although our 2010 hypothesis about fMet as a degradation signal [67] was cited by

Giglione and colleagues [110], they did not interpret their findings with D2 protein in terms of fMet/N-degrons. In contrast, the results below, using the N-terminal segment of D2 as a part of protein reporters (Figs. 3 and 4), strongly suggest that the data by Giglione et al. [109, 110] can be interpreted, in hindsight, as a likely example of protein degradation mediated by fMet/N-degrons.

Our 37-kDa reporter, termed $P1^{T2}$ ("protein-1 containing Thr at position 2"), comprised the 11-residue N-terminal sequence MTIAIGTYQEK of the wild-type D2 protein ($D2^{1-11}$), followed by the sequence GSGAWLLPVSLVKRKTTLAPNTQTASPRALADSLMQLARQVSRG (a 45-residue segment derived from the previously used e^K sequence [extension (e) containing lysine (K)] [67, 71, 111]), by the 9-residue ha epitope tag (YPYDVPDYA), by the AFLGQ linker [67], and by the 267-residue Ura3 protein of the yeast *Saccharomyces cerevisiae* (Fig. 3A). The Ura3 moiety is a frequently employed component of protein reporters [67, 69]. The e^K segment is another sequence often used in reporters, in part because e^K is conformationally disordered while lacking degrons in both *E. coli* and *S. cerevisiae* [67, 71, 111].

$P1^{T2}$ was expressed from the constitutive P_{KmR} promoter in wild-type, null *fmt*, and null *fmt def E.coli* strains, followed by extraction of proteins, SDS-PAGE, and immunoblotting with anti-ha antibody (Fig. 3A, D). Extracts were adjusted for equal total loads using Bradford assay [112] and Coomassie staining of proteins fractionated by SDS-PAGE (Fig. 3D). The levels of the $P1^{T2}$ reporter in both *fmt* and *fmt def* cells were strikingly higher than in congenic wild-type cells, in agreement with the above prediction of the fMet/N-degron hypothesis (Fig. 3A, D).

The ~70-residue N-terminal segment ($D2^{1\text{-}11}$-e^{K}-ha) of the 37 kDa $P1^{T2}$ reporter is a biologically irrelevant mix of different sequences (Fig. 3A). A nascent protein exemplified by $P1^{T2}$, with its disordered N-terminal region, may be less amenable to the PDF-mediated deformylation and would be, therefore, a relatively favored target for the capture and degradation by the postulated fMet/N-recognin/protease in fMet-containing wild-type cells (see Discussion for a more detailed exposition). Conversely, one would expect that an up-regulation of such a reporter in formyltransferase-lacking cells may be particularly high, in agreement with the observed increase of $P1^{T2}$ in *fmt* and *fmt def E. coli* (Fig. 3A, D).

Bypass of Met formylation can equalize the levels of efficacious and poor substrates of deformylase

When the D2 protein, encoded by chloroplast DNA, is expressed in chloroplasts, it bears the formylated N-terminal fMet, similarly to nascent bacterial proteins. The fMet of D2 is deformylated by two functionally overlapping PDFs in chloroplasts [21]. The Thr residue at position 2 of the D2 protein (denoted as $D2^{T2}$) becomes its N-terminal residue once MetAP cleaves off the (previously deformylated) N-terminal Met (Fig. 1B). The N-terminal sequence fMet-Thr (fMT) of a nascent $D2^{T2}$ protein is a favorable sequence context for the PDF-mediated deformylation of fMet, as had been shown, in particular, in a detailed study of substrate preferences of *E. coli* PDF for amino acid residues downstream from fMet [17].

When Giglione and colleagues [109, 110] carried out pulse-chases to monitor the degradation of the wild-type $D2^{T2}$ protein in chloroplasts, they found this protein to be

relatively long-lived under normal conditions. However, $D2^{T2}$ became short-lived in the presence of actinonin, which inhibited the PDF-mediated deformylation of nascent $D2^{T2}$. To address the reason for this effect, Giglione et al. [109, 110] mutated Thr at position 2 of $D2^{T2}$ to either Asp (D) or Glu (E). The resulting mutant proteins $D2^{T2D}$ and $D2^{T2E}$ were short-lived in chloroplasts even in the absence of actinonin, i.e., in the absence of PDF inhibition [109, 110]. The deformylated N-terminal Met of wild-type $D2^{T2}$ was expected to be cleaved off by MetAP, because Thr is smaller than Val (see Introduction). In contrast, N-terminal Met was expected to be retained in the mutant $D2^{T2D}$ and $D2^{T2E}$ proteins, inasmuch as both Asp and Glu are larger than Val. Therefore Giglione and colleagues interpreted the accelerated degradation of $D2^{T2D}$ and $D2^{T2E}$ (compared to $D2^{T2}$) in chloroplasts as resulting from the retention of their deformylated N-terminal Met, i.e., as the consequence of the inability of MetAP to remove deformylated Met from the N-termini of $D2^{T2D}$ and $D2^{T2E}$, in contrast to wild-type $D2^{T2}$ [110].

However, our results (Fig. 3) suggest a different, formyl-based interpretation of the above D2 findings [110]. This alternative interpretation ascribes the destruction of the mutant $D2^{T2D}$ and $D2^{T2E}$ proteins to a *relatively slow* PDF-mediated deformylation of N-terminal fMet if it is followed by either Asp or Glu, in comparison to the at least 10-fold faster deformylation of fMet if it is followed, for example, by the Thr residue, which is present at position 2 of wild-type $D2^{T2}$. Thus, we suggest that the correct interpretation of the earlier data about the protein $D2^{T2}$ is the one in which $D2^{T2}$ can be degraded through its fMet/N-degron if deformylation of fMet in $D2^{T2}$ is inhibited by actinonin. Further, the data described below (Fig. 3E, F) suggest that the previously observed rapid destruction of the mutant $D2^{T2D}$ and $D2^{T2E}$ proteins [109, 110] is also mediated by their fMet/N-degrons,

because the N-terminal fMet-Asp and fMet-Glu sequences of $D2^{T2D}$ and $D2^{T2E}$ are the least favorable sequence contexts for the PDF-mediated deformylation of N-terminal fMet, as had been shown in a detailed study of the sequence preferences of *E. coli* PDF [17].

The $P1^{T2}$ protein ($D2^{1-11}$-e^{K}-ha-Ura3) and the otherwise identical $P1^{T2D}$ protein, with Asp replacing Thr at position 2, were expressed from the arabinose-inducible P_{ara} promoter (Fig. 3A, B and Table S2). These reporters were identical, in their 11-residue N-terminal segments, to the N-terminal sequences of the wild-type $D2^{T2}$ and mutant $D2^{T2D}$ proteins that had been studied in the cited chloroplast-based experiments [109, 110]. Two other plasmids expressed the otherwise identical Ub-$P1^{T2}$ and Ub-$P1^{T2D}$, i.e., the Ub-fusion counterparts of $P1^{T2}$ and $P1^{T2D}$ (Fig. 3C and Table S2).

Ub is not recognized as a degron in wild-type *E. coli*. However, a Ub fusion can be cotranslationally cleaved in *E. coli* if they express a deubiquitylating (DUB) enzyme such as Ubp1 of *S. cerevisiae* [75, 113, 114]. Placing the Ub moiety in front of two reporters and expressing the resulting Ub fusions in Ubp1-containing *E. coli* allowed the production of $P1^{T2}$ and $P1^{T2D}$ through the site-specific removal, by Ubp1, of the N-terminal Ub moiety. (This version of the Ub fusion technique was developed in our studies of the *E. coli* N-end rule pathway [75, 113, 114].) The difference between two modes of reporter expression, the direct one and the Ub fusion-mediated one, is the transient presence of the *formylated* fMet residue at the N-termini of directly produced $P1^{T2}$ and $P1^{T2D}$ vs. the presence of *unformylated* N-terminal Met in the otherwise identical $P1^{T2}$ and $P1^{T2D}$ that had been generated from Ub-$P1^{T2}$ and Ub-$P1^{T2D}$ through the removal of their Ub moiety (Fig. 3C). It should be noted that although N-terminal fMet was present at the N-terminus of nascent Ub upon the expression of Ub-$P1^{T2}$ and U-$P1^{T2D}$ in *E. coli*, the rapid folding of the emerging

Ub moiety would be expected to facilitate deformylation of its N-terminal fMet, thereby abrogating its fMet/N-degron (Fig. 1D).

Equal total protein loads were controlled as described above for $P1^{T2}$ in wild-type and *fmt* cells (Fig. 3D). Extracts from wild-type *E. coli* containing the directly expressed $P1^{T2}$ and $P1^{T2D}$ reporters were fractionated by SDS-PAGE, followed by immunoblotting with anti-ha antibody (Fig. 3E, F). Whereas the band of $P1^{T2}$ could be detected in cells growing in the presence of arabinose, the level of the otherwise identical $P1^{T2D}$, containing Asp at position 2 (this is an unfavorable sequence context for fMet deformylation [17]) was either too low for detection in one experiment (Fig. 3F, lanes 1-4) or was detectable but considerably lower than the level of $P1^{T2}$ in another, independent experiment (Fig. 3E, lanes 1-4).

In contrast, when the same two reporters, $P1^{T2}$ and $P1^{T2D}$, were expressed as Ub fusions in *E. coli* that also expressed the yeast Ubp1 DUB enzyme, two changes were observed. First, the yields of both reporters were greatly increased. Second, their steady-state levels, instead of being strongly different upon reporters' direct expression, became equal (Fig. 3C, E, F). Expression of the same Ub fusions in *E. coli* lacking the Ubp1 DUB yielded equal levels of the larger, unprocessed Ub-$P1^{T2}$ and Ub-$P1^{T2D}$ fusions (Fig. 3F, lanes 9-12).

These findings (Fig. 3B, C, E, F), together with the data about $P1^{T2}$ in wild-type vs. *fmt E. coli* (Figs. 3A, D), suggested that the N-terminal fMet residue of both nascent and just completed, newly formed proteins can participate in two alternative transitions: the PDF-mediated deformylation of N-terminal fMet vs. its capture by the postulated

fMet/N-recognin/protease and the ensuing processive degradation of a targeted protein (Fig. 1C-E and Discussion).

Formylation-dependent selective destabilization of a reporter protein

In these ^{35}S-pulse-chase assays, our reporters were derivatives of a natural cytosolic *E. coli* protein, the 164-residue PpiB peptidyl-prolyl cis-trans isomerase [115]. One feature of these assays (Fig. 4) was a "built-in" reference protein. fMVTF, the N-terminal sequence of PpiB, is a motif favored by the *E. coli* PDF deformylase [17]. This sequence is indicated by the superscript on the left side of the term $^{\mathrm{MVTF}}_{\mathrm{wt}}\mathrm{PpiB_f}$, which denotes the C-terminally flag-tagged wild-type PpiB, a reference protein. It was coexpressed with one of two otherwise identical reporters, termed, respectively, $^{\mathrm{MYFY}}\mathrm{PpiB_f}$-Ub and $^{\mathrm{MDDD}}\mathrm{PpiB_f}$-Ub (Fig. 4). The reference protein $^{\mathrm{MVTF}}_{\mathrm{wt}}\mathrm{PpiB_f}$ and the reporter $^{\mathrm{MYFY}}\mathrm{PpiB_f}$-Ub were coexpressed from two identical, arabinose-inducible, tandemly arranged P_{ara} promoters (Fig. 4A, B). An otherwise identical plasmid coexpressed the reference $^{\mathrm{MVTF}}_{\mathrm{wt}}\mathrm{PpiB_f}$ and the reporter $^{\mathrm{MDDD}}\mathrm{PpiB_f}$-Ub (Fig. 4C, D and Table S2).

The two reporters, $^{\mathrm{MYFY}}\mathrm{PpiB_f}$-Ub and $^{\mathrm{MDDD}}\mathrm{PpiB_f}$-Ub, differed from the reference $^{\mathrm{MVTF}}_{\mathrm{wt}}\mathrm{PpiB_f}$ at two places: by the sequence of three residues following N-terminal Met and by the presence of the ~8 kDa Ub moiety C-terminally to the $\mathrm{PpiB_f}$ moiety (Fig. 4A, C). The Ub moiety was linked, C-terminally, to the PpiB moiety solely for making it easy to distinguish, by SDS-PAGE, the resulting reporters $^{\mathrm{MYFY}}\mathrm{PpiB_f}$-Ub and $^{\mathrm{MDDD}}\mathrm{PpiB_f}$-Ub from the reference $^{\mathrm{MVTF}}_{\mathrm{wt}}\mathrm{PpiB_f}$ (Fig. 4).

Three residues, Val-Thr-Phe, which follow N-terminal Met in wild-type PpiB, were replaced, in ^{MYFY}PpiB$_f$-Ub and in ^{MDDD}PpiB$_f$-Ub, by the sequences Tyr-Phe-Tyr (YFY) and Asp-Asp-Asp (DDD), respectively (Fig. 4). ^{MYFY}PpiB$_f$-Ub was our "rapidly deformylatable" reporter (also called reporter-1), since N-terminal sequences of the kind exemplified by the sequence fMYFY are kinetically favorable contexts for the PDF-mediated deformylation of N-terminal fMet (Fig. 4A) [17]. The N-terminal sequence fMVTF, of the reference $^{MVTF}_{wt}$PpiB$_f$, is also a favorable motif for the PDF-mediated deformylation of N-terminal fMet [17].

The encoded N-terminal sequence of ^{MDDD}PpiB$_f$-Ub (reporter-2) was Met-Asp-Asp-Asp (MDDD) (Fig. 4C). ^{MDDD}PpiB$_f$-Ub was our "slowly deformylatable" reporter, because the N-terminal sequence fMDDD has been shown to be among the most unfavorable contexts for the PDB-mediated deformylation of N-terminal fMet [17]. Deformylation, by purified *E. coli* PDF, of synthetic peptides bearing N-terminal fMet was at least 10-fold faster for most favorable fMet sequence contexts, in comparison to least unfavorable ones [17]. These sequence motifs were exemplified, in our reporters, by fMYFY and fMVTF (favorable contexts) vs. fMDDD (unfavorable context) (Fig. 4A, C).

If fMet/N-degrons exist (in other words, if the postulated fMet/N-recognin/protease exists), the relatively slowly deformylated reporter-2 and the relatively rapidly deformylated reporter-1 would be vulnerable both to the PDF-mediated deformylation of their N-terminal fMet (a step that abrogates fMet/N-degrons) and to the alternative, competing event of capture and processive degradation of a reporter protein through its fMet/N-degron. In the latter outcome, the postulated fMet/N-recognin/protease succeeds in

binding to N-terminal fMet before its deformylation by PDF. Either one of these mutually exclusive steps would take place while the polypeptide chain of a nascent reporter continues to emerge from the ribosomal tunnel at the rate of 10-20 residues/sec.

Given this disposition, one key prediction of the fMet/N-degron hypothesis is as follows: if the N-terminal fMet residue of one nascent protein (reporter-2) is deformylated significantly slower than fMet of another (nearly identical) nascent protein (reporter-1) (Fig. 4A, C), the molecules of reporter-2 would be targeted for destruction more often through its (more frequently retained) fMet/N-degron, resulting in a higher rate of degradation of reporter-2.

Because these events are expected to involve largely nascent, still growing polypeptide chains, the second prediction is that a difference in degradation rates between reporter-1 and reporter-2 in wild-type *E. coli* may be largely confined to previously glimpsed proteolytic processes referred to as the "time-zero", "before-chase" proteolysis [67-69, 71, 97, 116-118]. These effects result from the processive *cotranslational* degradation, in contrast to *posttranslational* degradation. While the posttranslational degradation of a protein is measured during a chase, the extent of cotranslational degradation of the same protein is determined by comparing time-zero (before chase) levels of this protein and an otherwise identical protein that lacks (or nearly lacks) the relevant degron [67-69, 71, 97, 116-118]. Given the second prediction above, the presence, in our assays, of the "built-in" reference protein $^{\mathrm{MVTF}}_{\mathrm{wt}}\mathrm{PpiB_f}$ (Fig. 4) was particularly important, because a reference greatly increases the accuracy of quantifying both cotranslational and

posttranslational degradation, with the cotranslational mode revealing itself through time-zero, before-chase effects.

The third and equally critical prediction of the fMet/N-degron hypothesis: if a faster degradation of the more slowly deformylated reporter-2 is actually observed in wild-type cells (possibly as a time-zero, before-chase effect), this effect should vanish if ^{35}S-pulse-chases are performed in *fmt* cells, which lack formyltransferase and therefore lack fMet/N-degrons.

Experiments designed as described above were carried out. The results were in agreement with all three predictions of the fMet/N-degron hypothesis (Fig. 4).

In the first set of ^{35}S-pulse-chases, wild-type *E. coli* and its *fmt* mutant (lacking Met formylation) were transformed with pKP458, which expressed, from two identical P_{ara} promoters, the rapidly deformylatable $^{\mathrm{MVTF}}_{\mathrm{wt}}\mathrm{PpiB_f}$ reference and the also rapidly deformylatable $^{\mathrm{MYFY}}\mathrm{PpiB_f}$-Ub reporter-1 (Fig. 4A, B and Table S2). Arabinose was added to induce expression of the two proteins, followed by 1-min pulse with ^{35}S-methionine/cysteine at 37°C, chases for 1, 3, 7, 15 and 30 min, preparation of cell extracts, immunoprecipitation of $^{\mathrm{MVTF}}_{\mathrm{wt}}\mathrm{PpiB_f}$ and $^{\mathrm{MYFY}}\mathrm{PpiB_f}$-Ub with anti-flag antibody, fractionation of precipitated proteins by SDS-PAGE, and autoradiography. The data were quantified by plotting, on a semi-logarithmic scale, the ratios of ^{35}S in the band of the $^{\mathrm{MYFY}}\mathrm{PpiB_f}$-Ub reporter-1 to ^{35}S in the band of the reference $^{\mathrm{MVTF}}_{\mathrm{wt}}\mathrm{PpiB_f}$ (Fig. 4A, B, E).

$^{\mathrm{MVTF}}_{\mathrm{wt}}\mathrm{PpiB_f}$ and $^{\mathrm{MYFY}}\mathrm{PpiB_f}$-Ub were relatively stable over the 30-min chase in wild-type and *fmt E. coli*. In addition, no significant differences in ^{35}S ratios of $^{\mathrm{MYFY}}\mathrm{PpiB_f}$-Ub to $^{\mathrm{MVTF}}_{\mathrm{wt}}\mathrm{PpiB_f}$ at the time-zero (before chase) point were observed between wild-type and *fmt*

cells (Fig. 4E; curves 1 and 2). That was expected, given the approximately equal rates of the PDF-mediated deformylation of the reference and reporter-1, as described above.

In the second set of ^{35}S-pulse-chases, wild-type and *fmt E. coli* were transformed with pKP459, which expressed, from the two P_{ara} promoters, the rapidly deformylatable $^{MVTF}_{wt}PpiB_f$ and the relatively slowly deformylatable $^{MDDD}PpiB_f$-Ub reporter-2 (Fig. 4C, D and Table S2). This comparison revealed a strikingly high ~8-fold difference between the rates of time-zero, before-chase degradation of the rapidly deformylatable $^{MYFY}PpiB_f$-Ub reporter-1 and the relatively slowly deformylatable $^{MDDD}PpiB_f$-Ub reporter-2, indicating a much higher rate of the early, presumably cotranslational degradation of the (relatively) slowly deformylated $^{MDDD}PpiB_f$-Ub in wild-type cells (Fig. 4E; curves 2 and 4). Crucially, the bulk of this effect was abrogated when the otherwise identical ^{35}S-pulse-chases were performed in *fmt* cells, which did not formylate N-terminal Met and therefore could not create fMet/N-degrons (Fig. 4E; curves 1 and 3).

While the degradation of the $^{MDDD}PpiB_f$-Ub reporter-2 in wild-type cells was largely of the time-zero, before-chase kind, this reporter was also destroyed, relatively slowly, during chases in both wild-type and *fmt* cells (Fig. 4C-E; curves 3 and 4). In contrast, little posttranslational degradation was observed with the $^{MYFY}PpiB_f$-Ub reporter (differing from $^{MDDD}PpiB_f$-Ub by three residues after N-terminal Met) in either wild-type or *fmt* cells (Fig. 4A, B, E). A parsimonious interpretation of the slow posttranslational degradation of $^{MDDD}PpiB_f$-Ub is that the sequence of three Asp residues after N-terminal Met may have created a weak, largely posttranslational and formylation-unrelated degron.

The design of these assays, i.e., their built-in reference protein as well as two identical transcriptional promoters expressing a reference and a reporter in wild-type vs. *fmt* cells, controlled for variables other than protein degradation (Fig. 4A, C). The ~8-fold difference in the time-zero, before-chase levels of the rapidly deformylated reporter-1 and the relatively slowly deformylated reporter-2 in wild-type cells, and the dependence of this effect on the presence of formyltransferase (Fig. 4E) seem to allow only one plausible and parsimonious interpretation. Specifically, we posit that this difference and its dependence on Nt-formylation indicated the presence, in our reporters, of PDF-vulnerable fMet/N-degrons (Figs. 1C-E and 4).

Discussion

Key results of the present study are the evidence that rapidly and slowly deformylated protein reporters are destroyed at different rates in wild-type *E. coli*, and that this effect is abrogated in formylation-lacking *fmt* mutants. These and related findings strongly suggest that the formylated N-terminal fMet residue can act as an N-degron, termed fMet/N-degron, of a novel bacterial N-end rule pathway, termed the fMet/N-end rule pathway (Figs. 1-4).

Incomplete deformylation of nascent bacterial proteins *in vivo*

N-terminal fMet of nascent polypeptides can be incompletely deformylated by PDF *in vivo* [60, 119]. The incomplete deformylation is particularly pronounced with DNA-encoded, ribosome-generated small natural peptides [120]. For example, the bulk of

secreted 7-residue microcin-C peptide is not deformylated *in vivo* [120], although this peptide's second residue, in the N-terminal sequence fMet-Arg, is one of position-2 residues that are optimal for deformylation of fMet by PDF [17].

The molar concentration of PDF in *E. coli* is 2-3 μM, an order of magnitude below that of the ribosomes, ~30 μM [7, 23, 37]. Consequently, an efficacious deformylation of nascent proteins requires that molecules of PDF "hop" among the PDF-binding sites of different ribosomes. Given the resulting stochasticity of deformylation, given low steady-state levels of PDF in the bulk solvent (since most PDF molecules are ribosome-bound), and given a significant dependence of the rate of deformylation by PDF on fMet-proximal sequence contexts [17, 18], one should expect an incomplete deformylation of bacterial proteins to be a frequent occurrence [60, 119]. For example, a 2-D electrophoretic study of abundant *Bacillus subtilis* proteins indicated that some of them retained, at steady-state, a small but significant fraction of their initial (formylated) N-terminal fMet [121].

Analyses, using 2-D electrophoresis, of the *in vivo* inhibition of fMet deformylation by the PDF-specific inhibitor LBM-415 in *Staphylococcus aureus* and *Streptococcus pneumoniae* demonstrated the accumulation of formylated (non-deformylated) counterparts of normally deformylated proteins [122]. Interestingly, while a subset of proteins in LBM-415-treated bacterial cells exhibited a telltale double-spot appearance on 2-D gels (a formylated plus deformylated species), many other proteins remained as single spots, without formylated counterparts [122]. This finding, remarked upon but not explained by the authors [122], might signify the selective degradation of some formylated proteins through fMet/N-degrons suggested by the results of our study (Figs. 1-4). In this interpretation of the data in ref. [122], those proteins that accumulate, in the presence of

PDF inhibitor, as formylated (non-deformylated) species, might be partially protected from degradation owing to a steric shielding (sequestration) of their fMet/N-degrons, either through intramolecular protein folding or through the formation of "protective" oligomeric complexes with cognate protein ligands. The latter mechanism would be analogous to the previously discovered shielding-mediated conditionality of natural eukaryotic Ac/N-degrons [68].

Working model of fMet/N-degrons

The idea of fMet/N-degrons was sketched in ref. [67]. It is now described in detail (Fig. 1C-E) vis-á-vis the data (Figs. 2-4).

First, we presumed that a distinct fMet/N-recognin/protease (envisioned as a transient complex of both) can recognize, in a competition with PDF, the N-terminal fMet moiety of a nascent protein and thereby initiate a processive destruction of this protein either cotranslationally or posttranslationally. The latter distinction is based on whether the protein's N-terminal fMet is captured by the fMet/N-recognin/protease before or after the protein's nascent polypeptide chain is released from the last tRNA molecule at the ribosome's peptidyltransferase site. Cotranslational protein degradation is defined as the processive degradation of a nascent, growing polypeptide that exists, at the time of proteolytic attack, as a ribosome-associated peptidyl-tRNA.

A proteolytic pathway that targets a specific degron in a protein and converts the bulk of it to short peptides must be highly processive. A nonprocessive protease would tend to release an initially captured protein and thereby would lose it for good if a protein's segment containing the degron had already been destroyed. The postulated bacterial

fMet/N-recognin/protease is envisioned to be a processive proteasome-like protease, possibly one of the known ones, such as, for example, FtsH, Lon, or a ClpP-containing protease [123] (see also *Concluding Remarks*). One protease of the latter class, ClpXP, is unlikely to be involved, because its *in vitro* activity toward a test protein was shown to be independent of the presence or absence of Nt-formylation [22].

The degradation of an fMet-bearing nascent protein, i.e., of a ribosome-bound peptidyl-tRNA, would proceed to completion once it begins, after the recognition of protein's N-terminal fMet. During this (postulated) degradation, the fMet/N-recognin/protease, having captured the protein's N-terminal fMet, would remain associated with the translating ribosome. The emerging chain of a nascent protein would continue to be delivered into the protease's chamber and destroyed to short peptides until the natural (i.e., not premature) chain termination event at the ribosome's peptidyl-transferase site. An alternative possibility is that the initiation of cotranslational degradation of a ribosome-associated peptidyl-tRNA would lead, through allosteric effects, to a premature termination of translation.

Second, the fMet/N-recognin/protease or at least its fMet/N-recognin part was presumed to have a non-zero affinity for the ribosomes, forming a "cloud" of fMet/N-recognin/protease molecules (or fMet/N-recognin alone) "hugging" the ribosomes. The analogous cloud of ribosome-hopping PDF molecules [23] would partially overlap with the (presumed) cloud of fMet/N-recognin/protease molecules. One version of this model envisions a "tighter cloud" of ribosome-hopping PDF molecules, i.e., a smaller time-averaged distance between them and the ribosomes, in comparison to a "looser cloud" of fMet/N-recognin/protease molecules, reflecting their (presumed) lower affinity for the

ribosomes. In such a setting, which was partly characterized for PDF [23] and is postulated here for the fMet/N-recognin/protease (or its fMet/N-recognin part), a molecule of ribosome-bound PDF would have a stochastically better "shot" at binding to and deformylating N-terminal fMet of an emerging nascent protein. The term "looser cloud" implies a larger time-averaged distance of the fMet/N-recognin/protease from the tunnel's exit, in comparison to PDF. Whether the "cloud" model is relevant to a postulated fMet/N-recognin rather than to a "downstream" protease remains to be seen, particularly if the protease in question is the inner membrane-embedded FtsH protease (see *Concluding Remarks*).

In this working model of fMet/N-degrons, some non-wild-type N-terminal sequences, once they emerge from the ribosomal tunnel, would either not collapse rapidly enough, or would collapse into globules that impede deformylation of N-terminal fMet by PDF. In the latter case, a collapse may prevent, at least in part, an exposure of the roughly 10-residue N-terminal region (including its fMet) on the globule's surface. As a result, the ribosome-bound PDF would often fail to deformylate fMet, given the narrow kinetic/stochastic window of opportunity that PDF is allowed to have (Fig. 1C-E). As to the former case, the radii of gyration of folded polypeptides with lengths of up to 100 residues are 1.0-1.2 nm, whereas the radii of gyration of unfolded polypeptides increase from ~1.0 to ~3.0 nm as their length increases from 8 to 100 residues [124]. In such a setting, the N-terminal fMet residue of a (largely) unfolded polypeptide may be stochastically and partially buried in a fluctuating, partially folded conformation, thereby impeding the capture and deformylation of fMet by the ribosome-bound PDF (Fig. 1C-E).

Results of a study based on the ribosome profiling technique suggested that the PDF-mediated deformylation of nascent bacterial proteins takes place, in the main, before they become significantly larger than ~100 residues [28]. Thus, the postulated targeting of a nascent Nt-formylated protein for processive degradation through its fMet/N-degron (Fig. 1C-E) may be "decided upon" largely on the basis of protein's first 100 or so residues. In other words, significantly more distal regions of a protein may often not be involved.

Given this disposition, we suggest that ~100-residue N-terminal regions of bacterial proteins evolve under a selection pressure that tends to maximize their ability to collapse into a "molten globule" [125] in which roughly 10 N-terminal residues, including N-terminal fMet, tend to be extruded from the globule and exposed to solvent. Consequently, PDF would be able to deformylate a nascent protein before the N-terminal fMet residue would move too far away from the ribosome-bound PDF, owing to the ongoing elongation of the protein's polypeptide chain (Fig. 1C, D). Entries in Protein Data Bank (PDB; http://www.rcsb.org/pdb/home/home.do) exhibit a tendency for N-terminal regions to be weakly ordered in crystal structures. Moreover, such regions are often absent altogether in published structures, having been removed from the proteins' natural N-termini to allow crystallization. For example, the first high-resolution structures of "soluble" eukaryotic proteins with intact natural N-terminal regions (usually in complexes with their cognate protein ligands) have been determined only recently [126-128].

Third, the kinetic advantage of PDF in targeting the N-terminal fMet residue would be transient, because a stochastic failure of PDF to capture and deformylate fMet of a nascent protein would soon (within seconds) position that fMet outside the physical reach of a ribosome-bound PDF molecule, owing to the ongoing elongation of the protein's

polypeptide chain. It would be, then, the stochastic and also transient turn of the less tightly ribosome-bound fMet/N-recognin/protease or its fMet/N-recognin part (resulting in its larger time-averaged distance from the ribosomes) to capture the N-terminal fMet residue, whose distance from the tunnel's exit may continue to increase as the nascent polypeptide keeps emerging from the ribosome.

Fourth, the main (but not necessarily the sole) function of postulated fMet/N-degrons (Fig. 1E) is envisioned to be the quality control of nascent bacterial proteins and just released, newly formed proteins. This role of bacterial fMet/N-degrons would be similar to the previously identified quality-control function of eukaryotic Ac/N-degrons [67-70]. The naturally high ($\sim 10^{-3}$ per residue) frequency of amino acid misincorporation during protein synthesis can be further increased by antibiotics that elevate the ribosome's error rate. Such antibiotics are endemic in natural bacterial habitats [7, 51]. On the assumption that the error rate is approximately uniform along the sequence of a translated polypeptide, a significant fraction of N-terminal regions of nascent proteins would be mutant vis-á-vis their wild-type DNA-encoded sequences even in the absence of stress. The frequency of abnormal (mistranslated) sequences would be further elevated in the presence of fidelity-decreasing antibiotics or other stresses.

Fifth, some molecules of just completed, newly formed proteins would stochastically and at least transiently bypass the targeting by both PDF and the postulated fMet/N-recognin/protease. The non-ablated fMet/N-degrons of such proteins are envisioned to be often rapidly repressed through their steric shielding (sequestration), owing to interactions of newly formed proteins with their cognate ligands, which can be other proteins, RNA or DNA. In contrast, a nascent or a newly formed Nt-formylated

protein that cannot form such "protective" complexes efficaciously enough or cannot form them at all (owing, for example, to its misfolding) would remain vulnerable to either the destruction by the postulated fMet/N-recognin/protease or to the PDF-mediated deformylation of N-terminal fMet, a step that abrogates the protein's fMet/N-degron. This model presumes a low level of PDF away from the ribosomes, in agreement with experimental evidence [23]. In contrast, the postulated fMet/N-recognin/protease (or its fMet/N-recognin part), while also ribosome-associated, is presumed to be present at significant levels in the bulk solvent as well.

Studies by Green and colleagues employed defined *in vitro* translation systems and showed that a bacterial (but apparently not eukaryotic) ribosome can sense a misincorporation of a non-cognate residue during protein synthesis and react through a further decreased fidelity of translation downstream from the incorrect amino acid residue [129, 130]. This error-induction response increases the probability of premature translation termination and the release of a mistranslated nascent polypeptide [129]. The extent of Green's effect remains to be determined *in vivo*. If the frequency of nascent polypeptides that are prematurely terminated in living bacteria owing to this effect is as high as it was observed to be *in vitro* [129], one would expect a significant frequency of Nt-formylated, mistranslated and prematurely terminated proteins that emerge from the ribosomal tunnel while bearing fMet/N-degrons. Owing to misincorporation events that led to their premature release, such (incomplete) proteins would often fold either abnormally or not at all. These properties may render them less susceptible to deformylation.

The temporal and geometric aspects of N-terminal fMet vis-á-vis other participants in this kinetic drama would vary from one nascent protein to another, at least in part

because the rate of PDF-mediated deformylation of fMet in a nascent protein depends on the identities of residues at position 2 and beyond [17]. In sum, the folding (or misfolding) of a growing nascent protein, and the propensity (or its absence) of N-terminal fMet to remain sterically accessible to PDF on the surface of a nascent protein globule would affect the outcomes of competition between the ribosome-associated PDF and the postulated fMet/N-recognin/protease. This glimpse of possible mechanics is an illustration of complexities that remain to be understood vis-á-vis the concept of fMet/N-degrons (Fig. 1C-E).

Concluding remarks

The fMet/N-degron hypothesis was proposed in 2010 [67]. The difficulty in viewing (let alone proving) the N-terminal fMet residue as a degradation signal stems from the transiency of the formyl group of N-terminal fMet in a majority of nascent bacterial proteins.

The rate of chain elongation by bacterial ribosomes *in vivo* at 37°C is 10-20 residues/sec, i.e., it is up to an order of magnitude higher than estimated rates of chain elongation by the cytosolic ribosomes in eukaryotes [49-52]. Faster emergence of nascent proteins from bacterial ribosomes may have precluded the adoption, during bacterial evolution, of cotranslationally (as distinguished from pretranslationally) created N-degrons, such as, for example, Ac/N-degrons in eukaryotes (Fig. S1B). Notably, the Nt-acetylation of many eukaryotic proteins is known to be incomplete [103], i.e., the cotranslational generation of Ac/N-degrons is often not efficacious enough even at relatively low rates of chain elongation in eukaryotes. This fact is consistent with the view that the observed

pervasiveness of the pretranslational formylation of N-terminal Met (all examined wild-type bacteria contain fMet) resulted from selection pressures to maximize the extent of Met formylation vis-á-vis high rates of polypeptide chain elongation.

Competition among bacteria and other microorganisms often involves antibiotics that increase the frequency of translational errors in susceptible strains. One function of fMet/N-degrons is envisioned to be the preferential degradation of misfolded nascent proteins. Thus, stresses caused by perturbed translation, including antibiotics-mediated conflicts in the microbial world, may be a source of selection pressures that retained the apparatus of bacterial fMet/N-degrons.

Now that the first evidence for fMet/N-degrons has been produced (Figs. 1-4), the next essential step is to identify the postulated, possibly two-component fMet/N-recognin/protease. A recent study by Bittner et al. [131] described the N-terminal degradation signal of YfgM, an inner membrane-embedded *E. coli* protein. Analyses by Bittner et al. [131] did not invoke either an fMet/N-degron or the formylation of N-terminal Met. However, specific properties of the cytosol-facing N-terminal degron of YfgM [131] suggested, to us, that this degradation signal may be an fMet/N-degron. If so, the inner membrane-embedded, ATP-dependent FtsH protease would be the one that targets the N-terminal fMet residue (either directly or through an unknown fMet/N-recognin), because Bittner al. [131] identified FtsH as the protease that destroys YfgM. Remarkably, our recent studies showed that the degron of YfgM is, in fact, an fMet/N-degron, thereby identifying FtsH as the relevant protease (T.T.M.V., K.P. and A.V., unpublished data).

Materials and Methods

Miscellaneous reagents

Anti-flag M2 Magnetic Beads (M8823), anti-flag M2 antibody, and anti-ha antibody were from Sigma-Aldrich. Complete EDTA-free Protease Inhibitor Cocktail Tablets were from Roche. Express [^{35}S] Protein Labeling Mix (1.175 Ci/mmol) was from Perkin-Elmer. Methionine/cysteine-free synthetic complete ("Hopkins") supplement mixture (SC) was from Sunrise Science Products. Actinonin was from Enzo Life Sciences.

Bacterial strains and mutagenesis

E. coli strains (Table S1) were grown at 37°C on Luria-Bertani (LB) medium. When used for selection, antibiotics were added to the following final concentrations: kanamycin (Km): 50 μg/ml; ampicillin (Amp): 100 μg/ml. Null *fmt* and *def-fmt E. coli* mutants (strains KPS73-KPS76) (Table S1) were constructed using a gene disruption strategy [132]. The resulting *E. coli* mutants were grown in LB under selective conditions. The desired deletions were verified by polymerase chain reaction (PCR), followed by sequencing of PCR-amplified, purified DNA fragments.

Construction of plasmids

E. coli DH5α (Invitrogen) was used for cloning and maintaining plasmids. Phusion High-Fidelity DNA polymerase (New England Biolabs) was used for PCR. Specific DNA

constructs were generated using standard techniques [112] and verified by DNA sequencing.

The plasmids containing one or two P_{ara} promoters were derived from the pBADET vector, a gift from Dr. V. Ksenzenko (Institute of Protein Research, Pushchino, Russia). The plasmids pKP249 and pKP250, which expressed $P1^{T2X}$ ($P1^{T2X}$-e^{K}-ha-Ura3) fusion proteins (X=Thr or Asp) from the P_{ara} promoter, were constructed by subcloning a *Nde*I/*Hind*III-digested DNA fragment (produced by PCR from pCH178; Table S2) into the *Nde*I/*Hind*III-cut plasmid pBADET (Table S2). (The DNA fragment from pCH178 that encoded e^{K}-ha-Ura3 was extended, by PCR, to yield fragments encoding either $P1^{T2}$-e^{K}-ha-Ura3 or $P1^{T2D}$-e^{K}-ha-Ura3.) To construct pKP251 and pKP252, which expressed Ub-$P1^{T2X}$ fusion proteins from the P_{ara} promoter, a DNA fragment containing the ORF of Ub was PCR-amplified (using the pCH178 plasmid as a template), digested with *NdeI*/*Bsp*EI and subcloned into *NdeI*/*Bsp*EI-cut pKP249 and pKP250 (Table S2). To construct pKP257 and pKP258, which expressed $P1^{T2X}$ proteins ($P1^{T2X}$-e^{K}-ha-Ura3) (X=Thr or Asp) from the P_{KmR} promoter, *Nde*I/*Hind*III-digested fragments, produced by PCR from pKP249 and pKP250, were subcloned into *Nde*I/*Hind*III-cut pACYC177 (Table S2). The plasmids pKP286 and pKP287, which expressed ^{MXXX}PpiB-His_8-flag ($^{MXXX}PpiB_f$) proteins (XXX=Val-Thr-Phe or Asp-Thr-Phe), were constructed by subcloning a *Nde*I/*Xba*I-digested DNA fragment (encoding PpiB and produced by PCR from MG1655 *E. coli* genomic DNA) into *Nde*I/*Xba*I-cut pBADET (Table S2). The plasmids pKP458 and pKP459, each of which expressed two PpiB-derived proteins from two identical P_{ara} promoters (Fig. 4) were constructed as follows. DNA fragment containing the P_{ara} promoter was PCR-amplified from pBADET (Table S2). DNA fragment encoding

^{MXXX}ppiB-His$_8$-flag-Ub (^{MXXX}PpiB$_f$-Ub) (XXX=Tyr-Phe-Tyr or Asp-Asp-Asp) was PCR-amplified from pKP335 (Table S2). The resulting DNA fragments were linked together using PCR, digested with *Afe*I/NsiI and thereafter subcloned into *Afe*I/NsiI-cut pKP286 (Table S2). Additional cloning details are available on request.

Immunoblotting assays

Methods for data in Fig. 3D: wild-type and mutant *E. coli* (CAG12184, KPS73 and KPS74; Table S1) carrying pKP257 (Table S2) were grown at 37°C overnight in Growth Medium (GM) (M9 medium (33.9 mg/ml Na_2HPO4, 15 mg/ml KH_2PO4, 5 mg/ml NH_4Cl, 2.5 mg/ml NaCl, pH 7.0), 0.5% glycerol, 0.2% glucose, 40 μg/ml Met, 40 μg/ml Cys, methionine/cysteine-free synthetic complete (SC) mixture (Sunrise Science Products) supplemented with ampicillin (Amp; 50 μg/ml)). Cultures were diluted 1:100 in 30 ml of GM medium and incubated on a shaker at 37°C until A_{600} of ~0.5. The resulting cultures (10 ml) were centrifuged at 5,000*g* for 5 min at 4°C, washed three times with 1-ml samples of ice-cold phosphate-buffered saline (PBS) and thereafter lysed in 0.1 ml volumes of 1% SDS. The resulting extracts were clarified by centrifugation at 14,000*g* for 5 min at 4°C, and protein concentration in the supernatants were determined using Pierce BCA Protein Assay (Fisher Scientific). Samples were mixed with equal volume of 2x SDS-sample buffer and heated at 95°C for 10 min. 25 μg of total protein in the resulting samples were subjected to SDS-4-12% NuPAGE (Invitrogen), followed by immunoblotting, using standard procedures [67, 68] with a monoclonal anti-ha antibody (1:2,000) (Sigma-Aldrich), with detection using ECL Plus (GE Healthcare).

Methods for data in Fig. 3E, F: wild-type *E. coli* CAG12184 (Table S1) carrying pKP249-252, and pJT184 (Table S2) were grown at 37°C overnight in GM medium as described above. Cultures were diluted 1:100 in 30 ml of GM medium and incubated at 37°C until A_{600} of ~0.35. Cells were pelleted by centrifugation 5,000*g* for 5 min at room temperature (RT), washed with 1 ml of Induction Medium-Ara-0.25 (IM-Ara-0.25) (M9 medium (pH 7.0), 0.5% glycerol, 0.25% arabinose, 40 μg/ml Met, 40 μg/ml Cys, methionine/cysteine-free synthetic complete (SC) mixture) and resuspended in 30 ml of IM-Ara-0.25 medium. After 90 min of incubation at 37°C, the resulting cultures (10 ml) were centrifuged at 5,000*g* for 5 min at 4°C, washed three times with 1-ml samples of ice-cold PBS and thereafter processed for lysis, SDS-PAGE, and immunoblotting with anti-ha antibody as described above.

Pulse-chase assays without immunoprecipitation

Methods for data in Fig. 2A: wild-type *E. coli* CAG12184 cells (Table S1) were grown in LB medium at 37°C overnight. 0.75 ml of overnight culture in LB was washed with 1 ml of GM medium, resuspended in 30 ml of GM, and was grown until A_{600} of ~0.35. Cells were pelleted by centrifugation at 5,000*g* for 5 min at RT, washed with 1 ml of pre-warmed IM-Ara-0.25 medium and resuspended in 30 ml of pre-warmed IM-Ara-0.25. After 90 min of incubation on a shaker at 37°C in IM-Ara-0.25, 15 ml of the culture were centrifuged at 5,000*g* for 5 min at RT, and washed 2 times with 1-ml samples of pre-warmed Pulse Medium-025 (PM-Ara-0.25), which differed from the IM-Ara-0.25 medium by lacking Met and Cys. Cell pellet was resuspended in 1 ml of PM-Ara-0.25 and divided into 4 equal samples, which were incubated for 10 min at 37°C with agitation. Actinonin

was added (to the final concentrations indicated in panels of Fig. 2A, B) at the beginning of 10-min incubations and was kept at the same concentrations throughout pulse-chases. Thereafter the cultures were labeled with 15 µl of Express [^{35}S] Protein Labeling Mix (1.175 Ci/mmol, Perkin Elmer) for 1 min at 37°C, followed by centrifugation at 14,000*g* for 30 sec at RT. Each supernatant was added to 0.3 ml of Chase Medium (CM) (M9 medium (pH 7.0), 0.5% glycerol, 0.5% glucose, 0.5 mg/ml Met, 0.5 mg/ml Cys, 0.2 mg/ml chloramphenicol, methionine/cysteine-free synthetic complete (SC) mixture), followed by a chase, also at 37°C. Samples (0.1 ml) were withdrawn at indicated times during chase, followed by immediate freezing in liquid nitrogen. For further analyses, one volume of 2x-SDS-PAGE sample buffer was added to a frozen sample, followed by heating at 95°C for 10 min, brief vortexing and centrifugation at 12,000g for 5 min. 5 µl of each "time-zero" sample were spotted on Whatman 3MM filters, immersed in ice-cold 10% CCl_3COOH for 5 min, boiled in 10 % CCl_3COOH for 10 min, rinsed (for 15 sec) 3 times in 5% CCl_3COOH, washed (for 5 min) 2 times with 5% CCl_3COOH, rinsed 3 times with 95% ethanol, and air-dried, followed by measurements of ^{35}S using Safety-Solve scintillation cocktail and scintillation spectrometer. 20,000 ^{35}S cpm of each time-zero sample (Fig. 2B), and equal volumes of samples at later time points were subjected to SDS- 4-12% PAGE, followed by autoradiography.

Methods for data in Fig. 2B: wild-type (CAG12184) and *fmt* (KPS73) *E. coli* (Table S1) were grown in LB medium at 37°C overnight. Cultures were diluted 1:200 in the GM medium and incubated at 37°C until A_{600} of ~0.5. The resulting culture (7 ml) was centrifuged at 5000*g* for 5 min at room temperature, washed three times with 1-ml samples of pre-warmed PM-Ara-0.25 medium, and resuspended in 70 µl of PM-Ara-0.25, followed

by incubation at 37°C for 10 min. A culture was labeled with 7 µl of Express [^{35}S] Protein Labeling Mix (1.175 Ci/mmol, Perkin Elmer) for 1 min at 37°C. The labeling was quenched by the addition of 0.5 ml of CM (lacking chloramphenicol) and a chase, also at 37°C. Samples (0.1 ml) were withdrawn at indicated times during chase and mixed with 80 µl of TDS buffer (1% SDS, 5 mM dithiothreitol (DTT), 50 mM Tris-HCl, pH 7.4) containing "complete protease-inhibitor mixture" (Roche), followed by immediate freezing of samples in liquid nitrogen. Frozen samples were directly heated at 95°C for 10 min, and thereafter processed and analyzed identically to pulse-chase samples described above.

Pulse-chase assays with immunoprecipitation

E. coli CAG12184, and pKP73 (Table S1) carrying pKP458 or pKP459 (Table S2) were grown at 37°C overnight in LB supplemented with Amp (50 µg/ml). Cultures were diluted 1:200 in fresh LB and grown until A_{600} of ~0.5. A resulting culture (7 ml) was centrifuged at 5000*g* for 5 min at room temperature, washed three times with 1 ml samples of pre-warmed PM-Ara-0.1 medium (containing 0.1% arabinose), and resuspended in 70 µl of PM-Ara-0.1, followed by incubation at 37°C for 10 min. Cultures were then pulse-labeled with 7 µl of Express [^{35}S] Protein Labeling Mix (1.175 Ci/mmol, Perkin Elmer) for 60 sec at 37°C. The labeling was quenched by the addition of 0.5 ml of Chase-Medium (CM: M9 medium, pH 7.0, 0.5% glycerol, 0.25% glucose, 0.1 mM $CaCl_2$, 2 mM $MgSO_4$, Methionine/Cysteine-free Synthetic Complete (SC) Mixture (Sunrise Science Products), 0.5 mg/ml unlabeled Met, 0.5 mg/ml unlabeled Cys). Chases were carried out also at 37°C. Samples (0.1 ml) were withdrawn at indicated times during chase and mixed with 80 µl of TDS buffer (1% SDS, 5 mM dithiothreitol (DTT), 50 mM Tris-HCl, pH 7.4) containing

"complete protease-inhibitor mixture" (Roche), followed by immediate freezing of samples in liquid nitrogen. For further analyses, one volume of 2x-SDS-PAGE sample buffer was added to a frozen sample, followed by heating at 95°C for 10 min. They were, thereafter, briefly vortexed and centrifuged at 12,000g for 5 min. Supernatants were diluted with 10 volumes of TNN buffer (0.5 % NP40, 0.25 M NaCl, 5 mM Na-EDTA, 50 mM Tris-HCl (pH 7.4), containing "complete protease-inhibitor mixture" (Roche)), and processed for immunoprecipitation. 5 µl of each "time-zero" sample were spotted on Whatman 3MM filters and processed for measurements of CCl_3COOH-insoluble ^{35}S as described above. $5.5x10^6$ ^{35}S cpm of each of the time-zero samples, and equal volumes of the following time points for each pulse-series were processed for immunoprecipitation, using magnetic beads with immobilized anti-flag antibody M2 (Sigma; 7 µl of settled beads for each sample). The samples were incubated with rocking at 4°C for 3 hrs, followed by four washes of the beads in TNN buffer, resuspension of pellets in 20 µl of SDS-sample buffer, incubation at 95°C for 5 min, and the removal of beads. The resulting samples were fractionated by SDS-PAGE using NuPAGE 4-12% Bis-Tris gradient gels, followed by autoradiography and quantification using PhosphorImager (Molecular Dynamics, Sunnyvale, CA).

Acknowledgements

We thank Bernd Bukau (ZMBH, Heidelberg, Germany), Vladimir Ksenzenko (Institute of Protein Research, Pushchino, Russia), and Didier Mazel (Institut Pasteur, Paris, France) for gifts of plasmids and *E. coli* strains. We thank Shu-ou Shan (Caltech, Pasadena,

USA) for a discussion of our findings. We also thank David Chan, Michael Elowitz, Brandon Wadas (Caltech), Daniel Finley (Harvard Medical School, Boston, USA), Gholson Lyon (Cold Spring Harbor Laboratory, Cold Spring Harbor, USA), and William Tansey (Vanderbilt University, Nashville, USA) for comments on the manuscript. We are grateful to members of the Varshavsky laboratory for their interest and helpful discussions. This work was supported by grants to A.V. from the National Institutes of Health (DK039520 and GM031530).

SUPPLEMENTAL MATERIAL

Figure S1, its legend, Tables S1 and S2, and supplemental references.

ABBREVIATIONS

fMet, formyl-methionine. MetAP, methionine aminopeptidase. PDF, peptide deformylase. TF, trigger factor. Ub, ubiquitin.

REFERENCES

1. Adams JM, Capecchi MR (**1966**). N-formylmethionyl-sRNA as the initiator of protein synthesis. **Proc. Natl. Acad. Sci. USA** 55: 147-155. PMID: 5328638.
2. Housman D, Gillespie D, Lodish HF (**1972**). Removal of formyl-methionine residue from nascent bacteriophage f2 protein. **J. Mol. Biol.** 65: 163-166. PMID: 4553255.
3. Guillon J-M, Mechulam Y, Schmitter J-M, Blanquet S, Fayat G (**1992**). Disruption of the gene for Met-tRNA (fMet) formyltransferase severely impairs growth of *Escherichia coli*. **J. Bact.** 174: 4294-4301. PMID: 1624424.
4. Mazel D, Pochet S, Marliére P (**1994**). Genetic characterization of polypeptide deformylase, a distinctive enzyme of eubacterial translation. **EMBO J.** 13: 914-923. PMID: 8112305.
5. Wu X-Q, RajBhandary UL (**1997**). Effect of the amino acid attached to *Escherichia coli* initiator tRNA on its affinity for IF2 and on the IF2 dependence of its binding to the ribosome. **J. Biol. Chem.** 272: 1891-1895. PMID: 8999877.
6. Schmitt E, Panvert M, Blanquet S, Mechulam Y (**1998**). Crystal structure of methionyl-tRNAfMet transformylase complexed with the initiator formyl-methionyl-tRNAfMet. **EMBO J.** 17: 6819-6826. PMID: 9843487.
7. Laursen BS, Sørensen HP, Mortensen KK, Sperling-Petersen HU (**2005**). Initiation of protein synthesis in bacteria. **Microbiol. Mol. Biol. Rev.** 69: 101-123. PMID: 15755955.
8. Lee CP, Dyson MR, Mandal N, Varshney U, Bahramian B, RajBhandary UL (**1992**). Striking effects of coupling mutations in the acceptor stem on recognition of tRNAs by *Escherichia coli* Met-tRNA synthetase and Met-tRNA transformylase. **Proc. Natl. Acad. Sci. USA** 89: 9262-9266. PMID: 1409632.
9. Kramer G, Boehringer D, Ban N, Bukau B (**2009**). The ribosome as a platform for cotranslational processing, folding and targeting of newly synthesized proteins. **Nat. Struct. Mol. Biol.** 16: 589-597. doi: 10.1038/nsmb.1614.

10. Steitz TA (**2008**). A structural understanding of the dynamic ribosome machine. **Nat. Rev. Mol. Cell Biol.** 9: 242-253. doi: 10.1038/nrm2352.

11. Ramakrishnan V (**2002**). Ribosome structure and mechanism of translation. **Cell** 108: 557-572. PMID: 11909526.

12. Yonath A (**2005**). Antibiotics targeting ribosomes: resistance, selectivity, synergism, and cellular regulation. **Annu. Rev. Biochem.** 74: 649-679. PMID: 16180279.

13. Korostelev A, Noller HF (**2007**). The ribosome in focus: new structures bring new insights. **Trends Biochem. Sci.** 32: 434-441. PMID: 17764954.

14. Mazel D, Coïc E, Blanchard S, Saurin W, Marlière P (**1997**). A survey of polypeptide deformylase function throughout the eubacterial lineage. **J. Mol. Biol.** 266: 939-949. PMID: 9086272.

15. Rajagopalan PT, Datta A, Pei D (**1997**). Purification, characterization, and inhibition of peptide deformylase from *Escherichia coli*. **Biochemistry** 36: 13910-13918. PMID: 9374870.

16. Becker A, Schlichting I, Kabsch W, Schultz S, Wagner AF (**1998**). Structure of peptide deformylase and identification of the substrate binding site. **J. Biol. Chem.** 273: 11413-11416. PMID: 9565550.

17. Hu Y-J, Wei Y, Zhou Y, Rajagopalan PTR, Pei D (**1999**). Determination of substrate specificity for peptide deformylase through the screening of a combinatorial peptide library. **Biochemistry** 38: 643-650. PMID: 9888804.

18. Ragusa S, Mouchet P, Lazennec C, Dive V, Meinnel T (**1999**). Substrate recognition and selectivity of peptide deformylase. Similarities and differences with metzincins and thermolysin. **J. Mol. Biol.** 289: 1445-1457. PMID: 10373378.

19. Giglione C, Serero A, Pierre M, Boisson B, Meinnel T (**2000**). Identification of eukaryotic peptide deformylases reveals universality of N-terminal protein processing mechanisms. **EMBO J.** 19: 5916-5929. PMID: 11060042.

20. Serero A, Giglione C, Meinnel T (**2001**). Distinctive features of the two classes of eukaryotic peptide deformylases. **J. Mol. Biol.** 314: 695-708. PMID: 11733990.

21. Dirk LM, Williams MA, Houtz RL (**2002**). Specificity of chloroplast-localized peptide deformylases as determined with peptide analogs of chloroplast-translated proteins. **Arch. Biochem. Biophys.** 406: 135-141. PMID: 12234499.

22. Spector S, Flynn JM, Tidor B, Baker TA, Sauer RT (**2003**). Expression of N-formylated proteins in *Escherichia coli*. **Protein Expr. Purif.** 32: 317-322. PMID: 14965779.

23. Bingel-Erlenmeyer R, Kohler R, Kramer G, Sandikci A, Antolic S, Maier T, Schaffitzel C, Wiedmann B, Bukau B, Ban N (**2008**). A peptide deformylase-ribosome complex reveals mechanism of nascent chain processing. **Nature** 452: 108-111. doi: 10.1038/nature06683.

24. Selmer M, Liljas A (**2008**). Exit biology: battle for the nascent chain. **Structure** 16: 498-500. doi: 10.1016/j.str.2008.03.002.

25. Dirk LM, Schmidt JJ, Cai Y, Barnes JC, Hanger KM, Nayak NR, Williams MA, Grossman RB, Houtz RL, Rodgers DW (**2008**). Insights into the substrate specificity of plant peptide deformylase, an essential enzyme with potential for the development of novel biotechnology applications in agriculture. **Biochem. J.** 413: 417-427. doi: 10.1042/BJ20071641.

26. Sandikci A, Gloge F, Martinez M, Mayer MP, Wade R, Bukau B, Kramer G (**2013**). Dynamic enzyme docking to the ribosome coordinates N-terminal processing with polypeptide folding. **Nat. Struct. Mol. Biol.** 20: 843-850. doi: 10.1038/nsmb.2615.

27. Frank JA, Lorimer D, Youle M, Witte P, Craig T, Abendroth J, Rohwer F, Edwards RA, Segall AM, Burgin AB, Jr. (**2013**). Structure and function of a cyanophage-encoded peptide deformylase. **ISME J.** 7: 1150-1160. doi: 10.1038/ismej.2013.4.

28. Oh E, Becker AH, Sandikci A, Huber D, Chaba R, Gloge F, Nichols RJ, Typas A, Gross CA, Kramer G, Weissman JS, Bukau B (**2011**). Selective ribosome profiling reveals the cotranslational chaperone action of trigger factor in vivo. **Cell** 147: 1295-1308. doi: 10.1016/j.cell.2011.

29. Hoffmann A, Bukau B, Kramer G (**2010**). Structure and function of the molecular chaperone trigger factor. **Biochim. Biophys. Acta** 1803: 650-661. doi: 10.1016/j.bbamcr.2010.01.017.

30. Cabrita LD, Dobson CM, Christodoulou J (**2010**). Protein folding on the ribosome. **Curr. Op Struct. Biol.** 20: 33-45. doi: 10.1016/j.sbi.2010.01.005.

31. Lakshmipathy SK, Gupta R, Pinkert S, Etchells SA, Hartl FU (**2010**). Versatility of trigger factor interactions with ribosome-nascent chain complexes. **J. Biol. Chem.** 285: 27911-27923. doi: 10.1074/jbc.M110.134163.

32. Hoffmann A, Becker AH, Zachmann-Brand B, Deuerling E, Bukau B, Kramer G (**2012**). Concerted action of the ribosome and the associated chaperone trigger factor confines nascent polypeptide folding. **Mol. Cell** 48: 63-74. doi: 10.1016/j.molcel.2012.07.018.

33. O'Brien EP, Christodoulou J, Vendruscolo M, Dobson CM (**2012**). Trigger factor slows cotranslational folding through kinetic trapping while sterically protecting the nascent chain from aberrant cytosolic interactions. **J. Am. Chem. Soc.**: 10920-10932. doi: 10.1021/ja302305u.

34. Martinez-Hackert E, Hendrickson WA (**2009**). Promiscuous substrate recognition in folding and assembly activities of the trigger factor chaperone. **Cell** 138: 923-934. doi: 10.1016/j.cell.2009.07.044.

35. Rutkowska A, Mayer MP, Hoffmann A, Merz F, Zachmann-Brand B, Schaffitzel C, Ban N, Deuerling E, Bukau B (**2008**). Dynamics of trigger factor interaction with translating ribosomes. **J. Biol. Chem.** 283: 4124-4132. PMID: 18045873.

36. Merz F, Boehringer D, Schaffitzel C, Preissler S, Hoffmann A, Maier T, Rutkowska A, Lozza J, Ban N, Bukau B, Deuerling E (**2008**). Molecular mechanism and structure of Trigger Factor bound to the translating ribosome. **EMBO J.** 27: 1622-1632. doi: 10.1038/emboj.2008.89.

37. Kaiser CM, Chang HC, Agashe VR, Lakshmipathy SK, Etchells SA, Hayer-Hartl M, Hartl FU, Barral JM (**2006**). Real-time observation of trigger factor function on translating ribosomes. **Nature** 444: 455-460. PMID: 17051157.

38. Baram D, Pyetan E, Sittner A, Auerbach-Nevo T, Bashan A, Yonath A (**2005**). Structure of trigger factor binding domain in biologically homologous complex with eubacterial ribosome reveals its chaperone action. **Proc. Natl. Acad. Sci. USA** 102: 12017-12022. PMID: 16091460.

39. Liu C-P, Perrett S, Zhou J-M (**2005**). Dimeric trigger factor stably binds folding-competent intermediates and cooperates with the DnaK-DnaJ-GrpE chaperone system to allow refolding. **J. Biol. Chem.** 280: 13315-13320. PMID: 15632130.

40. Agashe VR, Guha S, Chang HC, Genevaux P, Hayer-Hartl M, Stemp M, Georgopoulos C, Hartl FU, Barral JM (**2004**). Function of trigger factor and DnaK in multidomain protein folding: increase in yield at the expense of folding speed. **Cell** 117: 199-209. PMID: 15084258.

41. Kim YE, M.S. H, Bracher A, Hayer-Hartl M, Hartl FU (**2013**). Molecular chaperone functions in protein folding and proteostasis. **Annu. Rev. Biochem.** 82: 323-355. doi: 10.1146/annurev-biochem-060208-092442.

42. Bornemann T, Holtkamp W, Wintermeyer W (**2014**). Interplay between trigger factor and other protein biogenesis factors on the ribosome. **Nature communications** 5: 4180. doi: 10.1038/ncomms5180.

43. Shan SO, Walter P (**2005**). Co-translational protein targeting by the signal recognition particle. **FEBS Lett.** 579: 921-926. PMID: 15680975.

44. Zhang X, Shan SO (**2014**). Fidelity of cotranslational protein targeting by the signal recognition particle. **Annu. Rev. Biophysics.** 43: 381-408. doi: 10.1146/annurev-biophys-051013-022653.

45. Ariosa A, Lee JH, Wang S, Saraogi I, Shan SO (**2015**). Regulation by a chaperone improves substrate selectivity during cotranslational protein targeting. **Proc. Natl. Acad. Sci. USA** 112: E3169-E3178. doi: 10.1073/pnas.1422594112.

46. Solbiati J, Chapman-Smith A, Miller JL, Miller CG, Cronan JE, Jr. (**1999**). Processing of the N-termini of nascent polypeptide chains requires deformylation prior to methionine removal. **J. Mol. Biol.** 290: 607-614. PMID: 10395817.

47. Frottin F, Martinez A, Peynot P, Mitra S, Holz RC, Giglione C, Meinnel T (**2006**). The proteomics of N-terminal methionine cleavage. **Mol. Cell. Proteomics** 5: 2336-2349. PMID: 16963780.

48. Xiao Q, Zhang F, Nacev BA, Liu JO, Pei D (**2010**). Protein N-terminal processing: substrate specificity of *Escherichia coli* and human methionine aminopeptidases. **Biochemistry** 49: 5588-5599. doi: 10.1021/bi1005464.

49. Spencer PS, Siller E, Anderson JF, Barral JM (**2012**). Silent substitutions predictably alter translation elongation rates and protein folding efficiencies. **J. Mol. Biol.** 422: 328-335. doi: 10.1016/j.jmb.2012.06.010.

50. Zhang G, Ignatova Z (**2011**). Folding at the birth of the nascent chain: coordinating tranlation with co-translational folding. **Curr. Op. Struct. Biol.** 21: 25-31. doi: 10.1016/j.sbi.2010.10.008.

51. Wohlgemuth I, Pohl C, Rodnina MV (**2010**). Optimization of speed and accuracy of decoding in translation. **EMBO J.** 29: 3701-3709. doi: 10.1038/emboj.2010.229.

52. Proshkin S, Rahmouni AR, Mironov A, Nudler E (**2010**). Cooperation between translating ribosomes and RNA polymerase in transcription elongation. **Science** 328: 504-508. doi: 10.1126/science.1184939.

53. Guenneugues M, Caserta E, Brandi L, Spurio R, Meunier S, Pon CL, Boelens R, Gualerzi CO (**2000**). Mapping the fMet-tRNA(f)(Met) binding site of initiation factor IF2. **EMBO J.** 19: 5233-5240. PMID: 11013225.

54. Milon P, Carotti M, Konevega AL, Wintermeyer W, Rodnina MV, Gualerzi CO (**2010**). The ribosome-bound initiation factor 2 recruits initiator tRNA to the 30S initiation complex. **EMBO Rep.** 11: 312-316. doi: 10.1038/embor.2010.12.

55. Pavlov MY, Zorzet A, Andersson DI, Ehrenberg M (**2011**). Activation of initiation factor 2 by ligands and mutations for rapid docking of ribosomal subunits. **EMBO J.** 30: 289-301. doi: 10.1038/emboj.2010.328.

56. Nilsson AI, Zorzet A, Kanth A, Dahlström S, Berg OG, Andersson DI (**2006**). Reducing the fitness cost of antibiotic resistance by amplification of initiator tRNA genes. **Proc. Natl. Acad. Sci. USA** 103: 6976-6981. PMID: 16636273.

57. Steiner-Mosonyi M, Creuzenet C, Keates RA, Strub BR, Mangroo D (**2004**). The *Pseudomonas aeruginosa* initiation factor IF-2 is responsible for formylation-independent protein initiation in *P. aeruginosa*. **J. Biol. Chem.** 279: 52262-55229. PMID: 15385567.

58. Newton DT, Creuzenet C, Mangroo D (**1999**). Formylation is not essential for initiation of protein synthesis in all eubacteria. **J. Biol. Chem.** 274: 22143-22146. PMID: 10428776.

59. Brannigan JA, Dodson G, Duggleby HJ, Moody PC, Smith JL, Tomchick DR, Murzin AG (**1995**). A protein catalytic framework with an N-terminal nucleophile is capable of self-activation. **Nature** 378: 416-419. PMID: 7477383.

60. Bufe B, Schumann T, Kappl R, Bogeski I, Kummerow C, Podgórska M, Smola S, Hoth M, Zufall F (**2015**). Recognition of bacterial signal peptides by mammalian formyl peptide receptors: a new mechanism for sensing pathogens. **J. Biol. Chem.** 290: 7369-7387. doi: 10.1074/jbc.M114.626747.

61. Migeotte I, Communi D, Parmentier M (**2006**). Formyl peptide receptors: a promiscuous subfamily of G protein-coupled receptors controlling immune responses. **Cytokine Growth Factor Rev.** 17: 501-519. PMID: 17084101.

62. Varshavsky A (**1991**). Naming a targeting signal. **Cell** 64: 13-15. PMID: 1986863.

63. Bachmair A, Finley D, Varshavsky A (**1986**). *In vivo* half-life of a protein is a function of its amino-terminal residue. **Science** 234: 179-186. PMID: 3018930.

64. Bachmair A, Varshavsky A (**1989**). The degradation signal in a short-lived protein. **Cell** 56: 1019-1032. PMID: 2538246.

65. Hu R-G, Sheng J, Xin Q, Xu Z, Takahashi TT, Varshavsky A (**2005**). The N-end rule pathway as a nitric oxide sensor controlling the levels of multiple regulators. **Nature** 437: 981-986. PMID: 16222293.

66. Hu R-G, Wang H, Xia Z, Varshavsky A (**2008**). The N-end rule pathway is a sensor of heme. **Proc. Natl. Acad. Sci. USA** 105: 76-81. PMID: 18162538.

67. Hwang CS, Shemorry A, Varshavsky A (**2010**). N-terminal acetylation of cellular proteins creates specific degradation signals. **Science** 327: 973-977. doi: 10.1126/science.1183147.

68. Shemorry A, Hwang CS, Varshavsky A (**2013**). Control of protein quality and stoichiometries by N-terminal acetylation and the N-end rule pathway. **Mol. Cell** 50: 540-551. doi: 10.1016/j.molcel.2013.03.018.

69. Kim HK, Kim RR, Oh JH, Cho H, Varshavsky A, Hwang CS (**2014**). The N-terminal methionine of cellular proteins as a degradation signal. **Cell** 156: 158-169. doi: 10.1016/j.cell.2013.11.031.

70. Park SE, Kim JM, Seok OH, Cho H, Wadas B, Kim SY, Varshavsky A, Hwang CS (**2015**). Control of mammalian G protein signaling by N-terminal acetylation and the N-end rule pathway. **Science** 347: 1249-1252. doi: 10.1126/science.aaa3844.

71. Varshavsky A (**2011**). The N-end rule pathway and regulation by proteolysis. **Prot. Sci.** 20: 1298-1345. doi: 10.1002/pro.666.

72. Tasaki TS, Sriram SM, Park KS, Kwon YT (**2012**). The N-end rule pathway. **Annu. Rev. Biochem.** 81: 261-289. doi: 10.1146/annurev-biochem-051710-093308.

73. Gibbs DJ, Bacardit J, Bachmair A, Holdsworth MJ (**2014**). The eukaryotic N-end rule pathway: conserved mechanisms and diverse functions. **Trends Cell Biol.** 24: 603-611. doi: 10.1016/j.tcb.2014.05.001.

74. Cha-Molstad H, Sung KS, Hwang J, Kim KA, Yu JE, Yoo YD, Jang JM, Han DH, Molstad M, Kim JG, Lee YJ, Zakrzewska A, Kim SH, Kim ST, Kim SY, Lee HG, Soung NK, Ahn JS, Ciechanover A, Kim BY, Kwon YT (**2015**). Amino-terminal arginylation targets endoplasmic reticulum chaperone BiP for autophagy through p62 binding. **Nat. Cell Biol.** 17: 917-929. doi: 10.1038/ncb3177.

75. Tobias JW, Shrader TE, Rocap G, Varshavsky A (**1991**). The N-end rule in bacteria. **Science** 254: 1374-1377. PMID: 1962196.

76. Graciet E, Hu RG, Piatkov K, Rhee JH, Schwarz EM, Varshavsky A (**2006**). Aminoacyl-transferases and the N-end rule pathway of prokaryotic/eukaryotic specificity in a human pathogen. **Proc. Natl. Acad. Sci. USA** 103: 3078-3083. PMID: 16492767.

77. Mogk A, Schmidt R, Bukau B (**2007**). The N-end rule pathway of regulated proteolysis: prokaryotic and eukaryotic strategies. **Trends Cell Biol.** 17: 165-172. PMID: 17306546.

78. Dougan DA, Micevski D, Truscott KN (**2011**). The N-end rule pathway: from recognition by N-recognins to destruction by AAA+ proteases. **Biochim. Biophys. Acta** 1823: 83-91. doi: 10.1016/j.bbamcr.2011.07.002.

79. Rivera-Rivera I, Román-Hernández G, Sauer RT, Baker TA (**2014**). Remodeling of a delivery complex allows ClpS-mediated degradation of N-degron substrates. **Proc. Natl. Acad. Sci. USA** 111: E3853-E3859. doi: 10.1073/pnas.1414933111.

80. Humbard MA, Surkov S, De Donatis GM, Jenkins L, Maurizi MR (**2013**). The N-degradome of *Escherichia coli*: limited proteolysis *in vivo* generates a large pool of proteins bearing N-degrons. **J. Biol. Chem.** 288: 28913-28924. doi: 10.1074/jbc.M113.492108.

81. Shrader TE, Tobias JW, Varshavsky A (**1993**). The N-end rule in *Escherichia coli*: cloning and analysis of the leucyl, phenylalanyl-tRNA-protein transferase gene *aat*. **J. Bact.** 175: 4364-4374. PMID: 8331068.

82. Erbse A, Schmidt R, Bornemann T, Schneider-Mergener J, Mogk A, Zahn R, Dougan DA, Bukau B (**2006**). ClpS is an essential component of the N-end rule pathway in *Escherichia coli*. **Nature** 439: 753-756. PMID: 16467841.

83. Suto K, Shimizu Y, Watanabe K, Ueda T, Fukai S, Nureki O, Tomita K (**2006**). Crystal structures of leucyl/phenylalanyl-tRNA-protein transferase and its complex with an aminoacyl-tRNA analog. **EMBO J.** 25: 5942-5950. PMID: 17110926.

84. Dong XK-M, M., Muramatsu T, Mori H, Shirouzu M, Bessho Y, Yokoyama S (**2007**). The crystal structure of leucyl/phenylalanyl-tRNA-protein transferase from Escherichia coli **Prot. Sci.** 16: 528-534. PMID: 17242373.

85. Wang KH, Roman-Hernandez G, Grant RA, Sauer TT, Baker TA (**2008**). The molecular basis of N-end rule recognition. **Mol. Cell** 32: 406-414. doi: 10.1016/j.molcel.2008.08.032.

86. Wang KH, Oakes ESC, Sauer RT, Baker TA (**2008**). Tuning the strength of a bacterial N-end rule signal. **J. Biol. Chem.** 283: 24600-24607. doi: 10.1074/jbc.M802213200.

87. Hou JY, Sauer RT, Baker TA (**2008**). Distinct structural elements of the adaptor ClpS are required for regulating degradation by ClpAP. **Nat. Struct. Mol. Biol.** 15: 288-294. doi: 10.1038/nsmb.1392.

88. Schmidt R, Zahn R, Bukau B, Mogk A (**2009**). ClpS is the recognition component for *Escherichia coli* substrates of the N-end rule degradation pathway. **Mol. Microbiol.** 72: 506-517. doi: 10.1111/j.1365-2958.2009.06666.x.

89. Román-Hernández G, Grant RA, Sauer RT, Baker TA (**2009**). Molecular basis of substrate selection by the N-end rule adaptor protein ClpS. **Proc. Natl. Acad. Sci. USA** 106: 8888-8893. doi: 10.1073/pnas.0903614106.

90. Schuenemann VJ, Kralik SM, Albrecht R, Spall SK, Truscott KN, Dougan DA, Zeth K (**2009**). Structural basis of N-end rule substrate recognition in *Escherichia coli* by the ClpAP adaptor protein ClpS. **EMBO Rep.** 10: 508-514. doi: 10.1038/embor.2009.62.

91. Ninnis RL, Spall SK, Talbo GH, Truscott KN, Dougan DA (**2009**). Modification of PATase by L/F-transferase generates a ClpS-dependent N-end rule substrate in *Escherichia coli*. **EMBO J.** 28: 1732-1744. doi: 10.1038/emboj.2009.134.

92. Román-Hernández G, Hou JY, Grant RA, Sauer RT, Baker TA (**2011**). The ClpS adaptor mediates staged delivery of N-end rule substrates to the AAA+ ClpAP protease. **Mol. Cell** 43: 217-228. doi: 10.1016/j.molcel.2011.06.009.

93. Fung AW, Fahlman RP (**2015**). The molecular basis for the post-translational addition of amino acids by L/F-transferase in the N-end rule pathway. **Curr. Prot. Pept. Sci.** 16: 163-180. PMID: 25579118.

94. Kwon YT, Kashina AS, Varshavsky A (**1999**). Alternative splicing results in differential expression, activity, and localization of the two forms of arginyl-tRNA-protein transferase, a component of the N-end rule pathway. **Mol. Cell. Biol.** 19: 182-193. PMID: 9858543.

95. Piatkov KI, Brower CS, Varshavsky A (**2012**). The N-end rule pathway counteracts cell death by destroying proapoptotic protein fragments. **Proc. Natl. Acad. Sci. USA** 109: E1839-E1847. doi: 10.1073/pnas.1207786109.

96. Piatkov KI, Colnaghi L, Bekes M, Varshavsky A, Huang TT (**2012**). The auto-generated fragment of the Usp1 deubiquitylase is a physiological substrate of the N-end rule pathway. **Mol. Cell** 48: 926-933. doi: 10.1016/j.molcel.2012.10.012.

97. Brower CS, Piatkov KI, Varshavsky A (**2013**). Neurodegeneration-associated protein fragments as short-lived substrates of the N-end rule pathway. **Mol. Cell** 50: 161-171. doi: 10.1016/j.molcel.2013.02.009.

98. Wang H, Piatkov KI, Brower CS, Varshavsky A (**2009**). Glutamine-specific N-terminal amidase, a component of the N-end rule pathway. **Mol. Cell** 34: 686-695. doi: 10.1016/j.molcel.2009.04.032.

99. Kwon YT, Kashina AS, Davydov IV, Hu R-G, An JY, Seo JW, Du F, Varshavsky A (**2002**). An essential role of N-terminal arginylation in cardiovascular development. **Science** 297: 96-99. PMID: 12098698.

100. Gautschi M, Just S, Mun A, Ross S, Rücknagel P, Dubaquié Y, Ehrenhofer-Murray A, Rospert S (**2003**). The yeast N-alpha-acetyltransferase NatA is quantitatively anchored to the ribosome and interacts with nascent polypeptides. **Mol. Cell. Biol.** 23: 7403-7414. PMID: 14517307.

101. Polevoda B, Brown S, Cardillo TS, Rigby S, Sherman F (**2008**). Yeast N(alpha)-terminal acetyltransferases are associated with ribosomes. **J. Cell. Biochem.** 103: 492-508. PMID: 17541948.

102. Aksnes H, Hole K, Arnesen T (**2015**). Molecular, cellular, and physiological significance of N-terminal acetylation. **Int. Rev. Cell Mol. Biol.** 316: 267-305. doi: 10.1016/bs.ircmb.2015.01.001.

103. Arnesen T, Van Damme P, Polevoda B, Helsens K, Evjenth R, Colaert N, Varhaug JE, Vandekerckhove J, Lillehaug JR, Sherman F, Gevaert K (**2009**). Proteomics analyses reveal the evolutionary conservation and divergence of N-terminal acetyltransferases from yeast to humans. **Proc. Natl. Acad. Sci. USA** 106: 8157-8162. doi: 10.1073/pnas.0901931106.

104. Dorfel MJ, Lyon GJ (**2015**). The biological functions of Naa10 - From amino-terminal acetylation to human disease. **Gene** 567: 103-131. doi: 10.1016/j.gene.2015.04.085.

105. Starheim KK, Gevaert K, Arnesen T (**2012**). Protein N-terminal acettyltransferases: when the start matters. **Trends Biochem. Sci.** 37: 152-161. doi: 10.1016/j.tibs.2012.02.003.

106. Van Damme P, Evjenth R, Foyn H, Demeyer K, De Bock PJ, Lillehaug JR, Vandekerckhove J, Arnesen T, Gevaert K (**2011**). Proteome-derived peptide libraries allow detailed analysis of the substrate specificities of N(alpha)-acetyltransferases and point to hNaa10p as the post-translational actin N(alpha)-acetyltransferase. **Mol. Cell. Proteomics** 10: M110.004580. doi: 10.1074/mcp.M110.004580.

107. Jones JD, O'Connor CD (**2011**). Protein acetylation in prokaryotes. **Proteomics** 11: 3012-3022. doi: 10.1002/pmic.201000812.

108. Bienvenut WV, Giglione C, Meinnel T (**2015**). Proteome-wide analysis of the amino terminal status of *Escherichia coli* proteins at the steady-state and upon deformylation inhibition. **Proteomics** 15: 2503-2518. doi: 10.1002/pmic.201500027.

109. Giglione C, Vallon O, Meinnel T (**2003**). Control of protein life-span by N-terminal methionine excision. **EMBO J.** 22: 13-23. PMID: 12505930.

110. Adam Z, Frottin F, Espagne C, Meinnel T, Giglione C (**2011**). Interplay between N-terminal methionine excision and FtsH protease is essential for normal chloroplast

development and function in Arabidopsis. **The Plant cell** 23: 3745-3760. doi: 10.1105/tpc.111.087239.

111. Suzuki T, Varshavsky A (**1999**). Degradation signals in the lysine-asparagine sequence space. **EMBO J.** 18: 6017-6026. PMID: 10545113.

112. Ausubel FM, Brent R, Kingston RE, Moore DD, Smith JA, Seidman JG, Struhl K (**2010**). Current Protocols in Molecular Biology. Wiley-Interscience, New York. doi: 10.1002/0471142727.mb0718s108.

113. Varshavsky A (**2005**). Ubiquitin fusion technique and related methods. **Meth. Enzymol.** 399: 777-799. PMID: 16338395.

114. Piatkov K, Graciet E, Varshavsky A (**2013**). Ubiquitin reference technique and its use in ubiquitin-lacking prokaryotes. **PLoS One** 8: e67952. doi: 10.1371/journal.pone.0067952.

115. Compton LA, Davis JM, Macdonald JR, Bachinger HP (**1992**). Structural and functional characterization of *Escherichia coli* peptidyl-prolyl cis-trans isomerases. **Eur. J. Biochem.** 206: 927-934. PMID: 1606970.

116. Baker RT, Varshavsky A (**1991**). Inhibition of the N-end rule pathway in living cells. **Proc. Natl. Acad. Sci. USA** 87: 2374-2378. PMID: 1899923.

117. Piatkov KI, Oh J-H, Liu Y, Varshavsky A (**2014**). Calpain-generated natural protein pragments as short-lived substrates of the N-end rule pathway. **Proc. Natl. Acad. Sci. USA** 111: E817-E826. doi: 10.1073/pnas.1401639111.

118. Turner GC, Varshavsky A (**2000**). Detecting and measuring cotranslational protein degradation *in vivo*. **Science** 289: 2117-2120. PMID: 11000112.

119. Milligan DL, Koshland DE (**1990**). The amino terminus of the aspartate chemoreceptor is formylmethionine. **J. Biol. Chem.** 265: 4455-4460. PMID: 2155229.

120. Metlitskaya A, Kazakov T, Vondenhoff GH, Novikova M, Shashkov A, Zatsepin T, Semenova E, Zaitseva N, Ramensky V, Van Aerschot A, Severinov K (**2009**). Maturation

of the translation inhibitor microcin-C. **J. Bacteriol.** 191: 2380-2387. doi: 10.1128/JB.00999-08.

121. Bandow JE, Becher D, Büttner K, Hochgräfe F, Freiberg C, H. B, Hecker M (**2003**). The role of peptide deformylase in protein biosynthesis: a proteomic study. **Proteomics** 3: 299-306. PMID: 12627383.

122. Wang W, White R, Yuan Z (**2006**). Proteomic study of peptide deformylase inhibition in *Streptococcus pneumoniae* and *Staphylococcus aureus*. **Antimicrob. Agents. Chemother.** 50: 1656-1663. PMID: 16641432.

123. Sauer RT, Baker TA (**2011**). AAA+ Proteases: ATP-Fueled Machines of Protein Destruction. **Annu. Rev. Biochem.** 80: 587-612. doi: 10.1146/annurev-biochem-060408-172623.

124. Lobanov M, Bogatyreva NS, Galzitskaia OV (**2008**). Radius of gyration is indicator of compactness of protein structure. **Mol. Biol. (Russia)** 42: 701-706. PMID: 18856071.

125. Ptitsyn OB (**1995**). Molten globule and protein folding. **Adv. Prot. Chem.** 47: 83-229.

126. Zhang Z, Kulkarni K, Hanrahan SJ, Thompson AJ, Barford D (**2010**). The APC/C subunit Cdc16/Cut9 is a contiguous tetratricopeptide repeat superhelix with a homodimer interface. **EMBO J.** 29: 3733-3744. doi: 10.1038/emboj.2010.247.

127. Scott DC, Monda JK, Bennett EJ, Harper JW, Schulman BA (**2011**). N-terminal acetylation acts as an avidity enhancer within an interconnected multiprotein complex. **Science** 334: 674-678. doi: 10.1126/science.1209307.

128. Monda JK, Scott DC, Miller DJ, Lydeard J, King D, Harper JW, Bennett EJ, Schulman BA (**2012**). Structural conservation of distinctive N-terminal acetylation-dependent interactions across a family of mammalian NEDD8 ligation enzymes. **Structure** 21: 1-12. doi: 10.1016/j.str.2012.10.013.

129. Zaher HS, Green R (**2009**). Quality control by the ribosome following peptide bond formation. **Nature** 457: 161-166. doi: 10.1038/nature07582.

130. Eyler DE, Green R (**2011**). Distinct response of yeast ribosomes to a miscoding event during translation. **RNA (New York, N.Y.)** 17: 925-932. doi: 10.1261/rna.2623711.

131. Bittner LM, Westphal K, Narberhaus F (**2015**). Conditional proteolysis of the membrane protein YfgM by the FtsH protease depends on a novel N-terminal degron. **J. Biol. Chem.** 290: 19367-19378. doi: 10.1074/jbc.M115.648550.

132. Datsenko KA, Wanner BL (**2000**). One-step inactivation of chromosomal genes in *Escherichia coli* K-12 using PCR products. **Proc. Natl. Acad Sci. USA** 97: 6640-6645. PMID: 10829079.

FIGURE LEGENDS

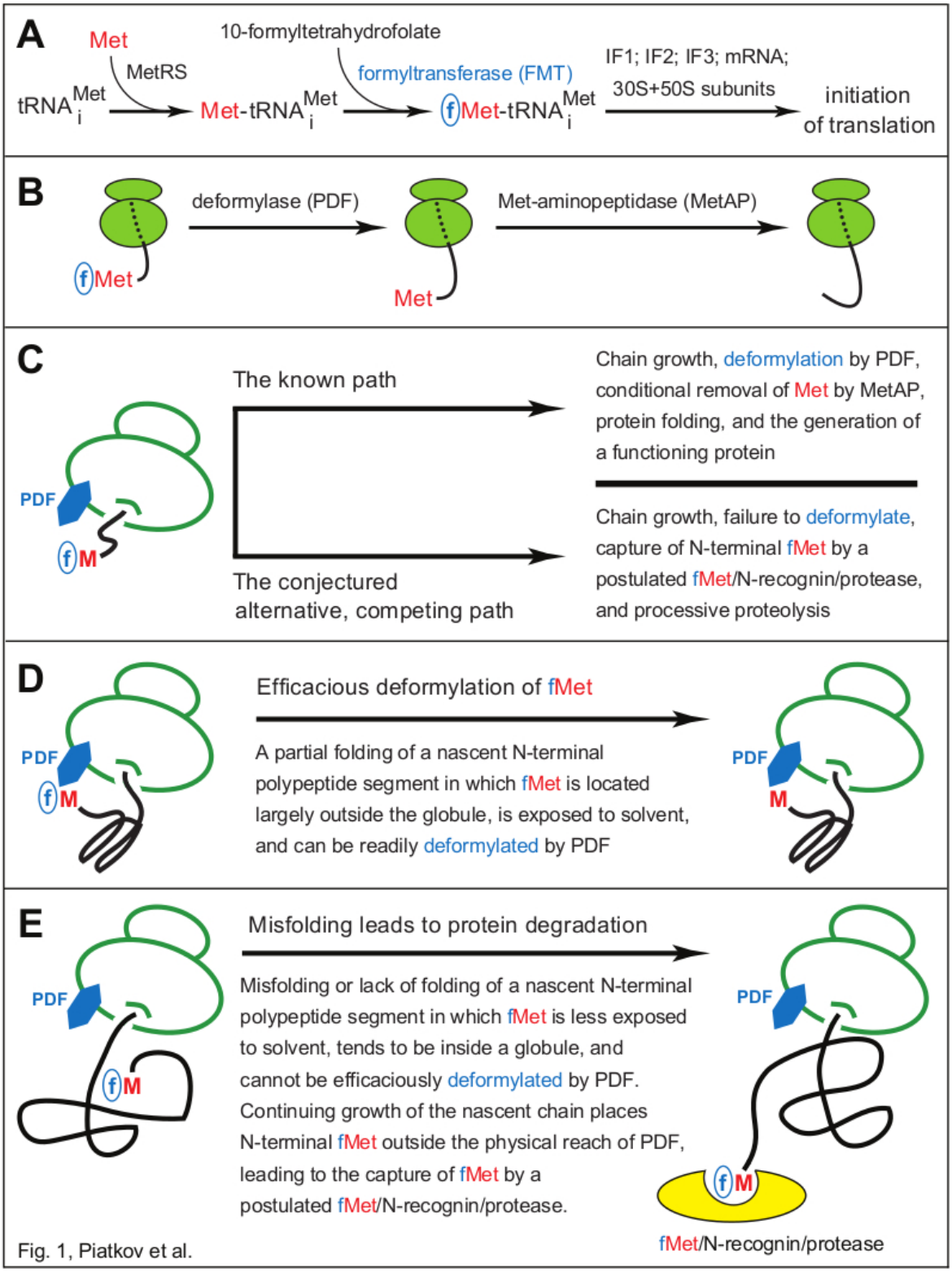

Fig. 1, Piatkov et al.

Figure 2.1. The working model of fMet/N-degrons. (A) Pretranslational enzymatic steps that result in formyl-Met (fMet) becoming the first residue of a nascent bacterial polypeptide. MetRS, Met-tRNA synthetase. IF proteins, initiation factors. **(B)** Translating ribosomes, with reversibly associated (not depicted) deformylase (PDF) and Met-aminopeptidase (MetAP) competing for their overlapping binding sites near the exit from the ribosomal tunnel. High-affinity binding by the TF chaperone to a nascent polypeptide chain occurs once its length exceeds ~100 residues, usually after deformylation of N-terminal Met. A nascent chain, depicted unfolded in this diagram, tends to become unstably folded as it emerges from the tunnel. The rate of the MetAP-mediated removal of the deformylated N-terminal Met residue depends on the identity of a residue at position 2. **(C-E)** Self-explanatory descriptions of the working model of fMet/N-degrons. See the main text for additional details and relevant citations.

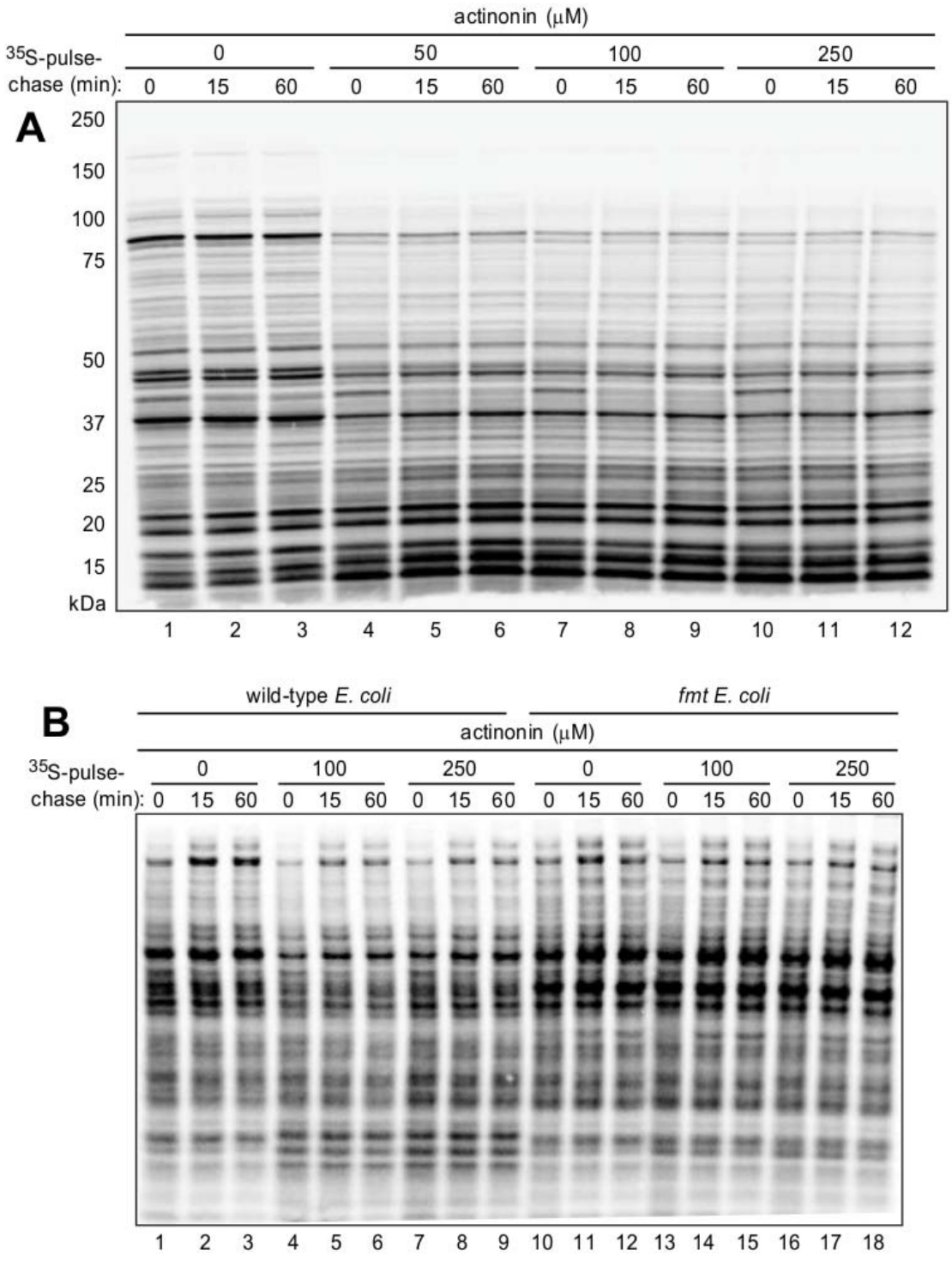

Fig. 2, Piatkov et al.

Figure 2.2. Pulse-chase analyses in wild-type and formylation-lacking *fmt E. coli* in the absence or presence of actinonin, an inhibitor of deformylation. (A) Wild-type *E. coli* were pulse-labeled with ^{35}S-methionine/cysteine for 1 min, followed by a chase (in the presence of chloramphenicol, a translation inhibitor) for indicated times, extraction of proteins, SDS-PAGE, and autoradiography. Pulse-chases were carried out either in the absence of actinonin (lanes 1-3) or in the presence of increasing concentrations of actinonin (lanes 4-12). Molecular masses of protein markers are indicated on the left. **(B)** Same as in **A** but pulse-chases were carried out in the absence of chloramphenicol in wild-type cells (lanes 1-9) and congenic *fmt E. coli* (lanes 10-18).

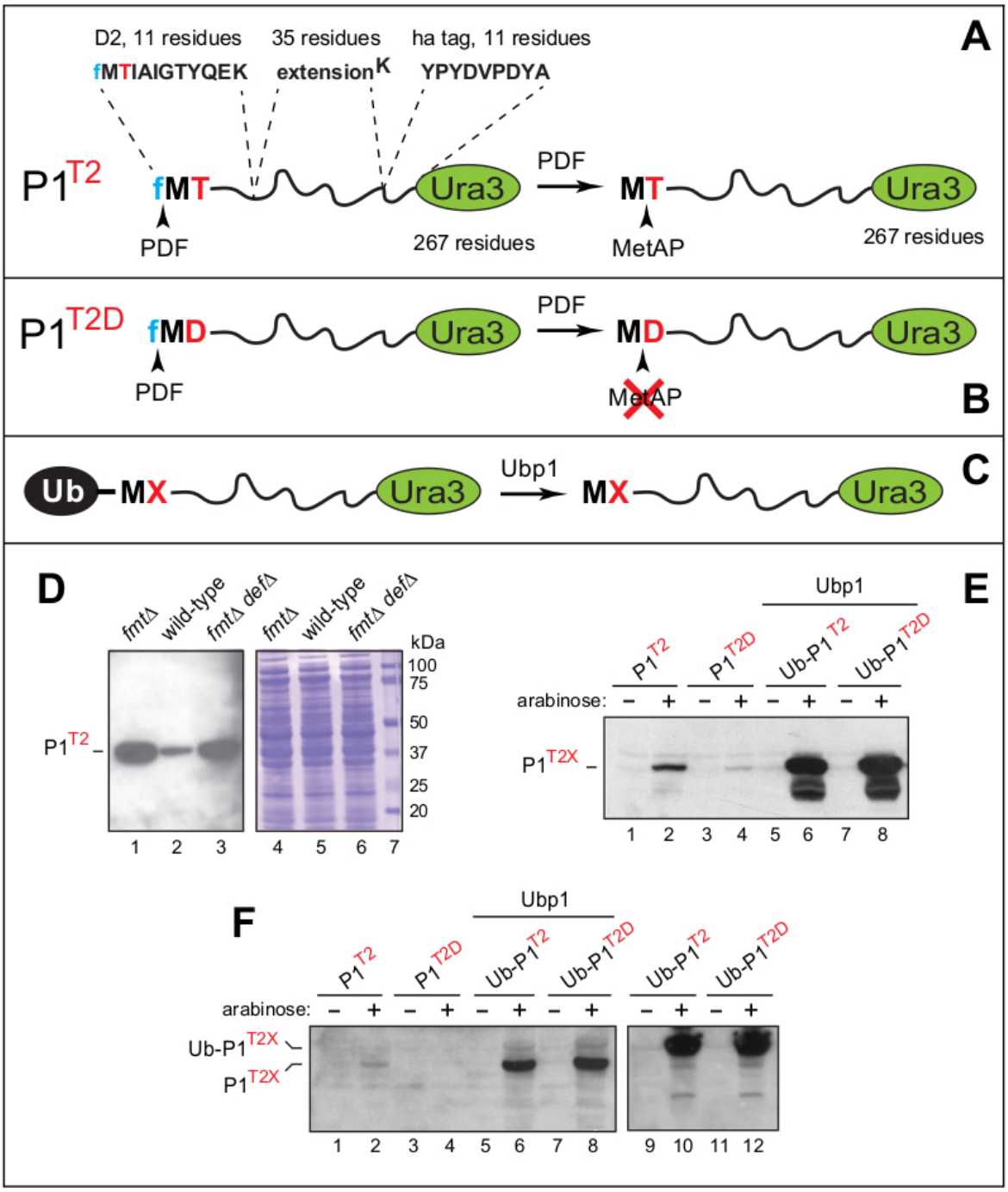

Fig. 3, Piatkov et al.

Figure 2.3. Analyses of reporter proteins in wild-type and formylation-lacking *fmt E. coli*. **(A)** Design of the $P1^{T2}$ ($D2^{1-11}$-eK-ha-Ura3) reporter protein. The term $P1^{T2}$ (protein-1 containing Thr at position 2) denotes a chimeric reporter containing the indicated N-terminal segments upstream of the 267-residue *S. cerevisiae* Ura3 moiety. Arrowheads indicate deformylation of N-terminal fMet by the PDF deformylase and the subsequent removal of Met by MetAP. See the main text for details. **(B)** Same as in **A** but the otherwise identical $P1^{T2D}$ reporter contains Asp (D) at position 2. The rate of PDF-mediated deformylation of N-terminal fMet with Asp at position 2 is at least 10-fold lower than the rate of deformylation with Thr at position 2. Another difference between $P1^{T2}$ and $P1^{T2D}$ is the retention of N-terminal Met in $P1^{T2D}$. See the main text for details and citations. **(C)** The use of ubiquitin (Ub) fusions to generate $P1^{T2}$ and $P1^{T2D}$ through the removal of the N-terminal Ub moiety by the *S. cerevisiae* Ubp1 deubiquitylase expressed in *E. coli*. **(D)** Immunoblotting analyses, after SDS-PAGE, of the $P1^{T2}$ reporter protein expressed in *fmt* (lane 1), wild-type (lane 2) and *fmt def* (lane 3) *E. coli*. Lanes 4-6, the corresponding total protein patterns (Coomassie staining). Lane 7, molecular mass markers. **(E)** Immunoblotting analyses, after SDS-PAGE, of the $P1^{T2}$ and $P1^{T2D}$ reporters expressed from the P_{ara} promoter in wild-type *E. coli* (lanes 1-4), and of the Ub fusions Ub-$P1^{T2}$ and Ub-$P1^{T2D}$ in wild-type *E. coli* expressing the *S. cerevisiae* Ubp1 deubiquitylase (lanes 5-8). (F) Same as in **E**, but independent experiments, in addition to expressing Ub-$P1^{T2}$ and Ub-$P1^{T2D}$ in the absence of coexpressed yeast Ubp1 (lanes 9-12). See the main text for details and citations.

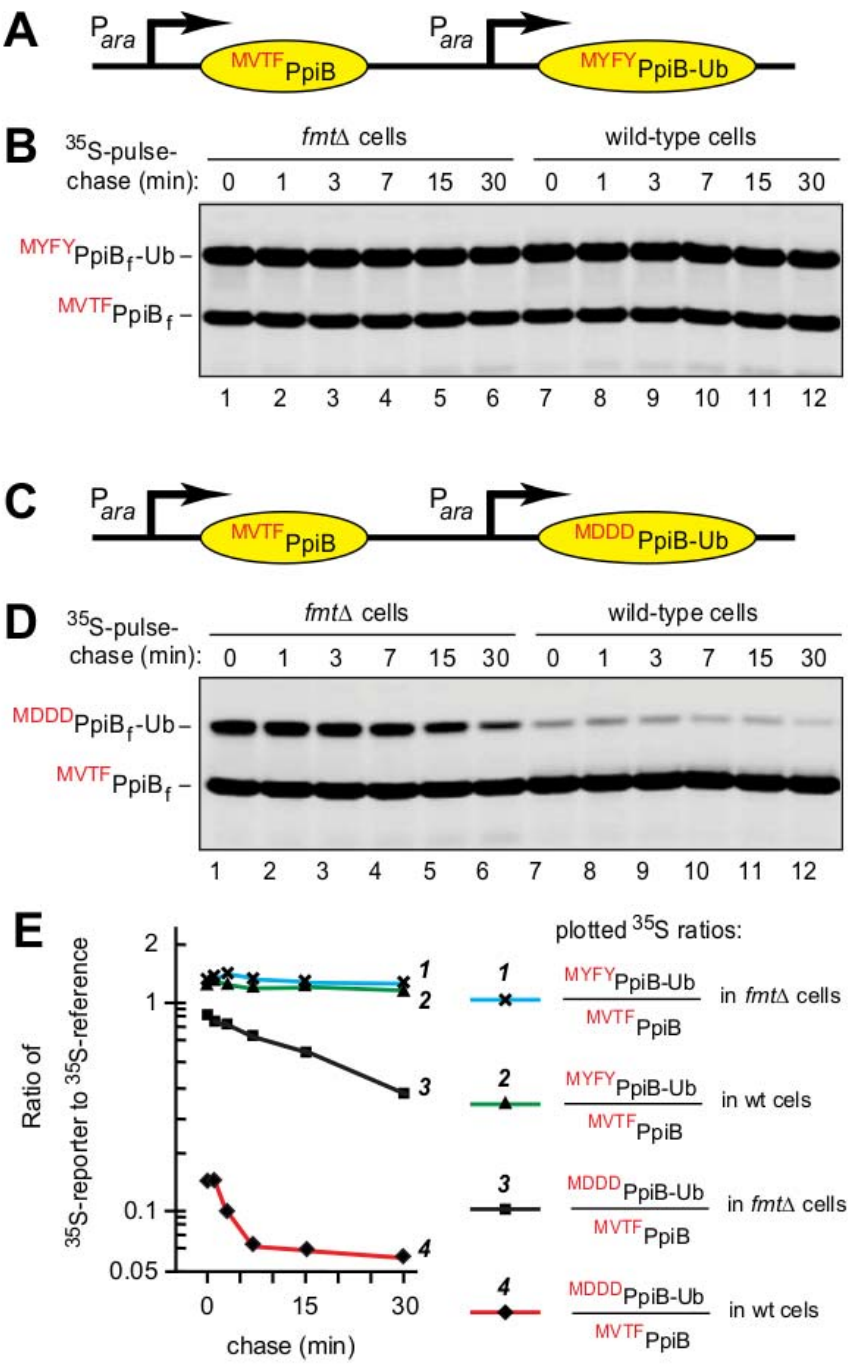

Fig. 4, Piatkov et al.

Figure 2.4. Formylation-dependent selective destabilization of PpiB-based reporter proteins. (A) Diagram of the expression cassette in which two identical tandem P_{ara} promoters express the C-terminally flag-tagged PpiB reference protein $^{\mathrm{MVTF}}_{\mathrm{wt}}\mathrm{PPiB_f}$ and the reporter protein $^{\mathrm{MYFY}}\mathrm{PpiB_f}$-Ub (reporter-1). The latter differs from $^{\mathrm{MVTF}}_{\mathrm{wt}}\mathrm{PPiB_f}$ by three amino acid residues adjacent to N-terminal fMet, and by the presence of C-terminal Ub moiety, added to make the two proteins distinguishable by size. **(B)** Lanes 1-6, formylation-lacking *fmt E. coli* were pulse-labeled with ^{35}S-methionine/cysteine for 1 min, followed by a chase (in the absence of chloramphenicol) for indicated times, extraction of proteins, immunoprecipitation with a monoclonal anti-flag antibody, SDS-PAGE, and autoradiography. Lanes 7-12, same but in wild-type *E. coli*. **(C)** Same as in **A**, with the reference $^{\mathrm{MVTF}}_{\mathrm{wt}}\mathrm{PPiB_f}$ and the reporter $^{\mathrm{MDDD}}\mathrm{PpiB_f}$-Ub (reporter-2), which differed from $^{\mathrm{MYFY}}\mathrm{PpiB_f}$-Ub in **A** and **B** by three residues (Asp-Asp-Asp) downstream from N-terminal fMet. **(D)** Same as in **B** but with $^{\mathrm{MVTF}}_{\mathrm{wt}}\mathrm{PPiB_f}$ and $^{\mathrm{MDDD}}\mathrm{PpiB_f}$-Ub (reporter-2). See the main text for the logic and details of these experiments.

SUPPLEMENTAL MATERIALS

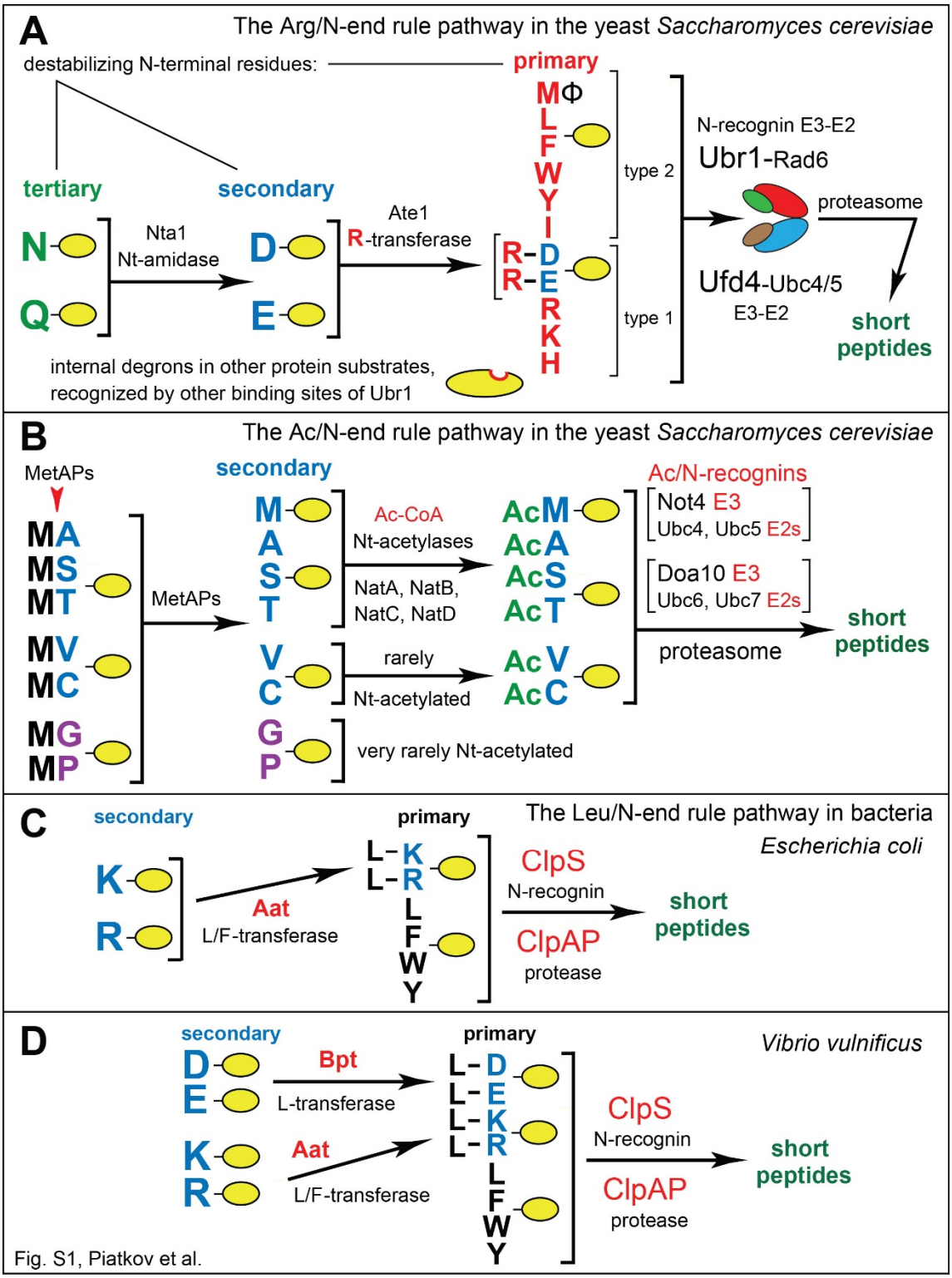

Fig. S1, Piatkov et al.

Figure S2.1. The Arg/N-End Rule Pathway and the Ac/N-End Rule Pathway. N-terminal residues are indicated by single-letter abbreviations. A yellow oval denotes the rest of a protein substrate. The N-end rule pathway recognizes proteins containing N-terminal degradation signals called N-degrons, polyubiquitylates these proteins and thereby causes their degradation by the 26S proteasome. Recognition components of the N-end rule pathway are called N-recognins. Eukaryotic N-recognins are E3 ubiquitin (Ub) ligases that can target N-degrons. The main determinant of an N-degron is a destabilizing N-terminal residue of a protein. In eukaryotes, the N-end rule pathway consists of two branches, described in panels **A** and **B**.

(A) The Arg/N-end rule pathway in *S. cerevisiae* [1-5]. The prefix "Arg" in the pathway's name refers to Nt-arginylation of N-end rule substrates. The Arg/N-end rule pathway targets specific unacetylated N-terminal residues. It is mediated by the Ubr1 N-recognin, a 225 kDa RING-type E3 Ub ligase and a part of the targeting complex containing the Ubr1-Rad6 and Ufd4-Ubc4/5 holoenzymes. The Ubr1 (N-recognin) component of this complex recognizes (binds to) the "primary" destabilizing N-terminal residues Arg, Lys, His, Leu, Phe, Tyr, Trp and Ile, as well as the unmodified N-terminal Met residue, if Met is followed by a bulky hydrophobic (Φ) residue [5]. The terms "secondary" and "tertiary" refer to the indicated enzymatic modifications of specific N-terminal residues. N-terminal Cys can be arginylated by the Ate1 arginyltransferase (R-transferase) only after the oxidation of Cys to Cys-sulfinate or Cys-sulfonate, in reactions that involve nitric oxide (NO) and oxygen [2-4, 6, 7]. Regulated oxidation of N-terminal Cys takes place in multicellular eukaryotes but not in fungi such as *S. cerevisiae*, which apparently do not produce NO under normal conditions.

(B) The Ac/N-end rule pathway in *S. cerevisiae* [3, 5, 8-10]. This pathway recognizes substrates through their N^{α}-terminally acetylated (Nt-acetylated) residues. The corresponding degradation signals and E3 Ub ligases are called Ac/N-degrons and Ac/N-recognins, respectively. Red arrow on the left indicates the removal of N-terminal Met by Met-aminopeptidases (MetAPs). N-terminal Met is retained if a residue at position 2 is larger than Val [11-13]. The term "secondary" refers to the requirement for a

modification (Nt-acetylation) of a destabilizing N-terminal residue before a protein can be recognized by an Ac/N-recognin.

(C) and **(D)** The bacterial Leu/N-end rule pathway, in *Escherichia coli* **(C)** and in *Vibrio vulnificus* **(D)** [14-32]. The Aat L/F-transferase conjugates (largely) Leu to N-terminal Arg or Lys. N-end rule substrates bearing primary (bulky hydrophobic) destabilizing N-terminal residues are recognized by the ClpS N-recognin and are delivered for degradation to the ClpAP protease. In *V. vulnificus*, the Leu/N-end rule pathway contains both the Aat L/F-transferase and the Bpt L-transferase. As a result, N-terminal Asp and Glu, which are not destabilizing residues in *E. coli*, function as secondary destabilizing residues in *V. vulnificus* [16].

Regulated degradation of proteins or their natural fragments by the N-end rule pathway mediates a broad range of biological functions (refs. [2-5, 8-10, 31] and refs therein).

Table S2.1 Bacterial strains used in this study.

***E. coli* strains**	**Genotype**	**Source or Ref.**
MG1655	*F-* □*- rph-1*	[33]
MG-D	*F-* □*- rph-1* Δ(def-fmt)::cm *ΔgloB*::frt	Gift from D. Mazel
DH5α	*φ80 lacZΔM15 endA1 recA1 gyrA96 thi-1 hsdR17 (r_k^- , m_k^-) relA1 supE44 deoR Δ(lacZYA–argF)U169*	Promega
CAG12184	□*- rph-1 tolC210::Tn10 (tet)*	[34]
KPS73	□*- rph-1 tolC210::Tn10 (tet) Δfmt ::Km*	This study
KPS74	□*- rph-1 tolC210::Tn10 (tet) Δdef-Δfmt ::Km*	This study

Table S2.2 Plasmids used in this study.

Plasmid name	Description	Source or Ref.
pJT184	Cm^R; pACYC184-based plasmid with 2.8-kb BamHI/SalI insert containing *S. cerevisiae* Ubp1.	[14]
pBADET	Ap^R; pBAD2-based plasmid containing arabinose-inducible promoter and expanded multiple cloning site.	Gift from V. Ksenzenko
pACYC177	Ap^R, Km^R; low copy vector containing p15A repl. origin.	[35, 36]
pKD46	Ap^R; ts replication (repA101ts); encodes lambda Red genes , *bet*, *gam*); native terminator (tL3) after *exo* gene; arabinose-nducible promoter for expression (P*ara*); encodes *araC* for epression of the Para promoter. This plasmid was used for chromosomal deletions of specific genes.	[37]
pKD3	Ap^R, Cm^R; R6K origin-based plasmid containing *cat*-cassette d by FRT sites. This plasmid was used as a template in PCR to create gene-specific *cat*-cassettes.	[37]
pCH178	Ap^R; p314CUP1-based plasmid expressing Ub-CK-e^K-ha-Ura3.	[9]
pKP249	Ap^R; pBADET-based plasmid expressing $P1^{T2}$-e^K-ha-Ura3 from P*ara* promoter.	This study
pKP250	Ap^R; pBADET-based plasmid expressing $P1^{T2D}$-e^K-ha-Ura3 from P*ara* promoter.	This study
pKP251	Ap^R; pBADET-based plasmid expressing Ub-$P1^{T2}$-e^K-ha-Ura3 from P*ara* promoter.	This study
pKP252	Ap^R; pBADET-based plasmid expressing Ub-$P1^{T2D}$-e^K-ha-Ura3 from P*ara* promoter.	This study
pKP257	Ap^R; pACYC177-based plasmid expressing $P1^{T2}$-e^K-ha-Ura3 from P_{KmR} promoter.	This study
pKP258	Ap^R; pACYC177-based plasmid expressing $P1^{T2D}$-e^K-ha-Ura3 from P_{KmR} promoter.	This study
pKP286	Ap^R; pBADET-based plasmid expressing PpiB-8his-flag from P*ara* promoter.	This study
pKP287	Ap^R; pBADET-based plasmid expressing $PpiB^{V2D}$-8his-flag from P*ara* promoter.	This study
pKP335	Ap^R; pBADET-based plasmid expressing PpiB-8his-flag-Ub-PpiB-8his-flag from P*ara* promoter	This study
pKP458	Ap^R; pBADET-based plasmid expressing ^{MVTV}PpiB-8his-flag ^{MDDD}PpiB-8his-flag-Ub from two identical and independent P*ara* promoters.	This study
pKP459	Ap^R; pBADET-based plasmid expressing ^{MVTV}PpiB-8his-flag ^{MYFY}PpiB-8his-flag-Ub from two identical and independent P*ara* promoters.	This study

Supplemental References

1. Hwang CS, Shemorry A, Varshavsky A (**2010**). The N-end rule pathway is mediated by a complex of the RING-type Ubr1 and HECT-type Ufd4 ubiquitin ligases. **Nat. Cell Biol.** 12: 1177-1185. doi: 10.1038/ncb2121.

2. Tasaki TS, Sriram SM, Park KS, Kwon YT (**2012**). The N-end rule pathway. **Annu. Rev. Biochem.** 81: 261-289. doi: 10.1146/annurev-biochem-051710-093308.

3. Varshavsky A (**2011**). The N-end rule pathway and regulation by proteolysis. **Prot. Sci.** 20: 1298-1345. doi: 10.1002/pro.666.

4. Gibbs DJ, Bacardit J, Bachmair A, Holdsworth MJ (**2014**). The eukaryotic N-end rule pathway: conserved mechanisms and diverse functions. **Trends Cell Biol.** 24: 603-611. doi: 10.1016/j.tcb.2014.05.001.

5. Kim HK, Kim RR, Oh JH, Cho H, Varshavsky A, Hwang CS (**2014**). The N-terminal methionine of cellular proteins as a degradation signal. **Cell** 156: 158-169. doi: 10.1016/j.cell.2013.11.031.

6. Hu R-G, Sheng J, Xin Q, Xu Z, Takahashi TT, Varshavsky A (**2005**). The N-end rule pathway as a nitric oxide sensor controlling the levels of multiple regulators. **Nature** 437: 981-986. PMID: 16222293.

7. Lee MJ, Tasaki T, Moroi K, An JY, Kimura S, Davydov IV, Kwon YT (**2005**). RGS4 and RGS5 are *in vivo* substrates of the N-end rule pathway. **Proc. Natl. Acad. Sci. USA** 102: 15030-15035. PMID: 16217033.

8. Shemorry A, Hwang CS, Varshavsky A (**2013**). Control of protein quality and stoichiometries by N-terminal acetylation and the N-end rule pathway. **Mol. Cell** 50: 540-551. doi: 10.1016/j.molcel.2013.03.018.

9. Hwang CS, Shemorry A, Varshavsky A (**2010**). N-terminal acetylation of cellular proteins creates specific degradation signals. **Science** 327: 973-977. doi: 10.1126/science.1183147.

10. Park SE, Kim JM, Seok OH, Cho H, Wadas B, Kim SY, Varshavsky A, Hwang CS (**2015**). Control of mammalian G protein signaling by N-terminal acetylation and the N-end rule pathway. **Science** 347: 1249-1252. doi: 10.1126/science.aaa3844.

11. Chen S, Vetro JA, Chang Y-H (**2002**). The specificity *in vivo* of two distinct methionine aminopeptidases in *Saccharomyces cerevisiae*. **Arch. Biochem. Biophys.** 398: 87-93. PMID: 11811952.

12. Xiao Q, Zhang F, Nacev BA, Liu JO, Pei D (**2010**). Protein N-terminal processing: substrate specificity of *Escherichia coli* and human methionine aminopeptidases. **Biochemistry** 49: 5588-5599. doi: 10.1021/bi1005464.

13. Frottin F, Martinez A, Peynot P, Mitra S, Holz RC, Giglione C, Meinnel T (**2006**). The proteomics of N-terminal methionine cleavage. **Mol. Cell. Proteomics** 5: 2336-2349. PMID: 16963780.

14. Tobias JW, Shrader TE, Rocap G, Varshavsky A (**1991**). The N-end rule in bacteria. **Science** 254: 1374-1377. PMID: 1962196.

15. Shrader TE, Tobias JW, Varshavsky A (**1993**). The N-end rule in *Escherichia coli*: cloning and analysis of the leucyl, phenylalanyl-tRNA-protein transferase gene *aat*. **J. Bact.** 175: 4364-4374. PMID: 8331068.

16. Graciet E, Hu RG, Piatkov K, Rhee JH, Schwarz EM, Varshavsky A (**2006**). Aminoacyl-transferases and the N-end rule pathway of prokaryotic/eukaryotic specificity in a human pathogen. **Proc. Natl. Acad. Sci. USA** 103: 3078-3083. PMID: 16492767.

17. Erbse A, Schmidt R, Bornemann T, Schneider-Mergener J, Mogk A, Zahn R, Dougan DA, Bukau B (**2006**). ClpS is an essential component of the N-end rule pathway in *Escherichia coli*. **Nature** 439: 753-756. PMID: 16467841.

18. Suto K, Shimizu Y, Watanabe K, Ueda T, Fukai S, Nureki O, Tomita K (**2006**). Crystal structures of leucyl/phenylalanyl-tRNA-protein transferase and its complex with an aminoacyl-tRNA analog. **EMBO J.** 25: 5942-5950. PMID: 17110926.

19. Dong XK-M, M., Muramatsu T, Mori H, Shirouzu M, Bessho Y, Yokoyama S (**2007**). The crystal structure of leucyl/phenylalanyl-tRNA-protein transferase from *Escherichia coli* **Prot. Sci.** 16: 528-534. PMID: 17242373.

20. Wang KH, Roman-Hernandez G, Grant RA, Sauer TT, Baker TA (**2008**). The molecular basis of N-end rule recognition. **Mol. Cell** 32: 406-414. doi: 10.1016/j.molcel.2008.08.032.

21. Wang KH, Oakes ESC, Sauer RT, Baker TA (**2008**). Tuning the strength of a bacterial N-end rule signal. **J. Biol. Chem.** 283: 24600-24607. doi: 10.1074/jbc.M802213200.

22. Hou JY, Sauer RT, Baker TA (**2008**). Distinct structural elements of the adaptor ClpS are required for regulating degradation by ClpAP. **Nat. Struct. Mol. Biol.** 15: 288-294. doi: 10.1038/nsmb.1392.

23. Schmidt R, Zahn R, Bukau B, Mogk A (**2009**). ClpS is the recognition component for *Escherichia coli* substrates of the N-end rule degradation pathway. **Mol. Microbiol.** 72: 506-517. doi: 10.1111/j.1365-2958.2009.06666.x.

24. Román-Hernández G, Grant RA, Sauer RT, Baker TA (**2009**). Molecular basis of substrate selection by the N-end rule adaptor protein ClpS. **Proc. Natl. Acad. Sci. USA** 106: 8888-8893. doi: 10.1073/pnas.0903614106.

25. Schuenemann VJ, Kralik SM, Albrecht R, Spall SK, Truscott KN, Dougan DA, Zeth K (**2009**). Structural basis of N-end rule substrate recognition in *Escherichia coli* by the ClpAP adaptor protein ClpS. **EMBO Rep.** 10: 508-514. doi: 10.1038/embor.2009.62.

26. Ninnis RL, Spall SK, Talbo GH, Truscott KN, Dougan DA (**2009**). Modification of PATase by L/F-transferase generates a ClpS-dependent N-end rule substrate in *Escherichia coli*. **EMBO J.** 28: 1732-1744. doi: 10.1038/emboj.2009.134.

27. Román-Hernández G, Hou JY, Grant RA, Sauer RT, Baker TA (**2011**). The ClpS adaptor mediates staged delivery of N-end rule substrates to the AAA+ ClpAP protease. **Mol. Cell** 43: 217-228. doi: 10.1016/j.molcel.2011.06.009.

28. Humbard MA, Surkov S, De Donatis GM, Jenkins L, Maurizi MR (**2013**). The N-degradome of *Escherichia coli*: limited proteolysis *in vivo* generates a large pool of proteins bearing N-degrons. **J. Biol. Chem.** 288: 28913-28924. doi: 10.1074/jbc.M113.492108.

29. Rivera-Rivera I, Román-Hernández G, Sauer RT, Baker TA (**2014**). Remodeling of a delivery complex allows ClpS-mediated degradation of N-degron substrates. **Proc. Natl. Acad. Sci. USA** 111: E3853-E3859. doi: 10.1073/pnas.1414933111.

30. Fung AW, Fahlman RP (**2015**). The molecular basis for the post-translational addition of amino acids by L/F-transferase in the N-end rule pathway. **Curr. Prot. Pept. Sci.** 16: 163-180. PMID: 25579118.

31. Dougan DA, Micevski D, Truscott KN (**2011**). The N-end rule pathway: from recognition by N-recognins to destruction by AAA+ proteases. **Biochim. Biophys. Acta** 1823: 83-91. doi: 10.1016/j.bbamcr.2011.07.002.

32. Mogk A, Schmidt R, Bukau B (**2007**). The N-end rule pathway of regulated proteolysis: prokaryotic and eukaryotic strategies. **Trends Cell Biol.** 17: 165-172. PMID: 17306546.

33. Blattner FR, Plunkett G, 3rd, Bloch CA, Perna NT, Burland V, Riley M, Collado-Vides J, Glasner JD, Rode CK, Mayhew GF, Gregor J, Davis NW, Kirkpatrick HA, Goeden MA, Rose DJ, Mau B, Shao Y (**1997**). The complete genome sequence of *Escherichia coli* K-12. **Science** 277: 1453-1462. PMID: 9278503.

34. Singer M, Baker TA, Schnitzler G, Deischel SM, Goel M, Dove W, Jaacks KJ, Grossman AD, Erickson JW, Gross CA (**1989**). A collection of strains containing genetically linked alternating antibiotic resistance elements for genetic mapping of *Escherichia coli*. **Microbiol. Rev.** 53: 1-24. PMID: 2540407.

35. Chang AC, Cohen SN (**1978**). Construction and characterization of amplifiable multicopy DNA cloning vehicles derived from the P15A cryptic miniplasmid. **J. Bacteriol.** 134: 1141-1156. PMID: 149110.

36. Rose RE (**1988**). The nucleotide sequence of pACYC184. **Nucl. Acids Res.** 16: 355.

37. Datsenko KA, Wanner BL (**2000**). One-step inactivation of chromosomal genes in *Escherichia coli* K-12 using PCR products. **Proc. Natl. Acad Sci. USA** 97: 6640-6645. PMID: 10829079.

CHAPTER 3:

THE ARG/N-END RULE PATHWAY AS A REGULATOR OF PROCESSES THAT CAN CAUSE EPILEPSY

Introduction

Epilepsy is the most common neurological disorder, occurring at the rate of 5 to 10 per 1000 people [1]. Epileptic seizures occur in many variations, with different levels of severity. Susceptibility to epilepsy depends on a variety of factors, including the age and gender of patients and their specific health problems [2]. Although there are drugs to alleviate the symptoms, about one third of patients become resistant to anti-epileptic drugs. Some patients, including those with drug-resistant epilepsy, have to undergo brain surgery, often with lifelong side effects [3, 4]. These difficulties make it particularly important to understand molecular causes and risk factors in epileptic seizures.

In this chapter, we summarize the current understanding of epilepsy, with an emphasis on one known risk factor for seizures: dysregulation of Ca^{2+} signaling. Increased Ca^{2+} transients, as a result of over-excitation of neurons, activate intracellular proteases such as Ca^{2+}-dependent calpains, leading to cellular injury and death. We demonstrate here that *Ate1*$^{-/-}$ mice, which lack the arginylation branch of the Arg/N-end rule pathway (Fig. 1.2), are not only hypersensitive to treatments that can induce epileptic seizures but also suffer higher levels of brain damage as a result of seizures. These and related findings, to be described below, indicate that at least the arginylation branch of the Arg/N-end rule pathway is, operationally, a repressor of epileptic seizures.

One plausible and testable explanation of this function of the Arg/N-end rule pathway is its previously demonstrated ability to conditionally destroy the Rgs4, Rgs5 and Rgs16 proteins., All three of these proteins are down-regulators of G_α subunits of specific G proteins, by virtue of the ability of these (and other) RGS proteins to increase the otherwise

low GTPase activity of G_α subunits [5]. Rgs4 is the most prominently and broadly expressed member of this set of three RGS proteins, all of which are expressed in the brain. A partially repressed signaling by metabotropic G-protein-coupled receptors (GPCRs) can result in longer durations and/or higher frequencies of Ca^{2+} transients. An example of this was demonstrated in the presynaptic neurons of embryonic chick dorsal root ganglia. Specifically, an intracellular injection of a small amount of purified Rgs4 inhibits the ability of these neurons to decrease intracellular Ca^{2+} though their metabotropic norepinephrine receptors [6]. We envision a similar dysfunction in *Ate1*$^{-/-}$ mice, in which the levels of the normally short-lived Rgs4 (Nt-arginylated by Ate1 and destroyed by the rest of the Arg/N-end rule pathway) are greatly elevated, as described below.

Seizures are monitored by EEGs

With humans as well as in in animal models, epileptic seizures are diagnosed using electroencephalograms (EEGs). To carry out an EEG recording, electrodes are placed on the scalp or are inserted intracranially. EEG readouts are plots of voltage differences between two electrodes over time. Since there are many ways of placing electrodes, there are many ways (called channels) of taking EEGs. The channels can be local (a region of the brain) or global (involving the whole brain). In normal human adults, there are several physiologically relevant EEG frequencies: the delta rhythms (<4 Hz), the theta rhythms (4-8 Hz), the alpha rhythms (8-14 Hz), the beta rhythms (14-30 Hz), and the gamma rhythms (> 30Hz). Epileptic seizures result in abnormal EEG rhythms. Measurements of EEG rhythms have shown that epileptic seizures are initiated in a small brain region (called focus) and spread out to a larger

region, sometimes to the entire brain. Some seizures may have more than one focus. Seizures are categorized by where they initiate and where they tend to spread. Two common types are absence seizures and temporal lobe epilepsy (TLE).

Absence seizures are a type of generalized seizures. These seizures involve cortical-thalamus circuits [7-9]. Seizures are initiated from the thalamus and spread to the cortical areas (although there is also evidence that the somatosensory region of the cortex can initiate seizures) [9]. Once initiated, these epileptic states spread between the cortex and the thalamus. Their EEGs are characterized by the so-called 3-Hz spike and wave complex, which are detected using an algorithm referred to as wavelet transformation [10].

Temporal lobe epilepsy (TLE) is an example of partial seizures. It often occurs as a result of hippocampal sclerosis, a damage in that region of the brain manifested as hippocampal scars. They are caused by injuries such as stroke, head trauma, or prolonged seizures. [11-13]. For some patients, surgical removal of the damaged hippocampus prevents recurrent seizures. However, about 30% of patients who undergo such surgeries still suffer from seizures [14]. Since partial seizures occur in 60% of epileptic patients and TLE is the most common partial seizure, TLE is the focus of the bulk of research on epileptic seizures. TLE is modeled in rodents that are treated with chemoconvulsants such as kainic acid (kainate; KA). KA treatments lead to hippocampal injuries and spontaneous recurrent seizures, mimicking the human disorder [14, 15].

TLE hippocampal EEGs show disruption of theta rhythms. KA-treated rodents have isolated spike, spike-and-wave, or poly-spikes at 1-3 Hz frequency [11, 12]. These seizures are usually initiated from the hippocampus [16]. They can also be initiated from the amygdala, the entorhinal cortex, and part of the thalamus [7]. They spread, thereafter, to other

limbic regions. In severe cases, they spread to the prefrontal cortex, leading to generalized seizures. As with absence seizures, TLE can be reliably diagnosed using specific mathematical transformations of raw EEG data [17].

Molecular understanding of epilepsy is still far from detailed

While EEGs allow us to diagnose epilepsy, they do not, by themselves, illuminate the molecular causes and genetic factors that increase susceptibility for seizures. Genetic-predisposition studies showed that epilepsy is facilitated by a number of distinct genetic defects rather than by one major defect [18]. Patients with absence seizures usually have mutations in genes encoding voltage-gated Ca^{2+} channels [19, 20], the $GABA_A$ channel [21-23], the NMDA receptor [23], voltage-gated K^+ channels [2], or voltage-gated Na^+ channels [24-27].

Patients with TLE do not seem to have a common set of genetic defects. There are clinical reports of a family of epileptic patients who shared specific mutations of the leucine-rich glioma-inactivated 1 (LGI1) gene. There are also reports of patients who have inherited mutations of their voltage-gated Na^+ channels. However, the number of patients with these mutations are too few to link these mutations, reliably, to TLE [28].

In the absence of a clear understanding of epilepsy, there are several hypotheses about its causes. One idea is that seizures result from an imbalance in activity among the excitatory and inhibitory neurons. This imbalance may result from dysfunctions in the channels and receptors that modulate synaptic transmissions. Another idea is that seizures are caused by cell death and inflammation in the brain that result in scars such as TLE hippocampal

sclerosis. Other causes of epilepsy may stem from glial cell dysfunctions or pathological Ca^{2+} transients. We now discuss these hypotheses in some detail, and thereafter consider a specific role that the Arg/N-end rule pathway plays in regulating events that are relevant to epilepsy, with an emphasis on the G protein regulators Rgs4, Rgs5 and Rgs16.

The glutamatergic and GABAergic receptors are implicated in epilepsy

In the brain, a neuron typically receives thousands of synaptic inputs from other neurons. In turn, a neuron sends output signals to many other neurons. Presynaptic neurons are categorized as either excitatory or inhibitory. Excitatory neurons make a postsynaptic neuron more likely to generate an action potential. Inhibitory neurons make a postsynaptic neuron less likely to generate an action potential. By working together, they form circuits carrying signals and making long-term changes to the probabilities of action potentials by specific neurons. The main excitatory neurons are the glutamatergic neurons. The main inhibitory neurons are the GABAergic neurons. Hippocampal circuits consist of both glutamatergic pyramidal neurons and GABAergic neurons. Similarly, the cortical-thalamus circuits comprise both GABAergic interneurons and glutamatergic neurons [8, 9, 22, 29, 30].

Glutamate is the principal neurotransmitter of glutamatergic neurons. Glutamate activates two classes of receptors: ionotropic ones (NMDA, AMPA, and kainate receptors) (iGluRs) and metabotropic receptors (mGluRs). The latter are G protein-coupled receptors (GPCRs). They belong to the same family (family C) as the metabotropic $GABA_B$ receptor that is described below. mGluRs are categorized into three main groups, based on their sequelogy (sequence similarity [31]) and specific molecular mechanisms [32]. Group I

includes mGluR1 and mGluR5. Group II includes mGluR2 and mGluR3. Group III includes mGluR4, mGluR6, mGluR7, and mGluR8. Like other GPCRs from family C, these mGluRs function as dimers. mGluR5, for example, is known to form a heterodimer with mGluR1. Interestingly, mGluR5 also forms heterodimers with the adenosine A_{2A} receptor or the dopamine D2 receptor [33]. Hippocampal and cortical-thalamus circuits express all of these mGluRs and iGluRs [8, 34, 35].

iGluRs receptors mediate the flows of Ca^{2+} and Na^{+} into cells. When iGluRs are located on postsynaptic neurons, the resulting ion flow "excites" a cell, i.e., it increases the probability of action potential. When iGluRs are located on presynaptic neurons, the receptor-mediated ion flows facilitate the release of neurotransmitters [35]. While iGluRs play the main role in synaptic excitation, specific mGluRs modulate synaptic transmissions [32]. Group I mGluRs increase postsynaptic neuron excitability. They activate the $G_{\alpha q/11}$ family of G proteins to mediate Ca^{2+} signaling [36, 37]. In contrast, group II and group III mGluRs decrease presynaptic neuron activities. They activate the $G_{\alpha i/o}$ family proteins to inhibit voltage-gated Ca^{2+} channels and to activate G protein-coupled inward rectifying K^{+} (GIRK) channels. This reduces Ca^{2+} influx and increases K^{+} efflux, hyperpolarizing the neurons. Furthermore, group II and group III mGluRs inhibit the synaptic SNARE complex, reducing presynaptic neurotransmitter exocytosis [8, 35].

All iGluRs and mGluRs are implicated in epilepsy. iGluR agonists such as NMDA and KA induce seizures [38-40]. Group I mGluRs are involved in audiogenic seizures in fragile X syndrome model mice [36, 37] and their antagonists alleviate absence seizures [41]. The roles of group II and group III mGluRs in epilepsy are more complicated, as their agonists and antagonists have mixed effects on epilepsy. But in general, agonists of group II

and group III mGluRs inhibit seizures and protect neurons from excitotoxicity [8, 41, 42].

GABA is the main inhibitory neurotransmitter in GABAergic neurons. Analogously to glutamate, GABA activates two major types of receptors: the fast acting $GABA_A$ and $GABA_C$ ionotropic channels, as well as the slower acting metabotropic $GABA_B$ receptor. $GABA_A$ and $GABA_C$ are chloride-ion (Cl^-) channels. GABA activation leads to Cl^- influx, hyperpolarizing neurons and thereby decreasing the probability of action potentials. Metabotropic $GABA_B$ receptors work similarly to group II and group III mGluRs. They activate $G_{\alpha i/o}$ family G proteins to inhibit voltage-gated Ca^{2+} channels, activate GIRKs, and reduce the release of neurotransmitters [43-45]. Mutations of genes encoding $GABA_A$ receptors increase the risk of absence seizures [23]. $GABA_B$ agonists and antagonists affect the severity of seizures depending on the animal model [46, 47].

Glutamatergic and GABAergic neurons work together to fine-tune neuronal circuits. Dysfunction in the glutamatergic and GABAergic receptors can lead to excessive glutamate release and, consequently, excessive Ca^{2+} transients. The resulting higher levels of intracellular cytosolic Ca^{2+} hyper-activate both specific kinases, nitric oxide synthases, and Ca^{2+}-dependent calpain proteases. These events can result in either necrotic or apoptotic cell death, as described below.

Astrocytes are implicated in epilepsy

In addition to comprising circuits of excitatory and inhibitory neurons, brains also contain other cell types, referred to as glial cells. Astrocytes are glial cells that play major roles in the maintenance and regulation of neuronal circuits. Dysfunction of astrocytes can

also facilitate epileptic seizures. Like the glutamatergic neurons, astrocytes relies on specific mGluRs for many of their functions.

Astrocytes detect synaptic glutamate levels through their mGluRs to modulate glutamate concentration and synaptic transmission [48-51]. For example, mGluR5 works with the ATP receptor P2Y1 to induce astrocyte release of glutamate and D-serine. The released glutamate activates presynaptic NMDA receptor to increase neurotransmitter release [52]. D-serine binds to postsynaptic NMDA receptor to increase its probability of activation, thereby increasing neuron long-term potentiation (LTP) [53]. In addition, mGluRs protect astrocytes from Ca^{2+}-mediated excitotoxicity [42].

Another role of astrocytes is their control of the interstitial volume (extracellular space; ECS) and K^+ concentration. Small ECS tends to increase K^+ concentration and the incidence of seizures [54]. ECS is regulated by volumes of individual astrocytes through the aquaporin AQP4 and the K^+ channel Kir4.1 which work together to control water and K^+ flows in the synapse [52]. This regulation is influenced by mGluRs, as astrocytes can be shown to swell upon activation of mGluRs [55].

Astrocytes also regulate specific cerebrovascular structures and modulate cerebral blood flow in part through their mGluRs [56-59]. To maintain the blood-brain barrier (BBB), astrocytes rely on other GPCRs. For example, astrocytes release the Sonic Hedgehog (Shh) protein, which causes capillary endothelial cells to upregulate tight junction proteins [60, 61]. On these endothelial cells, Shh activates the Hedgehog receptor to alleviate the inhibition of Smo, a GPCR. Smo activates specific Gli transcription factors that activate, in turn, specific gene regulons. Breakdown of the BBB leads, among other things, to thrombin leakage into the brain. Thrombin activates the protease activated receptor (PARs) [62]. PARs are GPCRs

that activate either the $G_{\alpha q/11}$, the $G_{\alpha i/o}$, or the $G_{\alpha 12/13}$ proteins. Not much is known about these receptors, but activation of PAR1 is reported to increase neuron excitability, neuronal death, or astrocyte proliferation [63, 64].

Purinergic receptors and inflammation are implicated in TLE (temporal lobe epilepsy)

Astrocytes also play a role in hippocampal sclerosis. These tissue scars comprise, in particular, dead neurons and live but altered cells, such as "transformed" astrocytes, which undergo a process called astrogliosis. Mildly transformed astrocytes upregulate a variety of proteins, including GFAP and extracellular matrix proteins [65, 66]. They also upregulate mGluRs, including mGluR3, mGluR5, and mGluR8, and cytokines such as TGFβ, TNFα, IL-1β, and IL-6. Severely transformed astrocytes proliferate and form long-lasting scars that inhibit axon regeneration [56]. At the same, not all manifestations of scars are physiologically detrimental. For example, scars can form borders protecting neuronal tissue against inflammatory cells of the immune system.

Astrogliosis is regulated by extracellular ATP and adenosine through purinergic receptors [67, 68]. ATP is released, in particular, from damaged cells, including transformed astrocytes. These astrocytes upregulate the connexin-43 hemichannel, increasing ATP efflux [69]. Extracellular ATP activates P2 receptors. There are two types of P2 receptors, ionotropic P2XRs and metabotropic P2YRs. P2XRs receptors allow influxes of Na^+, K^+, and Ca^{2+}. The P2YR1, 2, 4, 6, and 11 receptors activate $G_{\alpha q}$ proteins for Ca^{2+} signaling, while the P2YR12, 13, and 14 receptors activate the $G_{\alpha i}$ proteins to inhibit adenylyl cyclase.

Extracellular ATP is gradually converted into adenosine, which activates specific adenosine receptors. These receptors (A_1 and A_3), in turn, activate the $G_{\alpha i/o}$ G proteins, while the A_{2A} and A_{2B} receptors activate $G_{\alpha s}$ G proteins.

Astrocytes sense cell damage through activation of their P2YR receptors by extracellular ATP. This activation induces astrocytes to release glutamate. Glutamate and ATP work together to induce astrocytes to release the cytokines TNFα, IL-1β, and IL-6 [70, 71]. These cytokines worsen scar formation [72]. First, they attract and activate microglial cells (resident macrophages of the brain). Second, the released cytokine TNFα activates TNF receptors. TNF receptor activation, along with activation of the mGluR5 and P2Y1R receptors, induce astrocytes to release even more glutamate and ATP, resulting in positive feedback. Third, the interleukin IL-1β disrupts BBB permeability, causing neuroinflammation [61, 73]. Fourth, inflammatory cytokines reduce seizure threshold vis-à-vis the level of neuronal excitation [54, 74-76], because TNFα and IL-1β affect the activity of neuronal voltage-dependent Ca^{2+} and K^+ channels as well as the AMPA, NMDA, and GABA ionotropic receptors [77]. For example, it has been shown that blocking IL-1β signaling reduces severity of a seizure [78].

While extracellular ATP increases astrogliosis, the same ATP tends to be protective vis-à-vis neurons. Activation of the neuronal P2YR channel inhibits Ca^{2+} signaling and neurotransmitter exocytosis, decreasing excitotoxicity [79]. This may explain why ATP receptor agonists and antagonists have mixed effects on TLE-type epilepsies [80]. In sum, the roles of ATP receptors in regulating events linked to epilepsy remains to be better understood [79, 81].

Adenosine also has different effects on astrocytes and neurons. A_{2A} receptor

activation increases astrogliosis and leads to neuronal apoptosis [82]. Not much is known about the A_3 receptor, whose activation can be either protective or seizure-inducing. On the other hand, the A_1 adenosine receptor plays a major neuroprotective function. On presynaptic neurons, the A1 receptor inhibits Ca^{2+} channels, activates the GIRKs, and down-regulates the release of neurotransmitters. Through the A_1 receptor, adenosine suppresses seizures and protects neurons from excitotoxicity [35, 82-85].

The Arg/N-end rule pathway as a repressor of epileptic seizures

As described above, the brain relies on various GPCRs and Ca^{2+} signaling to modulate synaptic transmissions, maintain cerebrovascular structures, and control neuroinflammation. The Arg/N-end rule pathway plays a role in this regulation, in part through its Ate1-mediated arginylation branch (Fig. 1.2). One role of the Ate1 R-transferase is to mediate the conditional degradation of three G-protein down-regulators, Rgs4, Rgs5, and Rgs16 [86, 87].

Rsg4, the most broadly and highly expressed RGS among the above three RGS proteins, is present in both neurons and astrocytes [88, 89]. It acts on the $G_{\alpha i}$ and $G_{\alpha q}$ family of the G proteins and down-regulates their activity by increasing the otherwise weak intrinsic GTPase activity of these G_α proteins In particular, Rgs4 down-regulates the activity of the mGluR1, mGluR5, $GABA_B$, and A_1 receptors, thus impacting, simultaneously, a variety of brain functions [90, 91].

In the hippocampus, a neuron that emitted an action potential becomes hyperpolarized and enters the refractory period. This phase depends on the Ca^{2+}-activated K^+

efflux. The outflow of K^+ is inhibited when mGluR5 is activated. Rgs4 down-regulates the activity of mGluR5, thereby allowing hippocampal neurons to hyperpolarize [92]. In the paraventricular nucleus of the hypothalamus, postsynaptic neurons communicate with presynaptic neurons through glucocorticoids to inhibit the release of GABA from presynaptic neurons, and thereby to minimize the extent of long-term depression. Glucocorticoid release from postsynaptic neurons is upregulated by mGluR5. Rgs4 also down-regulates postsynaptic mGluR5 to maintain long-term depression [93]. In the prefrontal cortex and the hypothalamus, Rgs4 was shown to interact with the $GABA_B$ receptor complex [94]. $GABA_B$ receptor activates K^+ channels and inhibit Ca^{2+} channels to hyperpolarize neurons [95-98]. Rgs4 down-regulates $GABA_B$ to increase the excitability of neurons [96, 98]. Therefore, predictably, fragile X-syndrome model mice that in addition lack Rgs4 are less susceptible to audiogenic seizures [99, 100]. In cortical neurons, Rgs4 was shown to interact with neurabin to inhibit the adenosine A_1 receptor [101]. Adenosine is known to suppress seizures through the A_1 receptor [102]. Inhibiting Rgs4 decreases KA-induced seizures in mice [101].

Effects of Rgs4 on other GPCRs are less well understood. Rsg4 down-regulates P2YR1 and P2YR12 receptors *in vitro*, suggesting its role in astrocyte-mediated release of cytokines [103]. RGS4 interacts with PAR1 in COS7 cells, suggesting its involvement in thrombin- mediated neuroinflammation [104]. As for Rgs5, it is significantly expressed in the vascular structures [105]. In particular, Rgs5 represses Smoothened (Smo), a GPCR-like receptor that is part of the hedgehog signaling pathway, in murine embryonic mesenchymal C3H10T1/2 cells [106]. Rgs5 may act to weaken the blood-brain barrier (BBB) by reducing the ability of capillary endothelial cells to express tight junction proteins [107]. The third RGS protein, Rgs16, that is conditionally Nt-arginylated and destroyed by the Arg/N-end

rule pathway, is expressed in the suprachiasmatic nucleus of the hypothalamus [108] and in activated T-cells in germinal centers, [109] suggesting that Rgs16 may regulate circadian rhythm and adaptive immunity [91]. In sum, and focusing on Rgs4, it is already clear that mice in which the levels of (at least) Rgs4 are abnormally high suffer a number of neurological defects.

Yet another important role of the Ate1 R-transferase and the rest of the Arg/N-end rule pathway is to mediate the degradation of pro-apoptotic protein fragments that are generated by non-processive proteases such as calpains and caspases in the presence of pathologically high levels of Ca^{2+} transients [110-113]. Activation of calpains results in a large number of intracellular protein fragments [114]. They include pro-apoptotic fragments such as Glu-Bak [115]. Some pro-apoptotic fragments such as Asn-Bfl1 [116] and Asp-Bcl_{XL} are produced from cleavages of anti-apoptotic proteins [117]. Thus, activation of calpains shifts cells toward a pro-necrotic and/or pro-apoptotic state. This shift is inhibited by the Arg/N-end rule pathway and in part by the Ate1 R-transferase as well, because Ate1 Nt-arginylates and thereby targets for degradation not only Rgs4 but also a subset of natural C-terminal pro-apoptotic protein fragments that bear Nt-arginylatable N-terminal residues, such as N-terminal Asp, Glu or (oxidized) Cys (Fig. 1.2) [110, 111]. Some natural protein fragments, such as the cleaved ryanodine receptor Gln-Ryr1 [118], increase Ca^{2+} influx into the cytosol, worsening excitotoxic effects of Ca^{2+} [119].The Ate1 R-transferase may counteract such effects by mediating the degradation of protein fragments bearing Nt-arginylatable N-terminal residues (Asp, Glu, oxidized Cys), and indirectly N-terminal Asn and Gln as well, because these residues are rapidly deamidated by N-terminal amidases

Ntan1 and Ntaq1, the most "upstream" components of the Arg/N-end rule pathway (Fig. 1.2).

As one would expect, given the above connections between Nt-arginylation and the levels of Rgs4, Rgs5 and Rgs16, Ate1-lacking *Ate1*$^{-/-}$ mice exhibit a large variety of abnormal phenotypes. Specifically, unconditionally null *Ate1* $^{-/-}$ mice are embryonic lethals, dying on embryonic day 15 (E15) [120]. *Ate1* $^{-/-}$ embryos exhibit internal bleeding and have defective heart and vascular development. Mice with a conditional *Ate1* deletion (induced in adult mice using the cre-lox system) are viable but also exhibit a number of abnormal phenotypes [121]. Specifically, about 15% of mice die upon tamoxifen (TM)-induced deletion/disruption of both copies of the *Ate1* gene. The surviving mice fail to thrive, in comparison to control littermates. These mice are lean, have enlarged brain, heart, and kidney, are strikingly hyperkinetic, and are easily startled [121].

In the present study, we examined neurological abnormalities of *Ate1*$^{-/-}$ mice more closely, with an emphasis on the possible propensity of these mice to epileptic seizures.

Results and Discussion

Ate1$^{tetO/-}$*;R26rtTA* Mouse Strains

To complement our previously constructed *Ate1*$^{flox/-}$*;CaggCreER* mouse strains [121], we also constructed a doxycycline-inducible *Ate1*$^{tetO/-}$*;R26rtTA* mouse strain. These mice harbor one unconditionally null (deletion/disruption) *Ate1*− allele (derived, through matings, from the previously constructed unconditional heterozygous *Ate1*+/− mice [120]) and one *Ate1*^{tetO} allele. Mice with *Ate1*^{tetO} allele had negligible levels of Ate1 R-transferase

expression, from that allele, in the absence of doxycycline (Dox) (even in the presence of the *R26rtTA* gene in these mice). However the addition of Dox to mouse food resulted in a strong expression of the Ate1 R-transferase from the $Ate1^{tetO}$ allele (Fig. 4.1, Fig. 4.2, and Fig. 4.3).

To construct $Ate1^{tetO/-}$*;R26rtTA* mice, the endogenous P_{Ate1} bidirectional promoter (previously investigated in our laboratory [122]) was replaced with the Dox-inducible $(TetO)_7P_{miniCMV}$ promoter to produce the $Ate1^{tetO}$ allele (Fig. 4.2). Heterozygous matings among $Ate1^{tetO/+}$ mice, $Ate1^{+/-}$ mice, and *R26rtTA* mice were carried out to generate mice of the desired genotype [123]. These mice, in addition to containing the $Ate1^{tetO}$ configuration at the *Ate1* locus, also expressed a modified form of reverse tetracycline/Dox-controlled transactivator (rtTA) at the *Rosa26* locus. rtTA is a fusion of a TetR mutant (rTetR) and the C-terminal activation domain of VP16 of the herpes simplex virus [124]. Upon the addition of Dox, rTetR undergoes a conformation change that results in its binding to the *tetO* DNA elements [125]. The activation domain of VP16 attracts host transcription factors to initiate transcription (Fig. 4.1) [126]. When $Ate1^{tetO/-}$*;R26rtTA* mice were fed Dox-containing food, the single $Ate1^{tetO}$ allele overexpressed Ate1 R-transferase, generating approximately 2-fold higher steady-state levels of the Ate1 protein than the levels of Ate1 in wild-type mice (Fig 4.3).

To confirm that Dox induces expression of Ate1, immunoblotting analyses, using affinity-purified anti-Ate1 antibody, were carried out with extracts of the stomach, pancreas, brain, testis, heart, thymus, and ES cells of $Ate1^{tetO/tetO}$*;R26rtTA*, $Ate1^{tetO/+}$*;R26rtTA*, and $Ate1^{tetO/-}$ mice (Fig. 4.3 and Fig. 4.4). Mice that were fed control (Dox-deficient) diet had low or negligible Ate1 R-transferase expression in the above tissues, with the exception of the

thymus. In contrast, mice that were fed Dox-containing diet had high level of Ate1 R-transferase expression. In particular, the brains of *Ate1*$^{tetO/-}$ mice on Dox-deficient diet, contained negligible levels of Ate1 R-transferase. The resulting Ate1 R-transferase deficiency led to strikingly high steady-state levels of the Rgs4 protein (Fig. 4.4).

Increased susceptibility to epilepsy and increased severity of seizures in Ate1$^{flox/-}$;CaggCreER and Ate1$^{tetO/-}$ mice

To address the role of Ate1 and Nt-arginylation in epileptic seizures, we subjected *Ate1*$^{flox/-}$*;CaggCreER* mice, *Ate1*$^{tetO/-}$ mice, *Ate1*$^{tetO/-}$*;R26rtTA* mice, and their corresponding wild-type and heterozygous (control) littermates (*Ate1*$^{flox/+}$ mice, *Ate1*$^{tetO/+}$ mice, *Ate1*$^{+/-}$ mice, and *Ate1*$^{tetO/+}$*;R26rtTA* mice) to treatments with either NMDA or KA through intraperitoneal (IP) injections. *Ate1*$^{flox/-}$*;CaggCreER* mice were made Ate1-deficient through tamoxifen (TM) treatment [121]. *Ate1*$^{tetO/-}$ mice and *Ate1*$^{tetO/-}$*;R26rtTA* mice were fed a Dox-deficient diet, resulting in negligible activity of their single *Ate1* allele. We observed mice for 60-120 minutes after injections of either NMDA or KA and scored severity of seizures using the Racine scale. Remarkably, all three kinds of Ate1-deficient mice, *Ate1*$^{flox/-}$*;CaggCreER* mice, *Ate1*$^{tetO/-}$ mice, and *Ate1*$^{tetO/-}$*;R26rtTA* mice, suffered severe seizures upon either NMDA or KA treatments that resulted in mild effects on wild-type (*Ate1*$^{+/+}$) and heterozygous (*Ate1*$^{+/-}$) mice (Fig. 4.5 and Fig. 4.6). In the case of KA treatments on *Ate1*$^{flox/-}$*;CaggCreER* mice, one of the wild-type mice suffered fatality during seizure skewing the average Racine score for control mice (Fig. 4.6). We are investigating more mice to see if this is an anomaly or if there are other variables that affect mouse predisposition toward

epileptic seizures. For example, the time of day at which the experiment is carried out may affect endogenous Ate1 levels due to circadian rhythm regulation.

Previous studies have shown that in mice treated with KA or NMDA, the more severe seizures caused higher extents of brain injury [127, 128]. In these Ate1-deficient, highly epileptic mice, we found, using histochemical methods, widespread cell death in the thalamus, the hypothalamus, and the hippocampus. Sections of mouse brains were stained with Fluoro-Jade C to detect dead neurons. Fluoro-Jade C is a mixture of the sulfate ester of three fluorescein derivatives (see Materials and Methods) that specifically and reliably stains dead neurons [127]. TM-treated *Ate1*$^{flox/-}$*;CaggCreER* mice (converted to the *Ate1*$^{-/-}$*;CaggCreER* genotype in the brain and other tissues) that underwent KA treatment suffered a marked increase in cell death in the hippocampus, thalamus, and hypothalamus regions, in comparison to KA-treated wild-type mice (Fig. 4.7A, B, and C).

To observe apoptotic cells using a different method, we performed TUNEL assays with the brain sections. While TM-treated *Ate1*$^{flox/-}$*;CaggCreER* mice that underwent KA treatment exhibited a minor increase in hippocampal apoptosis in comparison with KA-treated wild-type mice (Fig 4.8A), we observed a moderate increase of apoptosis in the thalamus and a major increase of apoptosis in the hypothalamus of TM-treated *Ate1*$^{flox/-}$*;CaggCreER* mice, in comparison with KA-treated wild-type mice (Fig. 4.8B and C). The seemingly lower extents of apoptosis observed using conventional TUNEL assay may stem from a lower sensitivity of this assay, in comparison, e.g., to Fluoro-Jade C staining (Fig. 4.7). We plan to investigate cytological cell death patterns further using APO™-BrdU TUNEL assay. This version of a TUNEL assay includes a fluorescently labeled anti-BrdU

antibody, to amplify the readout signal (which is produced by the added terminal deoxynucleotidyl transferase).

A consequence of seizures is excitotoxicity. Pathologically high cytosolic Ca^{2+} transients ($[Ca^{2+}]_i$), caused by overexcitation of neurons, activate proteases such as Ca^{2+}-dependent calpains, which are one cause of cellular injury and death. To verify calpain activation, we assayed brain regions for the cleavage of spectrin, a known calpain substrate in the hippocampus and elsewhere in the brain. We observed a striking increase in the amount of spectrin cleavage (Fig. 4.9A) in TM-treated *Ate1$^{flox/-}$;CaggCreER* mice under KA treatment, in comparison with KA-treated wild-type mice (lane 2 and 4 versus lane 3 and 5 in Fig. 4.9 A).

Future Experiments

Our findings about the strong and apparently connection between the Ate1-mediated N-terminal aginylation and the propensity toward (as well as severity of) epileptic seizures indicate a major role of the Arg/N-end rule pathway as a suppressor of overexcitation and epilepsy. Mice that were made Ate1-deficient (TM-treated *Ate1$^{flox/-}$;CaggCreER* mice and *Ate1$^{tetO/-}$* mice fed a Dox-deficient diet) suffered more severe seizures, neuronal death, and elevated intracellular calpain activity. One advantage of *Ate1$^{tetO/-}$;R26rtTA* mice (in which one copy of Ate1 gene is unconditionally null while the other copy expresses Ate1 only in the presence of Dox) is the ability to reverse Ate1-deficiency through feeding these mice a Dox-containing diet. We intend to see whether a reversal of Ate1 deficiency in these mice would alleviate their epileptic phenotype. Furthermore, a plausible explanation for the bulk

of our observations about the connection between the Arg/N-end rule pathway and epilepsy is that these striking phenotypes of Ate1-deficient mice are caused at least in part by abnormally high steady-state levels of Rgs4, Rgs5, and Rgs16 G-protein regulators in these mice, as these RGS proteins are conditionally short-lived owing to their nitric oxide/oxygen-dependent, Ate1-dependent degradation by the Arg/N-end rule pathway [87, 129]. If so, a down-regulation or complete ablation of, for example, Rgs4 (the most prominently and broadly expressed RGS among the above three proteins) may at least partially rescue the above phenotypes of Ate1-deficient mice.

We are collaborating with the Neubig group [130-135] in testing their small-compound Rgs4 inhibitor with our Ate1-deficient mouse strains. We have recently received the CCG-203769 RGS4 inhibitor from Dr. Neubig and are about to initiate these experiments. We also are constructing, through compound heterozygous matings, double-mutant *Ate1*$^{flox/-}$ *Rgs4*$^{-/-}$*; CaggCreER* mice that unconditionally lack Rgs4 and can be caused to ablate their remaining copy of the *Ate1* gene. Behavioral and histological assays with the above drug-treated mice and with double-mutant mice (vis-à-vis controls) will further advance the mechanistic understanding of epilepsy and the role of Ate1-Rgs4 circuits in the control of neuronal excitation.

A major aspect of epilepsy is over-activation of calpain proteases. Such activation generates, *in vivo*, many intracellular protein fragments. As discussed above and shown by earlier studies in our lab [111], a large fraction of such fragments are natural substrates of the Arg/N-end rule pathway, and, in particular, of its Ate1-dependent arginylation branch. We shall, therefore, continue to address this aspect of abnormal phenotypes of Ate1-deficient mice, in part by applying mass-spectrometry (MS)-based methods such as PROTOMAP,

which makes it possible to detect and measure the *in vivo* generation of protein fragments [136].

In sum, the long-term aim of these ongoing studies is a more detailed understanding of the role of the Arg/N-end rule pathway as a regulator of epilepsy-relevant circuits as well as a broader set of functions of this proteolytic pathway in the brain.

Materials and Methods

Animal Care and Treatments

All animal procedures (protocol #1328) were done with approval by the Institutional Animal Care and Use Committee (IACUC) and the Office of Laboratory Animal Research (OLAR) at the California Institute of Technology. Mice were housed at 71-75º F (22-24º C), 30-70% humidity, and 13 hours light / 11 hours dark cycle. Mice were either kept either in elevated-barrier, in intermediate-barrier, or in low-barrier facilities depending on specific procedures. Mice were fed with PicoLab® Rodent Diet 20 5053 (LabDiet St. Louis, MO) *ad libitum*.

Ate1$^{flox/-}$*;CaggCreER* Mouse Strains

Ate1$^{flox/-}$;*CaggCreER* mice were constructed previously [121]. The mice harbored one unconditionally null *Ate1*− allele (derived, through matings, from the previously constructed heterozygous *Ate1*+/− mice bearing an unconditionally null *Ate1*− allele [120]) and one "floxed" (*lox* sites-bearing), conditionally active *Ate1flox* allele that could be made null in the presence of active Cre recombinase. These mice also contained the *CaggCreER* gene, expressed from the ubiquitously active chimeric *Cagg* promoter [137]. *CaggCreER* encoded CreER, a fusion between the phage P1 Cre recombinase and a derivative of the mouse estrogen receptor ligand-binding domain. CreER was functionally inactive (sequestered in the cytosol) but could be activated by intraperitoneal (IP) injection of tamoxifen (TM).

Mice aged between 3 and 8 weeks were treated at 1 mg/g of body weight (BW) dosage with TM (Sigma) (2 mg in 0.2 ml sesame oil) by daily IP injections over 5 days. Mice were weighed weekly, starting 3 days before the first TM treatment.

To produce *Ate1flox/−*;*CaggCreER* mice, we mated *Ate1flox/+* mice with *Ate1+/−*;*CaggCreER* mice (the latter were generated by mating *Ate1+/−* with *Ate1+/+*;*CaggCreER* mice). To produce *Ate1flox/flox*;*CaggCreER* mice, we mated *Ate1flox/+* mice with *Ate1flox/+*;*CaggCreER* mice (the latter were generated by mating *Ate1flox/+* mice with *Ate1+/+*;*CaggCreER* mice).

Construction of $Ate1^{tetO/-}$ and $Ate1^{tetO/-}$;*R26rtTA* Mouse Strains

The targeting vector was constructed using a DNA fragment between the BstXI and PacI restriction sites on the *Ate1* gene locus. This fragment encompasses *Ate1* exon 1A and exon 1B, with the bidirectional P_{Ate1} promoter in between the two exons [121]. The fragment was modified as follows. A hygromycin resistance marker, *Hph*, expressed from the P_{PGK} promoter and terminated with a polyA tail was inserted upstream of the *Ate1* exon 1B between the XbaI and XhoI restriction sites. The marker was flanked by two *loxP* sites. The $(TetO)_7$ $P_{miniCMV}$ promoter replaced the bidirectional P_{Ate1} promoter next to the StuI restriction site.

The targeting vector was electroporated into 129 embryonic stem (ES) cells. The resulting cell population was plated on hygromycin-containing plates to select for hygromycin-resistant ES cell colonies. ES cells were grown in DMEM supplemented with 15% fetal bovine serum (FBS), 0.1 mM non-essential amino acids, 0.1 mM β-

mercaptoethanol, 2 mM glutamine, 100 U/ml penicillin, 0.1 mg/ml streptomycin, 1 mM pyruvate, and 1,000 U/ml leukemia inhibitory factor (LIF) [138], using a feeder layer of hygromycin-resistant mouse primary fibroblasts that had been treated with 10 μg/ml mitomycin C for 3 hr at 37°C. Selection with hygromycin (at 0.2 mg/ml) was started 24 hr after electroporation. Correctly targeted ES cell clones were identified using Southern hybridization and PCR.

ES cell lines that had apparently normal karyotypes were injected into 3.5-day-postcoitum C57BL/6J blastocysts and implanted into pseudopregnant females. The resulting male chimeric offspring were mated with C57BL/6J females. In some of the progeny, *Ate1*^{tetO} containing ES cells became a part of germline [138, 139]. Mice with the correctly integrated *Ate1*^{tetO} allele were mated with Cre-expressing mice to remove the *Hph* marker, thereby producing the desired *Ate1*$^{tetO/+}$ mice. The loss of the resistance marker was checked by Southern DNA hybridization and by PCR as well. *Ate1*$^{tetO/+}$ mice were mated with the *Gt(ROSA)26Sor*$^{tm1(rtTA2S*M2)Whsu}$ (*R26rtTA*) mice obtained from the Jackson Laboratory [123]. *R26rtTA* mice express a modified form of reverse tetracycline/doxycycline (Dox)-controlled transactivator (rtTA) at the *Rosa26* locus. rtTA is a fusion of a TetR mutant (rTetR) and the C-terminal activation domain of VP16 of the herpes simplex virus [124]. The *R26rtTA* allele allows the overexpression of Ate1 from the *Ate1*^{tetO} allele upon addition of Dox in food.

To produce *Ate1*$^{tetO/-}$ mice, *Ate1*$^{tetO/+}$ mice were mated with *Ate1*$^{+/-}$ mice [120]. To produce *Ate1*$^{tetO/tetO}$ mice, *Ate1*$^{tetO/+}$ mice were mated with *Ate1*$^{tetO/+}$ mice. To produce *Ate1*$^{tetO/-}$*;R26rtTA*, *Ate1*$^{tetO/+}$*;R26rtTA*, and *Ate1*$^{tetO/tetO}$*;R26rtTA* mice, *Ate1*$^{tetO/-}$ mice, *Ate1*$^{tetO/+}$ mice, and *Ate1*$^{tetO/tetO}$ mice were mated with *R26rtTA* mice respectively. During the mating, pregnant female mice that carried litters containing *Ate1*$^{tetO/-}$*;R26rtTA*,

Ate1$^{tetO/+}$*;R26rtTA*, or *Ate1*$^{tetO/tetO}$*;R26rtTA* mice were fed *ad libitum* with Dox-containing diet TD.00502 (Envigo). The Dox-containing diet dosage is 0.5-0.9 mg of Dox per 3-5 g of food. The daily food intake of a 30-g BW adult mice is about 3-5 g of food giving the pregnant mice the daily dosage of 0.5-0.9 mg of Dox [140]. All other mice were fed with the control Dox-deficient diet 2018 (Envigo).

Construction of *Ate1*$^{flox/-}$ *Rgs4*$^{-/-}$*; CaggCreER* Mouse Strains

The previously constructed *Rgs4*$^{-/-}$ mice were a gift from Dr. Scott Heximer (University of Toronto, Canada) [95]. The functional null *Rgs4*$^{-}$ allele, termed *Rgs4*^{tm1Dgen} in the Jackson Laboratory database, was generated by Deltagen Inc. That allele was produced by a targeted insertion of the lacZ gene and the neomycin (Neo) marker. LacZ transcription was driven by the endogenous *Rgs4* promoter. *Rgs4*$^{-/-}$ mice are healthy with no apparent defect.

To produce *Ate1*$^{flox/-}$ *Rgs4*$^{-/-}$*; CaggCreER* mice, appropriate mating pairs were made between *Rgs4*$^{-/-}$ mice and *Ate1*$^{flox/-}$*; CaggCreER* mice. *Ate1*$^{flox/-}$ *Rgs4*$^{-/-}$*; CaggCreER* mice aged between 3 and 8-week old were treated with TM (Sigma) (2 mg in 0.2 ml sesame oil) by daily IP injections over 5 days. Mice were weighed weekly, starting 3 days before the first TM treatment.

Genotyping of Mouse Strains

Mouse tails and ears were digested overnight at 60^{o}C in "tail digestion buffer" (5 mM EDTA pH 8.0, 0.2 M NaCl, 0.3% SDS, 0.4 mg/ml Proteinase K, 0.1 M Tris-HCl pH 8.5).

Genomic DNA was precipitated using isopropanol and cleaned with 70% ethanol [121]. Genomic DNA was dissolved in "TE buffer" (1 mM EDTA, 10 mM Tris-HCl, pH 8.0). Specific gene alleles were verified by PCR using primers listed in Table 4.2. All PCR reactions except for those to detect the *CaggCreER* transgene were carried out using HotStar Taq DNA polymerase, standard buffer conditions (Qiagen), 35 cycles of template denaturation for 30 seconds at 95°C, followed by primer annealing for 30 seconds at 60°C and primer extension for 1 minute at 72°C. PCR reactions for detecting *CaggCreER* were carried out using 30 cycles of template denaturation for 30 seconds at 95°C, followed by primer annealing for 30 seconds at 58°C and primer extension for 45 seconds at 72°C.

Seizure Induction by Kainate (KA) or NMDA Injection

Mice at indicated ages were injected intraperitoneally (injection volume 100-300 µl) with either 20-40 mg/kg body weight BW of KA (Sigma K0250; 2 mg/ml in 0.9% saline) or 80-120 mg/kg BW of NMDA (Sigma M3262; 20 mg/ml in 0.9% saline). Mice were scored at 1 min intervals using a Racine scale (Table 4.3) for 60-120 min [141-143]. The mean and the standard error of the mean (SEM) were calculated for each test group.

Once the observations were completed, mice were sacrificed for analyses or returned to their cages. For mice that experienced high levels of seizure, diazepam was injected to calm them before returning them to their cages. If the seizure could not be controlled, mice were euthanized.

Tissue Extracts and Immunoblotting

Mouse tissues were harvested and lysed in "NP-40 buffer" (150 mM NaCl, 1% NP-40, 50 mM Tris-HCl, pH 8.0) or in "RIPA buffer" (150 mM NaCl, 1% NP-40, 0.5% sodium deoxycholate, 0.1% SDS, 50 mM Tris-HCl, pH 8.0). Buffers were supplemented with 1 mM dithiothreitol (DTT) and freshly dissolved "Complete EDTA-Free Protease Inhibitors" (Roche-05892953001). Tissues were disrupted using the MP FastPrep-24 instrument and Lysing Matrix D (MP Biomedicals) with 2 or 3 runs at 6.5 m/s for 25 sec each, and with 5 min incubations on ice between the runs. The lysates were clarified by centrifugation at 12,000g for 30 min at 4°C.

The lysates were subjected to gel electrophoresis using MES or MOPS buffer and Bis-Tris SDS-PAGE gels with the appropriate gel percentage (10%, 12%, or 4-12%). The proteins were transferred to either PVDF or nitrocellulose membrane using the iBlot® Dry Blotting System (ThermoFisher Scientific). Immunoblots were detected using the IRDye® Odyssey Imaging Systems (LI-COR).

In Vitro Arginylation Assay

The arginyltransferase (R-transferase) reaction (50 µl) contained extracts from a specific mouse tissue (2.5 mg of total protein per ml), 0.5 mg/ml α-lactalbulmin (Sigma), 0.6 mg/ml total *E. coli* tRNA (Roche 10109541001), 800 U/ml *E. coli* aminoacyl-tRNA synthetase (Sigma A3646), 5 mM MG132, 1 mM ATP, 30 mM KCl, 2 mM $MgCl_2$, 2 mM DTT, 10 mM Tris-HCl pH 8.0, and 0.3 mM ^{3}H-arginine (Arg) (PerkinElmer NET1123001MC). The reaction mixture was incubated for 30 min at 37ºC and was spotted onto 1-cm square 3MM Whatman filter papers. The filter papers were boiled for 10 min in

10% trichloroacetic acid (TCA). The filter papers were then washed in ice-cold 5%TCA three times and in ice-cold ethanol once. Incorporated hot TCA-insoluble ^{3}H-Arg was measured using a Beckman LS 6500 Scintillation Counter [144].

Analyses of Tissue Sections

48 hr after seizure induction, mice were fixed through transcardial perfusion with 4% formaldehyde (Electron Microscopy Sciences). Mouse brains were further fixed with 4% formaldehyde for 16 hr, rinsed once with PBS for 10 min, dehydrated in 15% Sucrose-PBS for 12 hr, and dehydrated again in 20% Sucrose-PBS for 12 hr. Tissues were thereafter frozen in Tissue-Tek O.C.T Compound (Sakura Finetek) using 70% ethanol-dry ice bath and stored at -80ºC. Frozen tissues were sectioned coronally into sections (12 μm or 20 μm).

The 12 μm sections were mounted on Superfrost Plus Microscope Slides (Fisher Scientific). They were used to assess apoptosis by TUNEL, a nuclear DNA fragmentation assay, using a TUNEL kit (Roche, Indianapolis, IN), fluorescein-dUTP, and manufacturer's instructions.

The 20 μm sections were mounted onto 1% gelatin coated glass slides. They were used to assess cell death using Fluoro-Jade C staining (Histo-Chem Inc). Fluoro-Jade C is a mixture of the sulfate ester of trisodium 5-(6-hydroxy-3-oxo-3H-xanthen-9-yl) benzene, 1,2,4, tricarboxylic acid, disodium 2-(6-hydroxy-3-oxo-3H-xanthen-9-yl)-5-(2,4-dihydroxybenzol) terephthalic acid, and disodium 2,5-bis(6-hydroxy-3-oxo-3H-xanthen-9-yl) terephthalic acid. Fluoro-Jade C reproducibly and specifically stains degenerating neurons through an unknown mechanism [127].

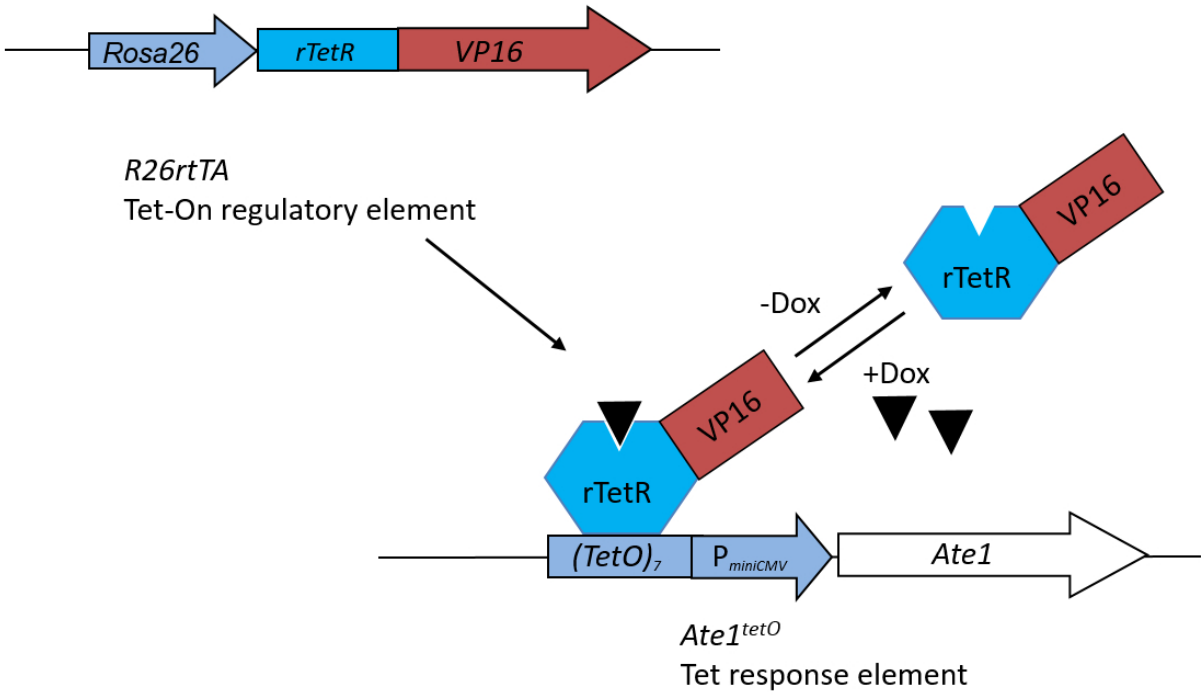

Figure 3.1 Regulation of gene expression by doxycycline (Dox). The *R26rtTA* mice express a modified form of reverse tetracycline/Dox-controlled transactivator (rtTA) whose gene is integrated in the *Rosa26* locus [123]. rtTA is a fusion of a TetR mutant (rTetR) and the C-terminal activation domain of VP16 of the herpes simplex virus [124]. Upon the addition of Dox, rTetR undergoes conformation change and binds to the *tetO* DNA elements [125]. The activation domain of VP16 attracts host transcription factors and RNA polymerase II to initiate transcription [126].

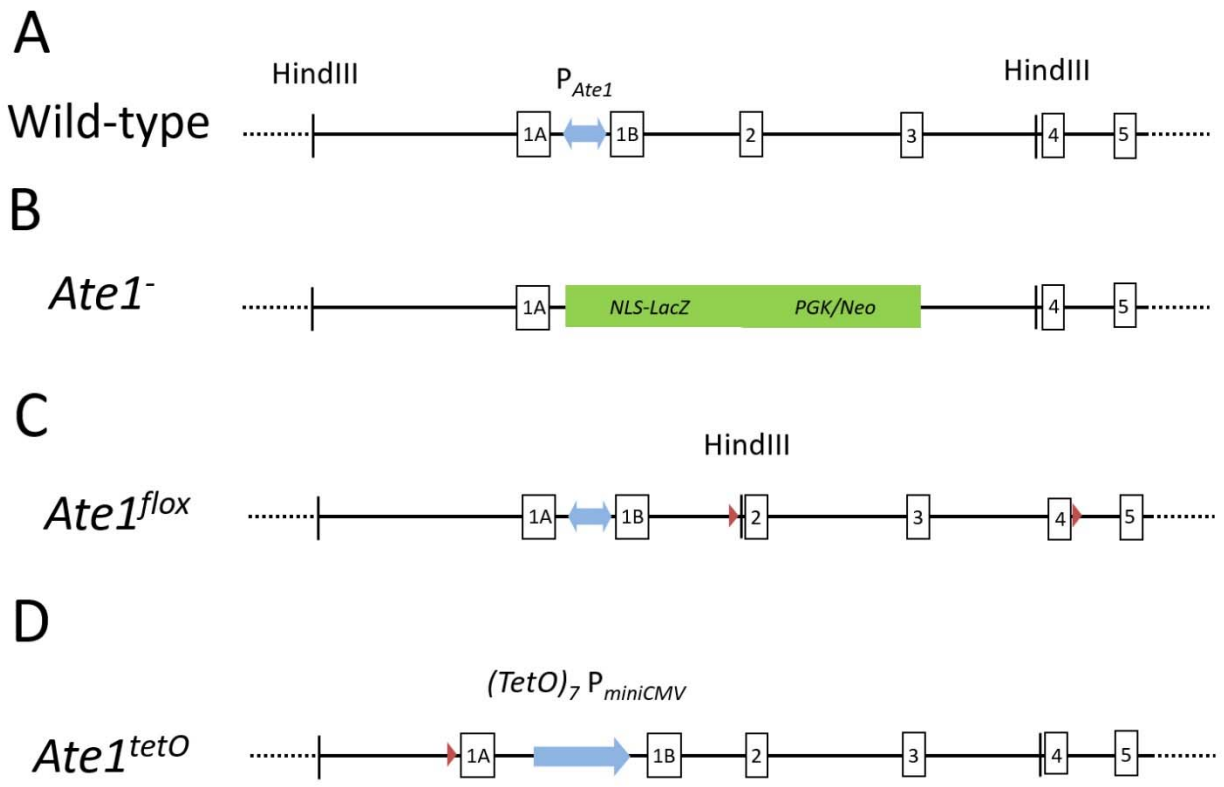

Figure 3.2 Mouse Ate1 alleles. The wild-type, *Ate1*$^{-}$, *Ate1*^{flox}, and *Ate1*^{tetO} alleles are shown. The differences between these alleles are confined to the region between *Ate1* exon 1A and exon 5. (A) A diagram of the 5' end of wild-type *Ate1* allele shows the bidirectional endogenous P$_{Ate1}$ promoter being flanked by the *Ate1* exon 1A and exon 1B [144]. (B) For *Ate1*$^{-}$ allele, the NLS-containing lacZ (*NLS-lacZ*) and the neomycin (Neo) selection marker expressed from the phosphoglycerate kinase P$_{PGK}$ promoter (*PGK/Neo*) replaced *Ate1* exon 1B, exon 2, exon 3, and the corresponding introns [120]. (C) For the *Ate1*^{flox} allele, *loxP* sites were inserted before exon 2 and after exon 4 [121]. For the *Ate1*^{tetO} allele, the *(TetO)*$_7$ P$_{miniCMV}$ promoter replaced the endogenous bidirectional element of the P$_{Ate1}$ promoter. There is an additional *loxP* site upstream of *Ate1* exon 1A that resulted from the removal of the hygromycin resistance marker that had been used, earlier, to insert the new *(TetO)*$_7$ P$_{miniCMV}$ promoter element.

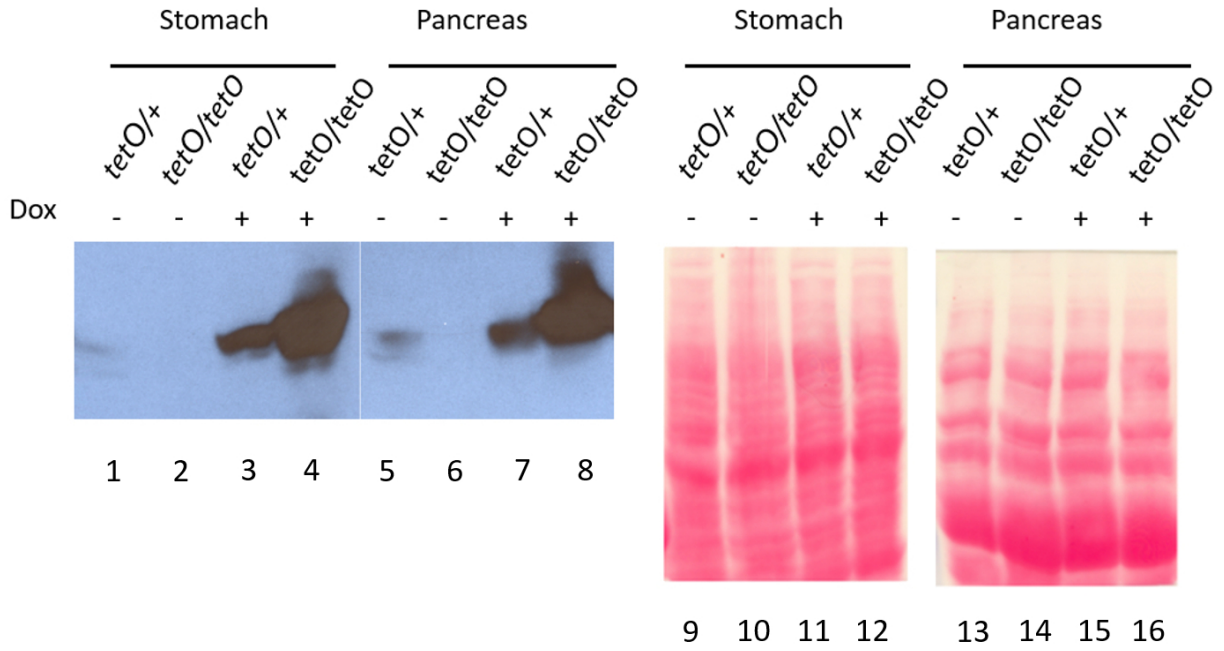

Figure 3.3 Dox induces Ate1 in *Ate1$^{tetO/tetO}$;R26rtTA* and *Ate1$^{tetO/+}$;R26rtTA* mice. Lysates from the stomachs and the pancreas of *Ate1$^{tetO/tetO}$;R26rtTA* and *Ate1$^{tetO/+}$;R26rtTA* mice were fractionated with 4-12% SDS-PAGE gels and immunoblotted against anti-Ate1. In extracts from the stomachs (lanes 1-4) and pancreas (lanes 5-6) of *Ate1$^{tetO/tetO}$;R26rtTA* and *Ate1$^{tetO/+}$;R26rtTA* mice, Ate1 R-transferase was expressed above its normal endogenous levels when mice were fed a Dox-containing diet. The corresponding total protein patterns (Ponceau S-stained) are shown in lanes 9-16.

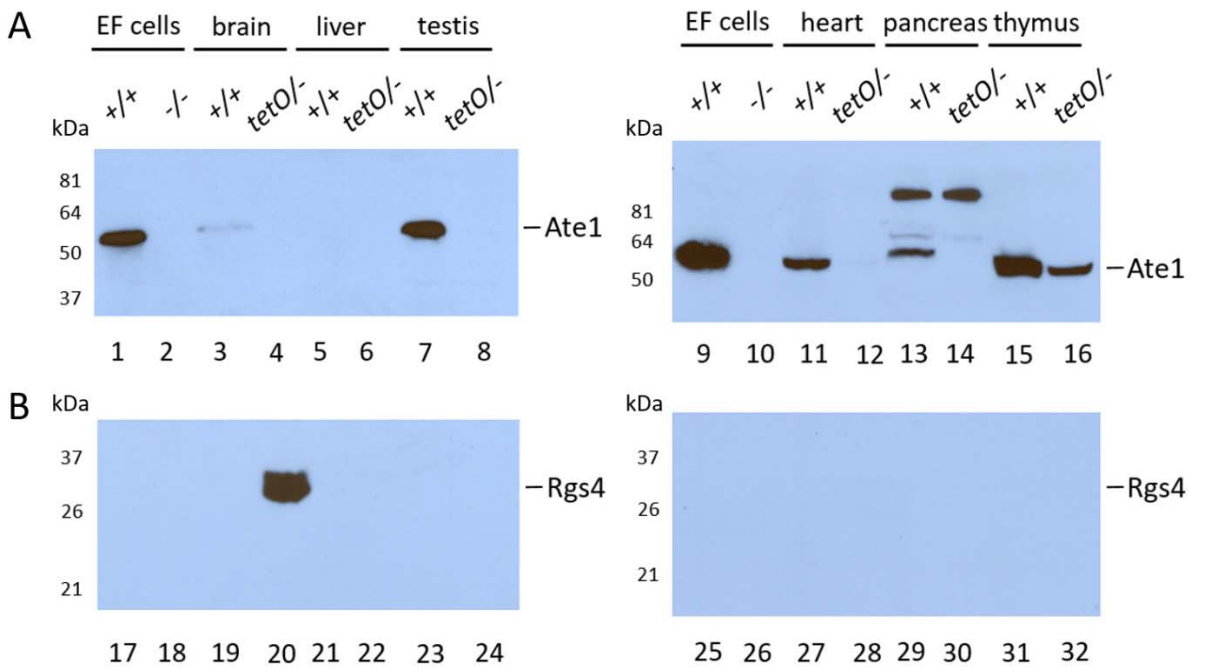

Figure 3.4 *Ate1*$^{tetO/-}$ mice are Ate1 R-transferase deficient. *Ate1*$^{tetO/-}$ mice and the control wild-type (*Ate1*$^{+/+}$) littermates were fed with Dox-deficient diet. (A) Lysate from embryonic fibroblast (EF) cell lines from *Ate1*$^{+/+}$ and *Ate1*$^{-/-}$ embryos (lane 1-2) and from the brain, liver, testis, heart, the pancreas of *Ate1*$^{+/+}$ or *Ate1*$^{tetO/-}$ mice (lane 3-16) were fractionated with 4-12% SDS-PAGE gels and immunoblotted against anti-Ate1. *Ate1*$^{tetO/-}$ mice that were on Dox-deficient diet lacked immunologically detectable levels of Ate1 R-transferase on all examined tissues. The only exception, among the examined tissues, was the thymus, which contained a below-wild-type but significant amount Ate1. (B) The above fractionated lysates were also immunoblotted against anti-Rgs4 (lane 17-32). In the brain, the reduction in protein level of Ate1 R-transferase in *Ate1*$^{tetO/-}$ mice was accompanied by a marked increase in the level of the Rgs4 protein, conditionally short-lived protein and an Nt-arginylation substrate of Ate1 (compare between lanes 3 and 4 and between lanes 19 and 20).

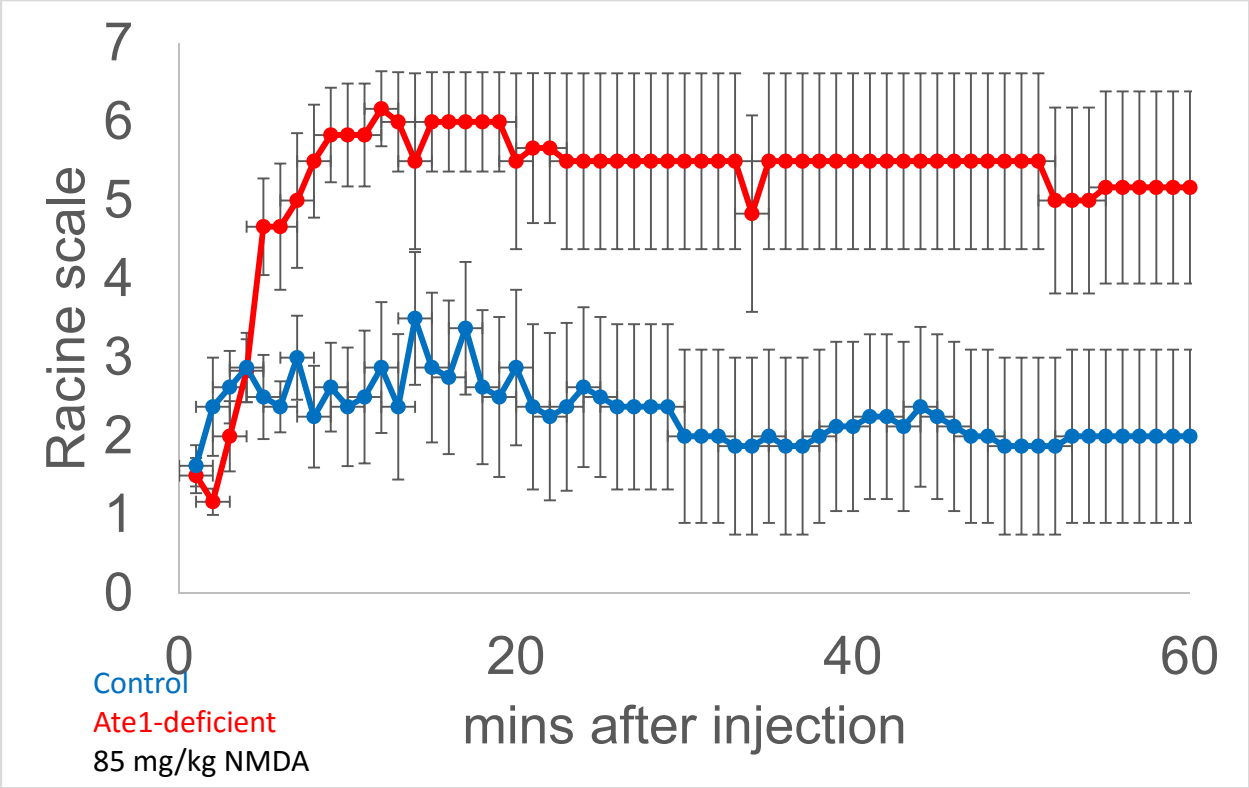

Figure 3.5 Increased epileptic tendency and seizure severity in Ate1-deficient (*Ate1*$^{tetO/-}$) mice versus control wild-type and heterozygous littermates (*Ate1*$^{tetO/+}$ mice, *Ate1*$^{+/-}$ mice, and *Ate1*$^{tetO/+}$*;R26rtTA* mice) upon NMDA injection. *Ate1*$^{tetO/-}$ mice and *Ate1*$^{tetO/-}$*;R26rtTA* mice were fed with Dox-deficient diet to ensure Ate1-deficiency. 8 control wild-type and heterozygous mice and 6 *Ate1*$^{tetO/-}$ or *Ate1*$^{tetO/-}$*;R26rtTA* mice were used for the study. The NMDA treated mice were 232 to 268-day old. They received a single NMDA IP injection at 85 mg/kg of BW, followed by observations over 1 hr. Seizure severity was scored using a Racine scale. The mean and the standard error of the mean (SEM) were plotted.

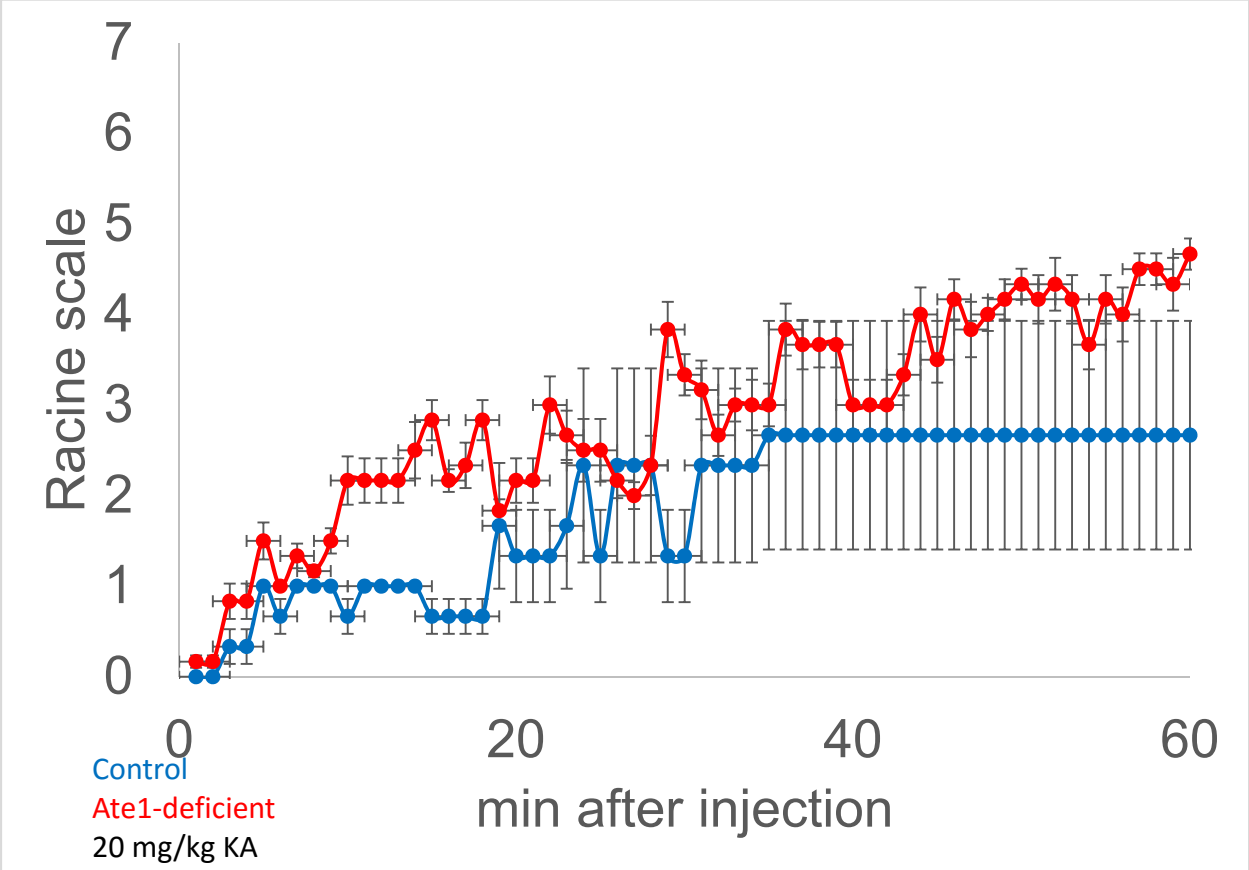

Figure 3.6 Increased epileptic tendency and seizure severity (*Ate1*$^{-/-}$) mice versus wild-type (*Ate1*$^{+/+}$) and heterozygous (*Ate1*$^{+/-}$) littermates upon KA injection. 3 control wild-type and 6 *Ate1*$^{flox/-}$*;CaggCreER* mice were used for the study. *Ate1*$^{flox/-}$*;CaggCreER* mice were made Ate1-deficient (*Ate1*$^{-/-}$) through TM treatment [121]. The KA-treated mice were of 60 to120-day old. They received a single KA IP injection at 20 mg/kg of body weight (BW), followed by observations over the next hour. Seizure severity was scored using Racine scale. The mean and the standard error of the mean (SEM) were plotted.

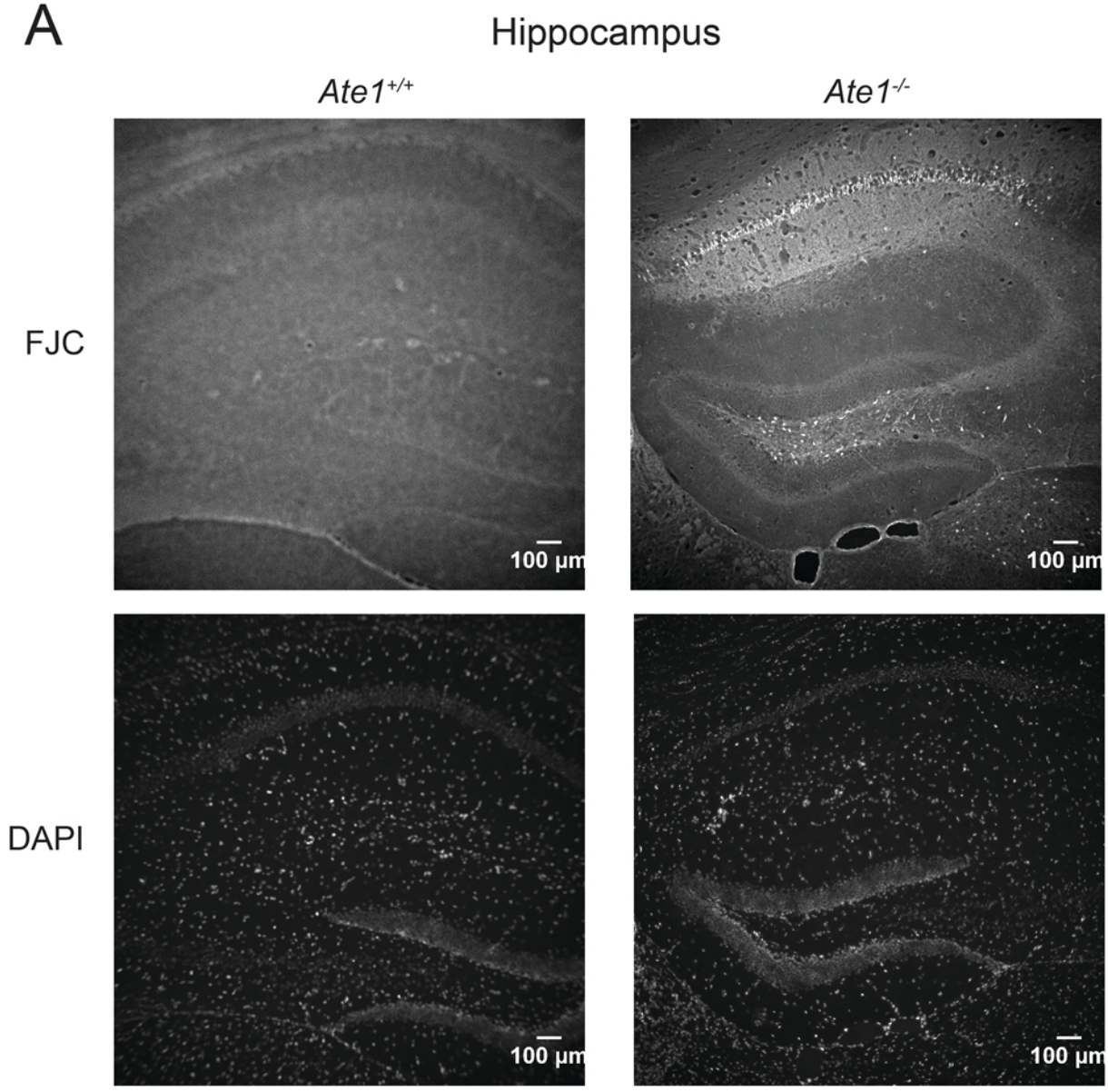
A
Hippocampus
Ate1+/+
Ate1-/-
FJC
DAPI
100 µm
100 µm
100 µm
100 µm

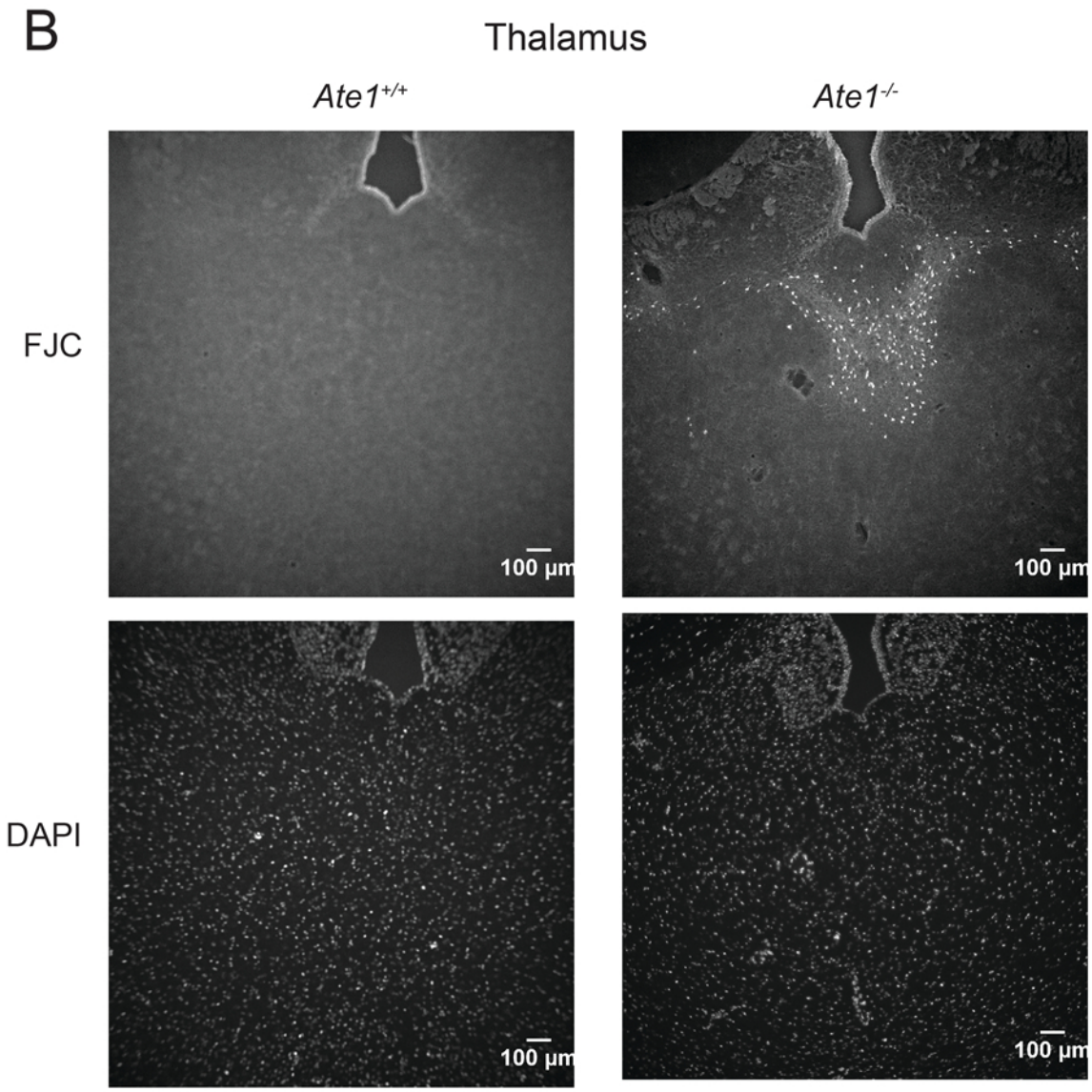
B
Thalamus
Ate1+/+
Ate1-/-
FJC
DAPI
100 µm
100 µm
100 µm
100 µm

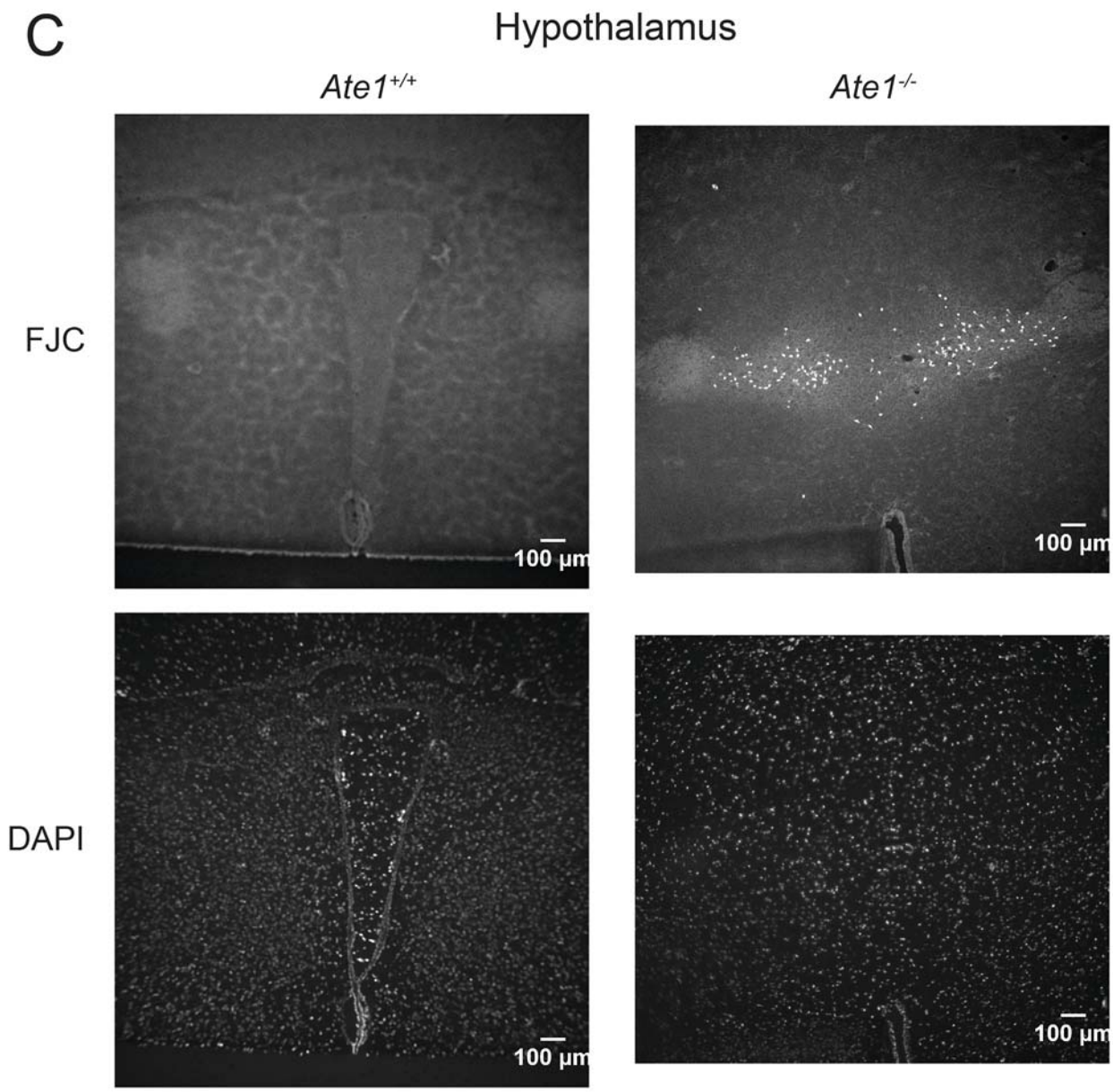
C
Hypothalamus
Ate1+/+
Ate1-/-
FJC
DAPI
100 µm
100 µm
100 µm
100 µm

D

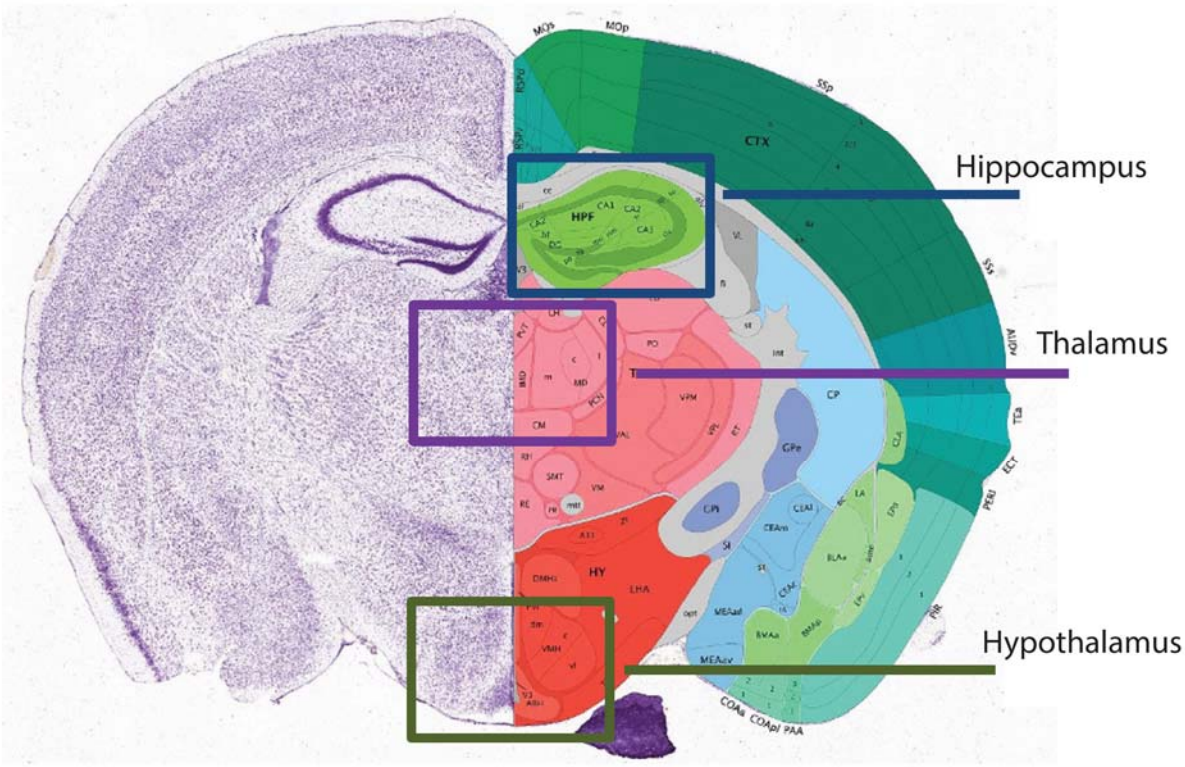

Figure 3.7. Extensive neuron death in KA-treated Ate1-deficient (*Ate1*$^{-/-}$) mice but not in identically treated wild-type (*Ate1*$^{+/+}$) mice. *Ate1*$^{flox/-}$*;CaggCreER* mice were made Ate1-deficient (*Ate1*$^{-/-}$) through TM treatment. (A) Fluoro-Jade C (FJC) and DAPI staining for *Ate1*$^{-/-}$ mice and the corresponding *Ate1*$^{+/+}$ littermates in the hippocampus region. (B) FJC and DAPI staining for *Ate1*$^{-/-}$ mice and the corresponding *Ate1*$^{+/+}$ littermates in the thalamus region (C) FJC and DAPI staining for *Ate1*$^{-/-}$ mice and the corresponding *Ate1*$^{+/+}$ littermates in the hypothalamus region. (D) The approximate field of visualization for each hippocampus, thalamus, and hippocampus region. (Image credit: Allen Institute)

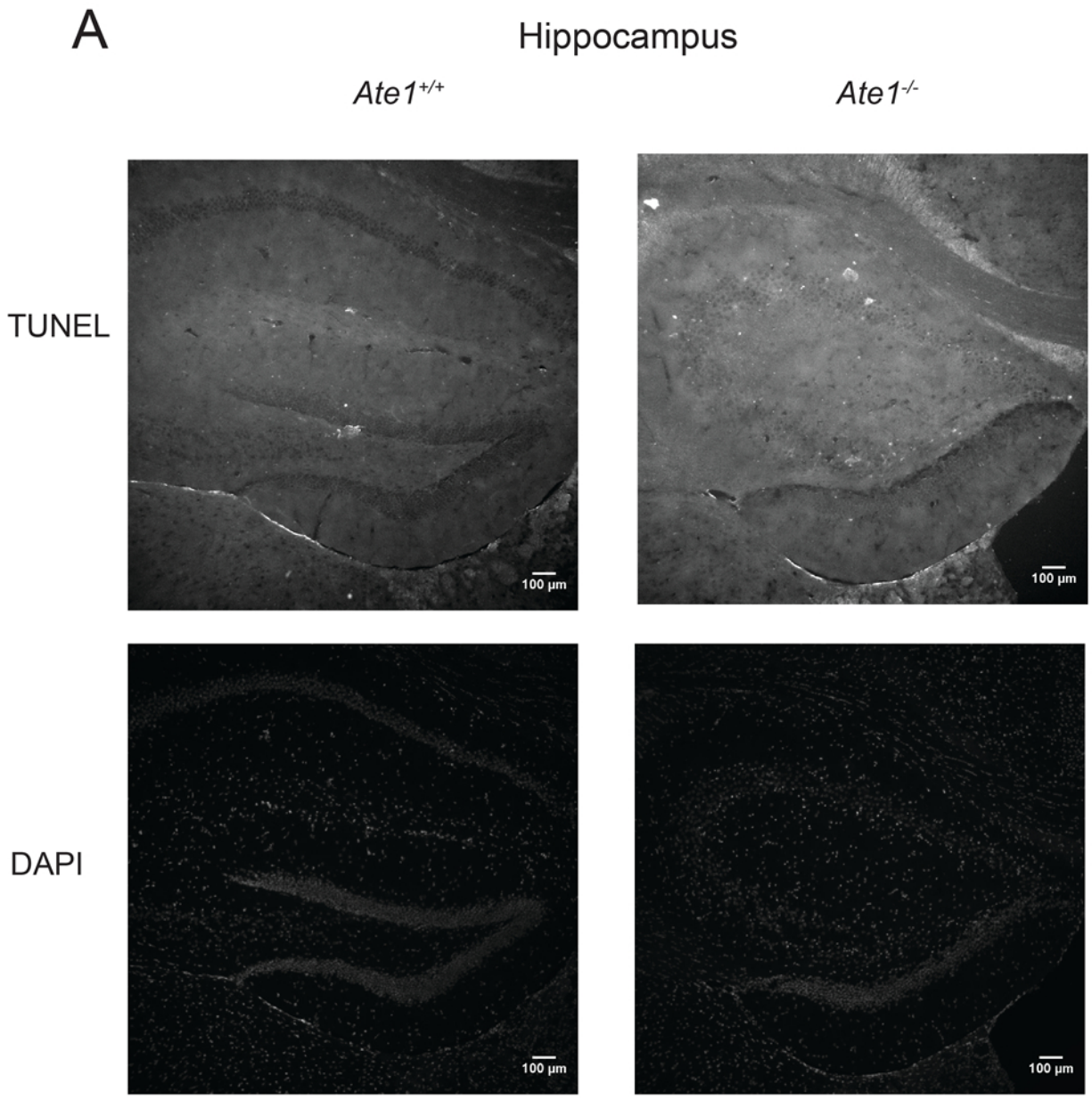
A
Hippocampus
Ate1+/+
Ate1-/-
TUNEL
DAPI
100 µm
100 µm
100 µm
100 µm

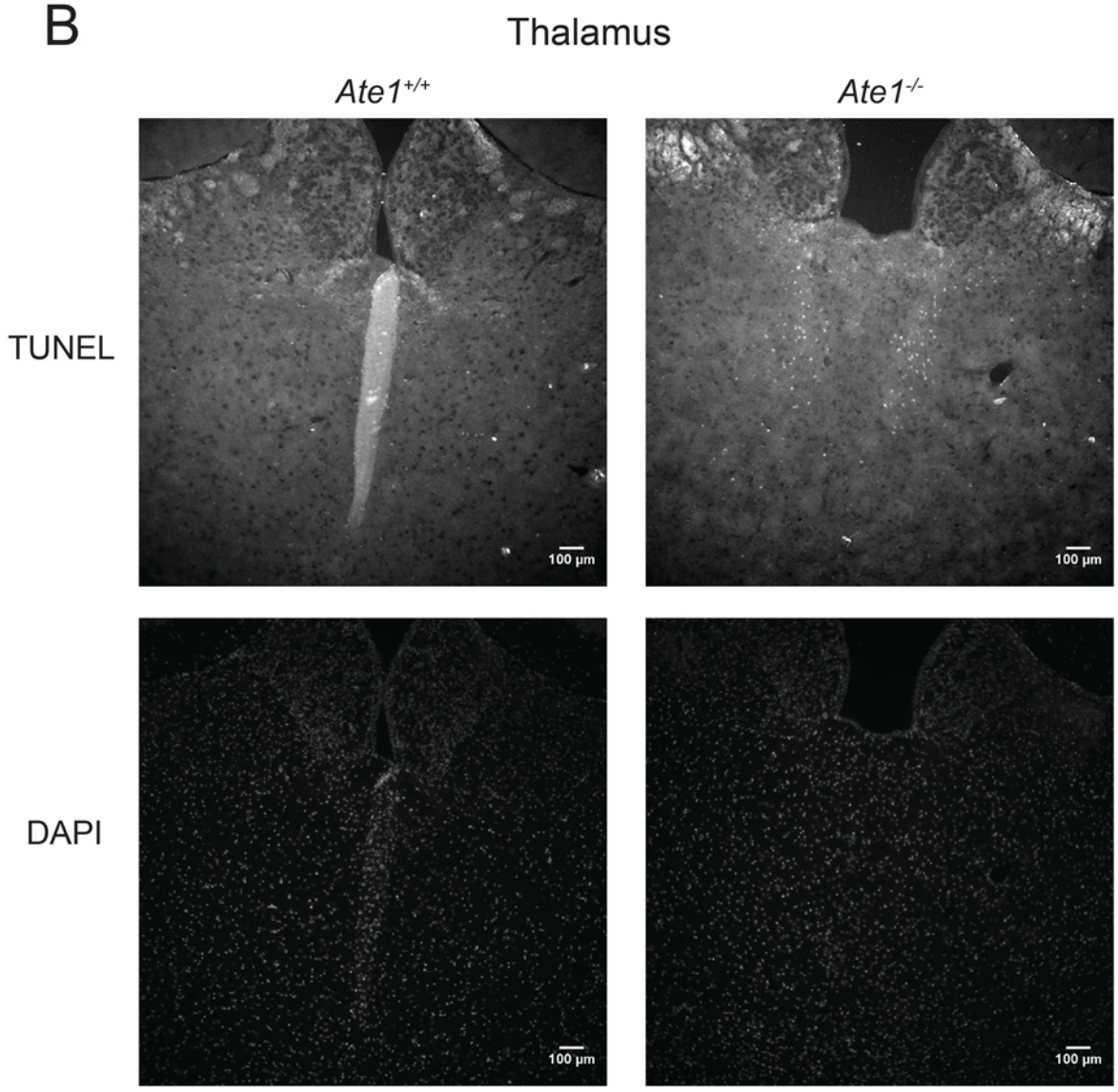
B
Thalamus
Ate1+/+
Ate1-/-
TUNEL
DAPI
100 µm
100 µm
100 µm
100 µm

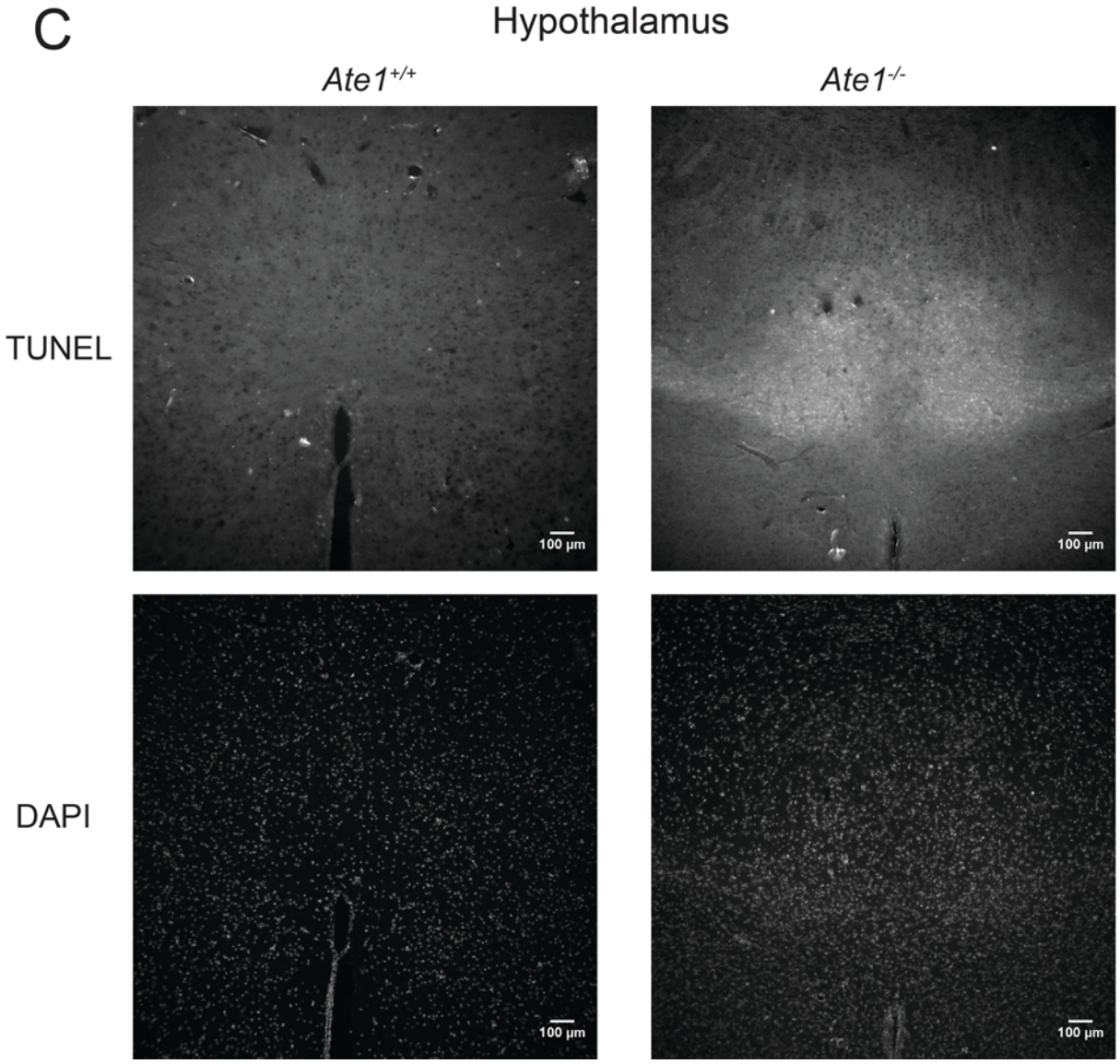

Figure 3.8 Increase apoptosis in hippocampus, thalamus, and hypothalamus in KA-treated Ate1-deficient (*Ate1*$^{-/-}$) mice but not in identically treated wild-type (*Ate1*$^{+/+}$) mice. *Ate1*$^{flox/-}$*;CaggCreER* mice were made Ate1-deficient (*Ate1*$^{-/-}$) through TM treatment. (A) TUNEL labeling and DAPI staining for *Ate1*$^{-/-}$ mice and the corresponding *Ate1*$^{+/+}$ littermates in the hippocampus region. (B) TUNEL labeling and DAPI staining for *Ate1*$^{-/-}$ mice and the corresponding *Ate1*$^{+/+}$ littermates in the thalamus region (C) TUNEL labeling and DAPI staining for *Ate1*$^{-/-}$ mice and the corresponding *Ate1*$^{+/+}$ littermates in the hypothalamus region.

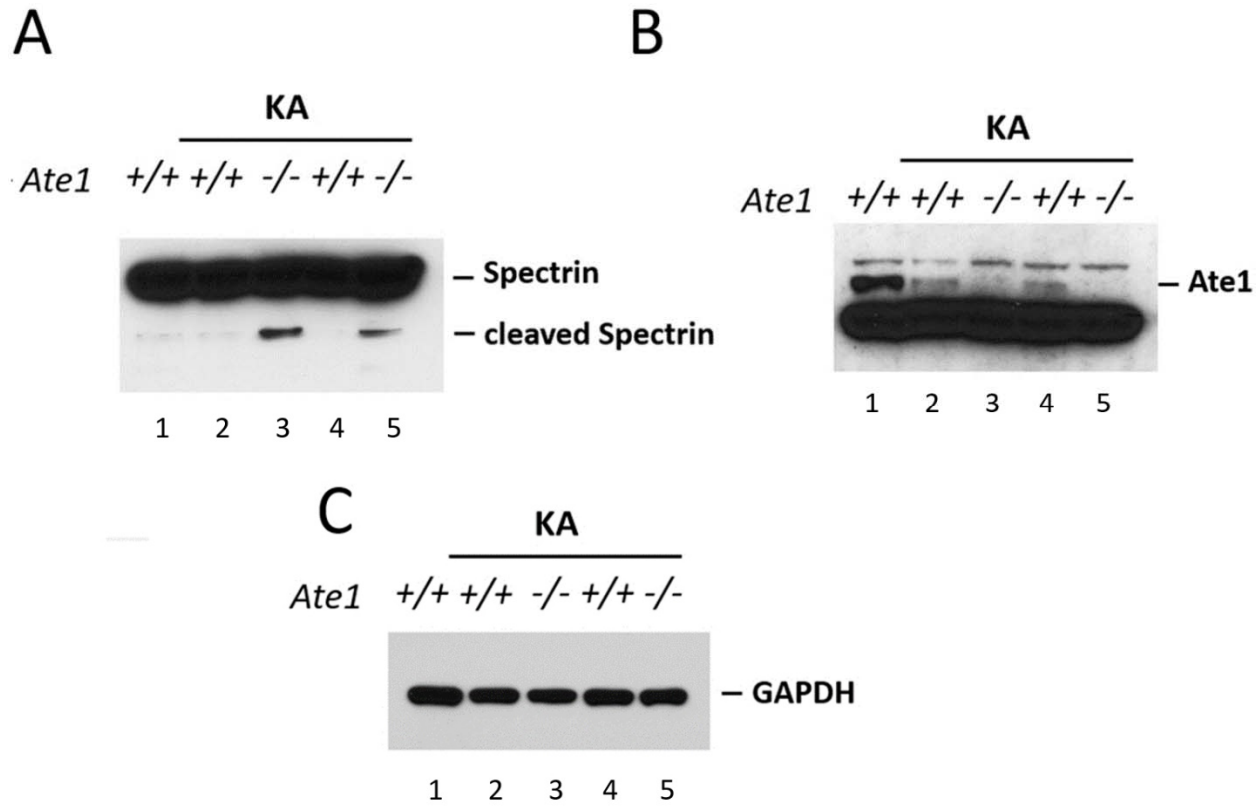

Figure 3.9 Elevated calpain activation in KA-treated Ate1-deficient (*Ate1*$^{-/-}$) mice. *Ate1*$^{flox/-}$*;CaggCreER* mice were made Ate1-deficient (*Ate1*$^{-/-}$) through TM treatment. Lysates from the hippocampus were fractionated with 4-12% SDS-PAGE gels and immunoblotted against (A) anti-Spectrin, (B) anti-Ate1, and (C) anti-GAPDH. In KA-treated *Ate1*$^{-/-}$ mice, the amount of spectrin cleavage was greatly elevated compare to KA-treated wild-type (*Ate1*$^{+/+}$) mice (lanes 2 and 4 versus lanes 3 and 5 in Fig. 4.9 A). anti-Ate1 and anti-GAPDH immunoblots were shown to verify Ate1-deficiency and similar loading inputs.

Table 3.1 The GPCRs in synaptic transmissions

G_α proteins	Glutamate	GABA	ATP	Adenosine
$G_{\alpha i/o}$	mGluR2, 3, 4, 6, 7, 8	$GABA_B$	P2YR12, 13, 14	A_1, A_3
$G_{\alpha q/11}$	mGluR1, 5		P2YR1, 2, 4, 6, 11	
$G_{\alpha s}$			P2YR11	A_{2A}, A_{2B}

The GPCRs in synaptic transmissions and their corresponding G_α proteins. There are three major family of G_α proteins: $G_{\alpha i/o}$, $G_{\alpha q/11}$, and $G_{\alpha s}$. The major neurotransmitters in synaptic transmissions include glutamate which activates the mGluRs, GABA which activates the $GABA_B$ receptor, ATP which activates the P2YRs, and adenosine which activates the A receptors [32, 67].

Table 3.2 PCR Primers		
Allele	Primer	Size (bp)
CaggCreER	GTTCGCAAGAACCTGATGGACA; CTAGAGCCTGTTTTGCACGTTC	Cre: 320
Ate1^{-}	GGTATTTGCTGCCGTCCTTTGGTGGT; CTGTTCCACATACACTTCATTCTCAG; CTGGAGACAAAGCCCCAGCCAGAC	Wild-type: 300; Ate1 null: 560
Ate1^{flox}	CAAGCAGGGGAAGGAGGC; TTCAGGAGTTAGCCATTGCC	Wild-type: 368; Ate1 flox: 408
Ate1^{tetO}	ACACGCCTACCTCGACCCGGG; CCGAGACGCACCCCTGCAACC; TACCCCCTAGGGAGGGCGAGG	Wild-type: 400; Ate1 tet: 609
Ate1^{floxOFF}	GTTTGTGTCACCACTCCTACC TTCAGGAGTTAGCCATTGCC	Ate1 flox-OFF: 470
Rgs4^{-}	GGGCCAGCTCATTCCTCCCACTCAT GGACATGAAACATCGGCTGGGGTTC CCATCTTGACCCAAATCTGGCTCAG	Wild-type: 441 Rgs4 null: 225

Table 3.3 Racine scale			
Scale	Behaviors	Severity	Error
0	no behavior alteration		
1	immobility, mouth and facial movements, facial clonus	Discomfiture	Sleeping
2	head nodding, forelimb and/or tail extension, rigid posture		
3	forelimb clonus, repetitive movements	Mild seizure	Grooming
4	rearing, forelimb clonus with rearing, rearing and falling	Seizure	
5	continuous rearing and falling, jumping		
6	severe tonic-clonic seizures		
7	death		

Racine scale with the corresponding behaviors and severities of seizures. Very mild epileptic episodes can be misinterpreted as normal mouse behaviors, such as sleeping or grooming.

REFERENCES

1. Fisher, R., et al., *ILAE Official Report: A practical clinical definition of epilepsy.* Epilepsia, 2014. **55**(4): p. 475-482.
2. Rakhade, S. and F. Jensen, *Epileptogenesis in the immature brain: emerging mechanisms.* Nature Reviews Neurology, 2009. **5**(7): p. 380-391.
3. Moshé, S., et al., *Epilepsy: new advances.* Lancet (London, England), 2015. **385**(9971): p. 884-898.
4. Pitkänen, A. and K. Lukasiuk, *Mechanisms of epileptogenesis and potential treatment targets.* The Lancet. Neurology, 2011. **10**(2): p. 173-186.
5. Hollinger, S. and J. Hepler, *Cellular regulation of RGS proteins: modulators and integrators of G protein signaling.* Pharmacological reviews, 2002. **54**(3): p. 527-559.
6. Diversé-Pierluissi, M.A., et al., *Regulators of G protein signaling proteins as determinants of the rate of desensitization of presynaptic calcium channels.* The Journal of biological chemistry, 1999. **274**(20): p. 14490-14494.
7. Bertram, E., *Neuronal circuits in epilepsy: Do they matter?* Experimental Neurology, 2013. **244**: p. 67-74.
8. Alexander, G. and D. Godwin, *Metabotropic glutamate receptors as a strategic target for the treatment of epilepsy.* Epilepsy Research, 2006. **71**(1): p. 1-22.
9. Luttjohann, A. and G. van Luijtelaar, *Dynamics of networks during absence seizure's on- and offset in rodents and man.* Frontiers in Physiology, 2015. **6**.
10. Adeli, H., Z. Zhou, and N. Dadmehr, *Analysis of EEG records in an epileptic patient using wavelet transform.* Journal of Neuroscience Methods, 2003. **123**(1): p. 69-87.
11. Arabadzisz, D., et al., *Epileptogenesis and chronic seizures in a mouse model of temporal lobe epilepsy are associated with distinct EEG patterns and selective neurochemical alterations in the contralateral hippocampus.* Experimental Neurology, 2005. **194**(1): p. 76-90.

12. Riban, V., et al., *Evolution of hippocampal epileptic activity during the development of hippocampal sclerosis in a mouse model of temporal lobe epilepsy.* Neuroscience, 2002. **112**(1): p. 101-111.
13. Engel, J., *Introduction to temporal lobe epilepsy.* Epilepsy Research, 1996. **26**(1): p. 141-150.
14. Lévesque, M. and M. Avoli, *The kainic acid model of temporal lobe epilepsy.* Neuroscience and biobehavioral reviews, 2013. **37**(10 Pt 2): p. 2887-2899.
15. Jessberger, S. and J. Parent, *Epilepsy and Adult Neurogenesis.* Cold Spring Harbor Perspectives in Biology, 2015. **7**(12): p. a020677.
16. Toyoda, I., et al., *Early Activation of Ventral Hippocampus and Subiculum during Spontaneous Seizures in a Rat Model of Temporal Lobe Epilepsy.* The Journal of Neuroscience, 2013. **33**(27): p. 11100-11115.
17. Bergstrom, R., et al., *Automated identification of multiple seizure-related and interictal epileptiform event types in the EEG of mice.* Scientific Reports, 2013. **3**.
18. Noebels, J., *Pathway-driven discovery of epilepsy genes.* Nature neuroscience, 2015. **18**(3): p. 344-350.
19. Zamponi, G., et al., *The Physiology, Pathology, and Pharmacology of Voltage-Gated Calcium Channels and Their Future Therapeutic Potential.* Pharmacological Reviews, 2015. **67**(4): p. 821-870.
20. Rajakulendran, S. and M. Hanna, *The Role of Calcium Channels in Epilepsy.* Cold Spring Harbor Perspectives in Medicine, 2016. **6**(1): p. a022723.
21. Chang, B. and D. Lowenstein, *Epilepsy.* N Engl J Med, 2003. **349**(13): p. 1257-1266.
22. Galanopoulou, A., *Mutations affecting GABAergic signaling in seizures and epilepsy.* Pflügers Archiv : European journal of physiology, 2010. **460**(2): p. 505-523.
23. Yuan, H., et al., *Ionotropic GABA and Glutamate Receptor Mutations and Human Neurologic Diseases.* Molecular Pharmacology, 2015. **88**(1): p. 203-217.
24. Liu, Y., et al., *Dravet syndrome patient-derived neurons suggest a novel epilepsy mechanism.* Annals of Neurology, 2013. **74**(1): p. 128-139.

25. Yu, F., et al., *Reduced sodium current in GABAergic interneurons in a mouse model of severe myoclonic epilepsy in infancy.* Nature neuroscience, 2006. **9**(9): p. 1142-1149.
26. Mathews, G., *A possible explanation for the paradox of hyperexcitability and epilepsy in "loss of function" voltage-gated sodium channel mutations.* Epilepsy currents / American Epilepsy Society, 2007. **7**(2): p. 54-55.
27. Ogiwara, I., et al., *Nav1.1 localizes to axons of parvalbumin-positive inhibitory interneurons: a circuit basis for epileptic seizures in mice carrying an Scn1a gene mutation.* The Journal of neuroscience : the official journal of the Society for Neuroscience, 2007. **27**(22): p. 5903-5914.
28. Salzmann, A. and A. Malafosse, *Genetics of Temporal Lobe Epilepsy: A Review.* Epilepsy Research and Treatment, 2012. **2012**: p. 1-19.
29. Guerriero, R., C. Giza, and A. Rotenberg, *Glutamate and GABA Imbalance Following Traumatic Brain Injury.* Current Neurology and Neuroscience Reports, 2015. **15**(5): p. 1-11.
30. Jinno, S., et al., *Neuronal Diversity in GABAergic Long-Range Projections from the Hippocampus.* The Journal of Neuroscience, 2007. **27**(33): p. 8790-8804.
31. Varshavsky, A., *'Spalog' and 'sequelog': neutral terms for spatial and sequence similarity.* Current biology : CB, 2004. **14**(5).
32. Niswender, C. and J. Conn, *Metabotropic Glutamate Receptors: Physiology, Pharmacology, and Disease.* Annual Review of Pharmacology and Toxicology, 2010. **50**(1): p. 295-322.
33. Jong, Y.-J., et al., *Location-Dependent Signaling of the Group 1 Metabotropic Glutamate Receptor mGlu5.* Molecular Pharmacology, 2014. **86**(6): p. 774-785.
34. Kyuyoung, C. and J. Huguenard, *Modulation of Short-Term Plasticity in the Corticothalamic Circuit by Group III Metabotropic Glutamate Receptors.* The Journal of Neuroscience, 2014. **34**(2): p. 675-687.
35. Pinheiro, P. and C. Mulle, *Presynaptic glutamate receptors: physiological functions and mechanisms of action.* Nature Reviews Neuroscience, 2008. **9**(6): p. 423-436.

36. Bianchi, R., et al., *Cellular Plasticity for Group I mGluR-Mediated Epileptogenesis.* The Journal of Neuroscience, 2009. **29**(11): p. 3497-3507.
37. Zhao, W., et al., *Extracellular Glutamate Exposure Facilitates Group I mGluR-Mediated Epileptogenesis in the Hippocampus.* The Journal of Neuroscience, 2015. **35**(1): p. 308-315.
38. Lau, A. and M. Tymianski, *Glutamate receptors, neurotoxicity and neurodegeneration.* Pflügers Archiv : European journal of physiology, 2010. **460**(2): p. 525-542.
39. Lewerenz, J. and P. Maher, *Chronic Glutamate Toxicity in Neurodegenerative Diseases—What is the Evidence?* Frontiers in Neuroscience, 2015. **9**.
40. DeLorenzo, R., et al., *An in vitro model of stroke-induced epilepsy: elucidation of the roles of glutamate and calcium in the induction and maintenance of stroke-induced epileptogenesis.* International review of neurobiology, 2007. **81**: p. 59-84.
41. Mercier, M. and D. Lodge, *Group III Metabotropic Glutamate Receptors: Pharmacology, Physiology and Therapeutic Potential.* Neurochemical Research, 2014. **39**(10): p. 1876-1894.
42. Corti, C., et al., *The Use of Knock-Out Mice Unravels Distinct Roles for mGlu2 and mGlu3 Metabotropic Glutamate Receptors in Mechanisms of Neurodegeneration/Neuroprotection.* The Journal of Neuroscience, 2007. **27**(31): p. 8297-8308.
43. Bettler, B. and J. Tiao, *Molecular diversity, trafficking and subcellular localization of GABAB receptors.* Pharmacology & Therapeutics, 2006. **110**(3): p. 533-543.
44. Betke, K., C. Wells, and H. Hamm, *GPCR mediated regulation of synaptic transmission.* Progress in Neurobiology, 2012. **96**(3): p. 304-321.
45. Turecek, R., et al., *Auxiliary GABAB Receptor Subunits Uncouple G Protein βγ Subunits from Effector Channels to Induce Desensitization.* Neuron, 2014. **82**(5): p. 1032-1044.
46. *Jasper's Basic Mechanisms of the Epilepsies (Contemporary Neurology Series)*, ed. J. Noebels, M. Avoli, and M. Rogawski. 2012: Oxford University Press.

47. Mares, P. and R. Slamberová, *Opposite effects of a GABA(B) antagonist in two models of epileptic seizures in developing rats.* Brain research bulletin, 2006. **71**(1-3): p. 160-166.
48. Yao, H.-H., et al., *Enhancement of glutamate uptake mediates the neuroprotection exerted by activating group II or III metabotropic glutamate receptors on astrocytes.* Journal of neurochemistry, 2005. **92**(4): p. 948-961.
49. Ye, Z.C. and H. Sontheimer, *Metabotropic glutamate receptor agonists reduce glutamate release from cultured astrocytes.* Glia, 1999. **25**(3): p. 270-281.
50. Vermeiren, C., et al., *Acute up-regulation of glutamate uptake mediated by mGluR5a in reactive astrocytes.* Journal of neurochemistry, 2005. **94**(2): p. 405-416.
51. Tian, G.-F., et al., *An astrocytic basis of epilepsy.* Nature Medicine, 2005. **11**(9): p. 973-981.
52. Wetherington, J., G. Serrano, and R. Dingledine, *Astrocytes in the Epileptic Brain.* Neuron, 2008. **58**(2): p. 168-178.
53. Henneberger, C., et al., *Long-term potentiation depends on release of d-serine from astrocytes.* Nature, 2010. **463**(7278): p. 232-236.
54. Devinsky, O., et al., *Glia and epilepsy: excitability and inflammation.* Trends in Neurosciences, 2013. **36**(3): p. 174-184.
55. Simard, M. and M. Nedergaard, *The neurobiology of glia in the context of water and ion homeostasis.* Neuroscience, 2004. **129**(4): p. 877-896.
56. Sofroniew, M., *Molecular dissection of reactive astrogliosis and glial scar formation.* Trends in Neurosciences, 2009. **32**(12): p. 638-647.
57. Nedergaard, M., B. Ransom, and S. Goldman, *New roles for astrocytes: Redefining the functional architecture of the brain.* Trends in Neurosciences, 2003. **26**(10): p. 523-530.
58. Zonta, M., et al., *Neuron-to-astrocyte signaling is central to the dynamic control of brain microcirculation.* Nature neuroscience, 2003. **6**(1): p. 43-50.
59. Anderson, C. and M. Nedergaard, *Astrocyte-mediated control of cerebral microcirculation.* Trends in neurosciences, 2003. **26**(7).

60. Alvarez, J.I., et al., *The Hedgehog Pathway Promotes Blood-Brain Barrier Integrity and CNS Immune Quiescence.* Science, 2011. **334**(6063): p. 1727-1731.
61. Wang, Y., et al., *Interleukin-1β Induces Blood–Brain Barrier Disruption by Downregulating Sonic Hedgehog in Astrocytes.* PLoS ONE, 2014. **9**(10): p. e110024.
62. Ben Shimon, M., et al., *Thrombin regulation of synaptic transmission and plasticity: implications for health and disease.* Frontiers in Cellular Neuroscience, 2015. **9**.
63. Maggio, N., et al., *Thrombin regulation of synaptic transmission: implications for seizure onset.* Neurobiology of disease, 2013. **50**: p. 171-178.
64. Noorbakhsh, F., et al., *Proteinase-activated receptors in the nervous system.* Nature Reviews Neuroscience, 2003. **4**(12): p. 981-990.
65. Wilhelmsson, U., et al., *Redefining the concept of reactive astrocytes as cells that remain within their unique domains upon reaction to injury.* Proceedings of the National Academy of Sciences of the United States of America, 2006. **103**(46): p. 17513-17518.
66. Robel, S. and H. Sontheimer, *Glia as drivers of abnormal neuronal activity.* Nature neuroscience, 2015. **19**(1): p. 28-33.
67. Burnstock, G., *An introduction to the roles of purinergic signalling in neurodegeneration, neuroprotection and neuroregeneration.* Neuropharmacology, 2015.
68. Burnstock, G., *Introduction to Purinergic Signalling in the Brain*, in *Glioma Signaling*, J. Barańska, Editor. 2013, Springer Netherlands. p. 1-12.
69. Lin, J., et al., *A Central Role of Connexin 43 in Hypoxic Preconditioning.* The Journal of Neuroscience, 2008. **28**(3): p. 681-695.
70. Halassa, M., T. Fellin, and P. Haydon, *The tripartite synapse: roles for gliotransmission in health and disease.* Trends in Molecular Medicine, 2007. **13**(2): p. 54-63.
71. Halassa, M., et al., *Synaptic Islands Defined by the Territory of a Single Astrocyte.* The Journal of Neuroscience, 2007. **27**(24): p. 6473-6477.

72. Brambilla, R., et al., *Cyclo-oxygenase-2 mediates P2Y receptor-induced reactive astrogliosis.* British journal of pharmacology, 1999. **126**(3): p. 563-567.
73. Librizzi, L., et al., *Seizure-induced brain-borne inflammation sustains seizure recurrence and blood-brain barrier damage.* Annals of neurology, 2012. **72**(1): p. 82-90.
74. Maroso, M., et al., *Toll-like receptor 4 and high-mobility group box-1 are involved in ictogenesis and can be targeted to reduce seizures.* Nature Medicine, 2010. **16**(4): p. 413-419.
75. Ortinski, P., et al., *Selective induction of astrocytic gliosis generates deficits in neuronal inhibition.* Nature Neuroscience, 2010. **13**(5): p. 584-591.
76. Vezzani, A., et al., *IL-1 receptor/Toll-like receptor signaling in infection, inflammation, stress and neurodegeneration couples hyperexcitability and seizures.* Brain, Behavior, and Immunity, 2011. **25**(7): p. 1281-1289.
77. Schäfers, M. and L. Sorkin, *Effect of cytokines on neuronal excitability.* Neuroscience letters, 2008. **437**(3): p. 188-193.
78. Vezzani, A., et al., *Powerful anticonvulsant action of IL-1 receptor antagonist on intracerebral injection and astrocytic overexpression in mice.* Proceedings of the National Academy of Sciences, 2000. **97**(21): p. 11534-11539.
79. Engel, T., et al., *ATPergic signalling during seizures and epilepsy.* Neuropharmacology, 2015.
80. Henshall, D. and T. Engel, *P2X purinoceptors as a link between hyperexcitability and neuroinflammation in status epilepticus.* Epilepsy & Behavior, 2015. **49**: p. 8-12.
81. Burnstock, G., *Purinergic signalling and disorders of the central nervous system.* Nature reviews. Drug discovery, 2008. **7**(7): p. 575-590.
82. Boison, D., *The adenosine kinase hypothesis of epileptogenesis.* Progress in Neurobiology, 2008. **84**(3): p. 249-262.
83. Navarrete, M. and A. Araque, *Basal Synaptic Transmission: Astrocytes Rule!* Cell, 2011. **146**(5): p. 675-677.

84. Panatier, A., et al., *Astrocytes Are Endogenous Regulators of Basal Transmission at Central Synapses.* Cell, 2011. **146**(5): p. 785-798.

85. Van Gompel, J., et al., *Increased cortical extracellular adenosine correlates with seizure termination.* Epilepsia, 2014. **55**(2): p. 233-244.

86. Lee, M., et al., *Characterization of Arginylation Branch of N-end Rule Pathway in G-protein-mediated Proliferation and Signaling of Cardiomyocytes.* Journal of Biological Chemistry, 2012. **287**(28): p. 24043-24052.

87. Lee, M.J., et al., *RGS4 and RGS5 are in vivo substrates of the N-end rule pathway.* Proceedings of the National Academy of Sciences of the United States of America, 2005. **102**(42): p. 15030-15035.

88. Paspalas, C.D., L.D. Selemon, and A.F.T. Arnsten, *Mapping the Regulator of G Protein Signaling 4 (RGS4): Presynaptic and Postsynaptic Substrates for Neuroregulation in Prefrontal Cortex.* Cerebral Cortex, 2009. **19**(9): p. 2145-2155.

89. Heraud-Farlow, J., et al., *Staufen2 regulates neuronal target RNAs.* Cell reports, 2013. **5**(6): p. 1511-1518.

90. Gerber, K., K. Squires, and J. Hepler, *Roles for Regulator of G Protein Signaling Proteins in Synaptic Signaling and Plasticity.* Molecular Pharmacology, 2016. **89**(2): p. 273-286.

91. Bansal, G., K. Druey, and Z. Xie, *R4 RGS proteins: regulation of G-protein signaling and beyond.* Pharmacology & therapeutics, 2007. **116**(3): p. 473-495.

92. Saugstad, J.A., et al., *RGS4 inhibits signaling by group I metabotropic glutamate receptors.* The Journal of neuroscience : the official journal of the Society for Neuroscience, 1998. **18**(3): p. 905-913.

93. Wamsteeker Cusulin, J., et al., *Glucocorticoid feedback uncovers retrograde opioid signaling at hypothalamic synapses.* Nature Neuroscience, 2013. **16**(5): p. 596-604.

94. Kim, G., et al., *The GABAB receptor associates with regulators of G-protein signaling 4 protein in the mouse prefrontal cortex and hypothalamus.* BMB reports, 2014. **47**(6): p. 324-329.

95. Cifelli, C., et al., *RGS4 Regulates Parasympathetic Signaling and Heart Rate Control in the Sinoatrial Node.* Circulation Research, 2008. **103**(5): p. 527-535.

96. Fowler, C., et al., *Evidence for association of GABA(B) receptors with Kir3 channels and regulators of G protein signalling (RGS4) proteins.* The Journal of physiology, 2007. **580**(Pt 1): p. 51-65.

97. Tedford, W. and G. Zamponi, *Direct G Protein Modulation of Cav2 Calcium Channels.* Pharmacological Reviews, 2006. **58**(4): p. 837-862.

98. Lur, G. and M. Higley, *Glutamate Receptor Modulation Is Restricted to Synaptic Microdomains.* Cell reports, 2015. **12**(2): p. 326-334.

99. Pacey, L., et al., *Genetic deletion of regulator of G-protein signaling 4 (RGS4) rescues a subset of fragile X related phenotypes in the FMR1 knockout mouse.* Molecular and cellular neurosciences, 2011. **46**(3): p. 563-572.

100. Pacey, L., S. Heximer, and D. Hampson, *Increased GABA(B) receptor-mediated signaling reduces the susceptibility of fragile X knockout mice to audiogenic seizures.* Molecular pharmacology, 2009. **76**(1): p. 18-24.

101. Chen, Y., et al., *Neurabin Scaffolding of Adenosine Receptor and RGS4 Regulates Anti-Seizure Effect of Endogenous Adenosine.* The Journal of Neuroscience, 2012. **32**(8): p. 2683-2695.

102. Fredholm, B., et al., *ACTIONS OF ADENOSINE AT ITS RECEPTORS IN THE CNS: Insights from Knockouts and Drugs.* Annual Review of Pharmacology and Toxicology, 2005. **45**(1): p. 385-412.

103. Bodor, E., et al., *Delineation of ligand binding and receptor signaling activities of purified P2Y receptors reconstituted with heterotrimeric G proteins.* Purinergic signalling, 2004. **1**(1): p. 43-49.

104. Ghil, S., K. McCoy, and J. Hepler, *Regulator of G Protein Signaling 2 (RGS2) and RGS4 Form Distinct G Protein-Dependent Complexes with Protease Activated-Receptor 1 (PAR1) in Live Cells.* PLoS ONE, 2014. **9**(4): p. e95355.

105. Cho, H., et al., *Pericyte-specific expression of Rgs5: implications for PDGF and EDG receptor signaling during vascular maturation.* The FASEB Journal, 2003.

106. Mahoney, W., et al., *Regulator of G-Protein Signaling – 5 (RGS5) Is a Novel Repressor of Hedgehog Signaling.* PLoS ONE, 2013. **8**(4): p. e61421.

107. Arensdorf, A., S. Marada, and S. Ogden, *Smoothened Regulation: A Tale of Two Signals.* Trends in Pharmacological Sciences, 2016. **37**(1): p. 62-72.

108. Grafstein-Dunn, E., et al., *Regional distribution of regulators of G-protein signaling (RGS) 1, 2, 13, 14, 16, and GAIP messenger ribonucleic acids by in situ hybridization in rat brain.* Molecular Brain Research, 2001. **88**(1-2): p. 113-123.

109. Estes, J., et al., *Follicular dendritic cell regulation of CXCR4-mediated germinal center CD4 T cell migration.* Journal of immunology (Baltimore, Md. : 1950), 2004. **173**(10): p. 6169-6178.

110. Piatkov, K., C. Brower, and A. Varshavsky, *The N-end rule pathway counteracts cell death by destroying proapoptotic protein fragments.* Proceedings of the National Academy of Sciences of the United States of America, 2012. **109**(27).

111. Piatkov, K., et al., *Calpain-generated natural protein fragments as short-lived substrates of the N-end rule pathway.* Proceedings of the National Academy of Sciences of the United States of America, 2014. **111**(9).

112. Luo, X., et al., *RGS proteins provide biochemical control of agonist-evoked [Ca2+]i oscillations.* Molecular cell, 2001. **7**(3): p. 651-660.

113. Berridge, M., M. Bootman, and L. Roderick, *Calcium: Calcium signalling: dynamics, homeostasis and remodelling.* Nature Reviews Molecular Cell Biology, 2003. **4**(7): p. 517-529.

114. Vosler, P.S., C.S. Brennan, and J. Chen, *Calpain-Mediated Signaling Mechanisms in Neuronal Injury and Neurodegeneration.* Molecular Neurobiology, 2008. **38**(1): p. 78-100.

115. Moldoveanu, T., et al., *The X-Ray Structure of a BAK Homodimer Reveals an Inhibitory Zinc Binding Site.* Molecular Cell, 2006. **24**(5): p. 677-688.

116. Valero, J., et al., *μ-Calpain Conversion of Antiapoptotic Bfl-1 (BCL2A1) into a Prodeath Factor Reveals Two Distinct alpha-Helices Inducing Mitochondria-Mediated Apoptosis.* PLoS ONE, 2012. **7**(6): p. e38620.

117. Nakagawa, T. and J. Yuan, *Cross-Talk between Two Cysteine Protease Families.* The Journal of Cell Biology, 2000. **150**(4): p. 887-894.

118. Wu, Y., et al., *Functional Interactions between Cytoplasmic Domains of the Skeletal Muscle Ca2+ Release Channel.* Journal of Biological Chemistry, 1997. **272**(40): p. 25051-25061.

119. Bevers, M. and R. Neumar, *Mechanistic role of calpains in postischemic neurodegeneration.* Journal of Cerebral Blood Flow & Metabolism, 2007. **28**(4): p. 655-673.

120. Kwon, Y., et al., *An Essential Role of N-Terminal Arginylation in Cardiovascular Development.* Science, 2002. **297**(5578): p. 96-99.

121. Brower, C. and A. Varshavsky, *Ablation of Arginylation in the Mouse N-End Rule Pathway: Loss of Fat, Higher Metabolic Rate, Damaged Spermatogenesis, and Neurological Perturbations.* PLoS ONE, 2009. **4**(11): p. e7757.

122. Brower, C., et al., *Mouse Dfa is a repressor of TATA-box promoters and interacts with the Abt1 activator of basal transcription.* The Journal of biological chemistry, 2010. **285**(22): p. 17218-17234.

123. Yu, H.-M., et al., *Development of a unique system for spatiotemporal and lineage-specific gene expression in mice.* Proceedings of the National Academy of Sciences of the United States of America, 2005. **102**(24): p. 8615-8620.

124. Urlinger, S., et al., *Exploring the sequence space for tetracycline-dependent transcriptional activators: Novel mutations yield expanded range and sensitivity.* Proceedings of the National Academy of Sciences, 2000. **97**(14): p. 7963-7968.

125. Gossen, M., et al., *Transcriptional activation by tetracyclines in mammalian cells.* Science, 1995. **268**(5218): p. 1766-1769.

126. Shen, F., et al., *Transcriptional Activation Domain of the Herpesvirus Protein VP16 Becomes Conformationally Constrained upon Interaction with Basal Transcription Factors.* Journal of Biological Chemistry, 1996. **271**(9): p. 4827-4837.

127. Schmued, L., et al., *Fluoro-Jade C results in ultra high resolution and contrast labeling of degenerating neurons.* Brain Research, 2005. **1035**(1): p. 24-31.

128. Schmued, L.C. and K.J. Hopkins, *Fluoro-Jade B: a high affinity fluorescent marker for the localization of neuronal degeneration.* Brain research, 2000. **874**(2): p. 123-130.

129. Hu, R.-G., et al., *The N-end rule pathway as a nitric oxide sensor controlling the levels of multiple regulators.* Nature, 2005. **437**(7061): p. 981-986.

130. Roman, D., et al., *Identification of small-molecule inhibitors of RGS4 using a high-throughput flow cytometry protein interaction assay.* Molecular pharmacology, 2007. **71**(1): p. 169-175.

131. Lerner, T. and A. Kreitzer, *RGS4 is required for dopaminergic control of striatal LTD and susceptibility to parkinsonian motor deficits.* Neuron, 2012. **73**(2): p. 347-359.

132. Blazer, L., et al., *Reversible, allosteric small-molecule inhibitors of regulator of G protein signaling proteins.* Molecular pharmacology, 2010. **78**(3): p. 524-533.

133. Blazer, L., et al., *A nanomolar-potency small molecule inhibitor of regulator of G-protein signaling proteins.* Biochemistry, 2011. **50**(15): p. 3181-3192.

134. Turner, E., et al., *Small Molecule Inhibitors of Regulators of G Protein Signaling (RGS) Proteins.* ACS Medicinal Chemistry Letters, 2012. **3**(2): p. 146-150.

135. Blazer, L., et al., *Selectivity and Anti-Parkinson's Potential of Thiadiazolidinone RGS4 Inhibitors.* ACS chemical neuroscience, 2015.

136. Dix, M., G. Simon, and B. Cravatt, *Global Mapping of the Topography and Magnitude of Proteolytic Events in Apoptosis.* Cell, 2008. **134**(4): p. 679-691.

137. Hayashi, S. and A. McMahon, *Efficient recombination in diverse tissues by a tamoxifen-inducible form of Cre: a tool for temporally regulated gene activation/inactivation in the mouse.* Developmental biology, 2002. **244**(2): p. 305-318.

138. Behringer, R., et al., *Manipulating the Mouse Embryo: A Laboratory Manual*. Manipulating the Mouse Embryo: A Laboratory Manual. Cold Spring Harbor Laboratory Press.

139. *Gene targeting: A practical approach*. Gene targeting: A practical approach, ed. A. Joyner. Oxford University Press.

140. *The Laboratory Mouse*, ed. H. Hedrich. 2012: Academic Press.

141. Racine, R.J., *Modification of seizure activity by electrical stimulation. II. Motor seizure.* Electroencephalography and clinical neurophysiology, 1972. **32**(3): p. 281-294.

142. Toscano, C., et al., *NMDA-induced seizure intensity is enhanced in COX-2 deficient mice.* NeuroToxicology, 2008. **29**(6): p. 1114-1120.

143. Ilhan, A., et al., *Pentylenetetrazol-induced kindling seizure attenuated by Ginkgo biloba extract (EGb 761) in mice.* Progress in neuro-psychopharmacology & biological psychiatry, 2006. **30**(8): p. 1504-1510.

144. Hu, R.-G., et al., *Arginyltransferase, Its Specificity, Putative Substrates, Bidirectional Promoter, and Splicing-derived Isoforms.* Journal of Biological Chemistry, 2006. **281**(43): p. 32559-32573.